Journal of the
OPTICAL SOCIETY
of AMERICA

VOLUME 36, NUMBER 11 NOVEMBER, 1946

Transparency of Ocean Water*

F. A. JENKINS
Department of Physics, University of California, Berkeley, California

AND

I. S. BOWEN
Mount Wilson Observatory, Carnegie Institution of Washington, Pasadena, California

(Received September 9, 1946)

INTRODUCTION

TWO recent papers in this journal raise questions that are answered in part by some measurements made by the authors in the Fall of 1941 in the ocean off San Diego. Hulburt's investigations[1] of the scattering and absorption by samples of sea water transported to the laboratory emphasize the desirability of measuring the properties of the water *in situ* to avoid uncertainties introduced by aging of the samples. The scattering is especially sensitive to changes in the suspended matter that is bound to occur upon standing in containers. The article by Ewing, Vine, and Worzel[2] on "Photography of the Ocean Bottom" points out that for judging the clarity of the water for photographic purposes neither of the two common methods of measuring water transparency, the Secchi disk and the readings of a photronic cell at different depths, really determine the desired quantity. What is needed is the fraction of light that is transmitted from a point source to the camera without scattering, and they suggest that a determination of the distance at which a light source could be seen through the water at night would be an appropriate measure. The present article describes some measurements of this kind, and, although the results are not of great accuracy, a certain amount of information is obtained on the scattering of light in the ocean.

MEASUREMENTS OF VISUAL RANGE

The critical distance, s, at which an object seen through a turbid medium disappears against the background of scattered light is called the visual range.[3] It depends strongly on the nature of the object and on the conditions of illumination. Thus the Secchi disk reading, which is the visual range of a white disk 30 cm in diameter lowered into the ocean, is a crude measure of transparency, but is not related in any simple way to the absorption and scattering coefficients of the water. The maximum possible visual range, and one of more significance, is that of a point source at night. Our measurements show that in

* This work represents one of the results of research carried out by the University of California Division of War Research under contracts with the Office of Scientific Research and Development, Section 6.1, National Defense Research Committee, and with the Bureau of Ships, Navy Department.

[1] E. O. Hulburt, J. Opt. Soc. Am. **35**, 698 (1945).

[2] Maurice Ewing, Allyn Vine, and J. L. Worzel, J. Opt. Soc. Am. **36**, 307 (1946).

[3] W. E. K. Middleton, *Visibility in Meteorology* (University of Toronto Press, Toronto, 1941).

BOSTON UNIVERSITY
COLLEGE OF LIBERAL ARTS
LIBRARY

offshore water the visual range of a light is roughly twice that of a Secchi disk, while a black disk in daylight has about half the range of the latter.

The light source for these measurements was a clear 1000-watt lamp designed especially for underwater use by the General Electric Company. Current was supplied through a two-conductor rubber-covered cable which was paid out from a reel provided with slip rings. To get exact depths, the bulb was attached to a small wire rope carrying a heavy weight at the end, and passing over a metering wheel. The attachment of the lamp was made so that it floated free of the wire rope in order to avoid strains which might hasten its bursting under pressure. It will be shown below that s is not very sensitive to the intensity of the source, provided that the latter has a certain minimum value.

Observations were first made with a glass-bottomed box floating alongside of a small boat. This proved impracticable, however, for use in the open ocean, and furthermore it does not avoid the effects of the first meter or so of relatively opaque water.[4] Hence an underwater viewing telescope was constructed, and mounted on gimbal rings in the floor of a temporary platform attached at deck level to the side of the experimental ship, the U.S.S. *Jasper*. Since this telescope proved to be very satisfactory for underwater observations in all kinds of weather, it will be briefly described. At either end of a four-inch brass tube 14 ft. 8 in. long were mounted 4-diopter meniscus spectacle lenses. The one at the lower end was protected by a disk of ¼-in. plate glass made watertight by a rubber gasket. Ordinary reading-glass lenses 4 inches in diameter and of 10-in. focal length were placed at distances slightly greater than 10 in. from each spectacle lens. A well-corrected lens of one-meter focal length and diameter 60 mm (actually half of a large camera lens) was mounted near the center, so that the two reading glass lenses were at conjugate foci. The whole constituted a telescopic system of unit magnification giving an angular field of view of 27°. The gimbal ring support was 10 ft. from the lower end, and 5 feet of the telescope were immersed.

TABLE I. Visual ranges for a light source and for a Secchi disk.

Date	Location	Depth of ocean (meters)	Visual range s 1000-watt lamp	Visual range s Secchi disk
7/31/41	5 mi. S of Coronados Islands	91	37	—
8/11/41	San Diego harbor	6	—	2
8/11/41	Tanner bank	27	—	26
8/11/41	32° 04′ N 120° 10′ W	3660	85	45
8/13/41	Off Catalina islands	550	61	—
8/28/41	San Diego harbor	6	5.5	—
9/18/41	33° 28′ N 117° 44′ W	736	76	24
10/10/41	32° 35′ N 117° 18′ W	95	62	—
10/11/41	32° 14′ N 117° 31′ W	1740	62	—
10/11/41	31° 52′ N 117° 45′ W	1560	62	—
10/11/41	31° 30′ N 118° 00′ W	1410	—	28
10/11/41	31° 05′ N 118° 17′ W	1370	—	30
10/11/41	30° 49′ N 118° 25′ W	2650	—	37
10/11/41	30° 31′ N 118° 38′ W	3380	—	40
10/11/41	29° 43′ N 119° 10′ W	3380	77	—
10/11/41	29° 20′ N 119° 25′ W	3660	81	—
10/12/41	28° 58′ N 119° 40′ W	3840	120	—
10/12/41	28° 57′ N 119° 54′ W	3750	137	—
10/12/41	29° 07′ N 120° 56′ W	4080	—	30
10/12/41	29° 07′ N 121° 24′ W	4130	—	47
10/12/41	29° 07′ N 122° 07′ W	3930	—	48
10/12/41	28° 35′ N 122° 46′ W	4200	152	—
10/12/41	28° 51′ N 122° 24′ W	4160	152	—
10/13/41	29° 06′ N 122° 04′ W	4100	152	—
10/13/41	29° 23′ N 121° 36′ W	4020	157	—
10/13/41	30° 15′ N 121° 00′ W	4020	—	48
10/13/41	30° 35′ N 120° 32′ W	4080	—	46
10/13/41	30° 22′ N 120° 15′ W	4020	—	50
10/13/41	30° 52′ N 119° 55′ W	3660	128	—
10/13/41	31° 10′ N 119° 10′ W	3330	73	—
10/14/41	31° 29′ N 118° 49′ W	640	62	—
10/14/41	31° 42′ N 118° 32′ W	2060	93	—
10/14/41	31° 49′ N 118° 22′ W	1460	69	—

Measurements were made by lowering the light until the observer judged that it was on the threshold of visibility. The distances recorded for disappearance and reappearance checked to within ±2 percent, as did the readings taken by different observers. Table I gives the results for the visual range of a light, and also includes, for comparative purposes, a number of Secchi disk readings. Since the latter must be observed in the daytime, they cannot be taken simultaneously with the values for a light source. However, the extensive set of readings taken on the cruise of October 10–14 give a good basis for correlation. Figure 1(a) shows plots of the readings taken on the trip. It shows that whereas the Secchi disk readings were consistently about half those of the light source up to a distance of about 225 miles from shore, beyond this point the water suddenly changed in character and the ratio no longer holds. The reason for this change appears when the optical data are compared with the temperature conditions, as recorded with a bathythermograph by Lt. R. Revelle on the same trip. Figure 1(b) is a plot of the isothermals, and shows, at the same distance from land, a great increase in the depth of the mixed layer of uniform temperature. The

[4] Wilson M. Powell and George L. Clarke, J. Opt. Soc. Am. 26, 111 (1936).

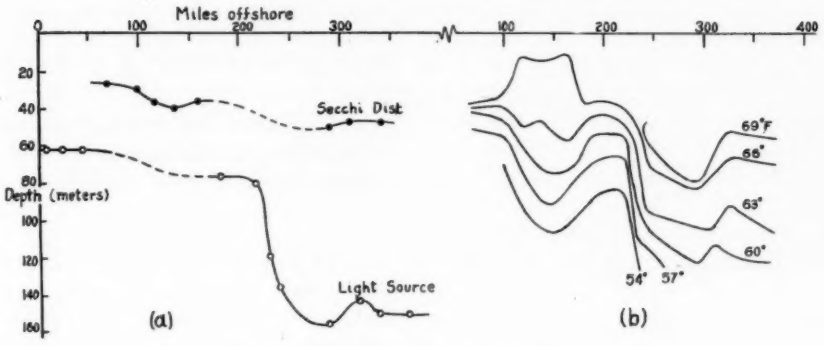

FIG. 1. (a) Visual ranges and (b) isothermals.

transition undoubtedly represents the boundary between the Subarctic water carried by the California current[5] and the Eastern North Pacific Central water. The change in optical characteristics will be discussed below, but it should be mentioned here that in the very clear water ($s \sim 150$ meters) the conditions during disappearance of the light were different, in that by the time the light became invisible the background of scattered light had entirely disappeared. Also, the end point was more difficult to judge in this case because the intensity of the light appeared to die off more gradually.

One test was made, in water having $s = 152$m, of the effect of increasing the intensity of the light source. The effective candlepower of the lamp was raised by running it for a short time above its rated power. The power was increased by a factor of 2.8, which should change the color temperature from 2700°K to 3500°K. The intensity at λ5000 is thereby increased by a factor of 10. The measured increase in range was 25 meters. As will be shown below, this is consistent with our other observations. It is worth remarking that the range obtained in this experiment, 177 meters or 580 feet, probably represents the largest distance that an object has been seen through water.

MEASUREMENTS OF SCATTERED LIGHT

It is possible to evaluate the scattering and absorption coefficients from our measurements of the visual range of a light by using an empirical relation determined by Langmuir and Westendorp[6] for disappearance of a point source against an illuminated background. If E_d represents the flux density at the eye coming directly from the source, and B_0 the brightness of the background, the source becomes invisible when

$$E_d = 3.5 \times 10^{-9} B_0^{\frac{1}{2}} \text{ lumen/cm}^2. \quad (1)$$

In our experiments the background is not uniformly bright, but decreases with increasing angle θ between the source and the line of sight. B_0 is now the brightness at the center of the field, in the immediate neighborhood of the source. To evaluate the total flux of scattered light reaching the eye, it is necessary to find the brightness as a function of θ, that is, we wish to find $f(\theta)$ in the expression

$$B(\theta) = B_0 f(\theta). \quad (2)$$

Since $f(\theta)$ depends in a complicated way on the law of angular scattering, we undertook to make a direct experimental measurement of this function.

A small cartridge type gas-filled photo-cell was installed in a watertight housing at the principal focus of a combination of two plano-convex condensing lenses 6 in. in diameter. The cell responded to light from a field about 6° in angular diameter. The housing was mounted on the end of a long pole and immersed just under the water surface. At each of several depths of the light, readings were taken at 10° intervals of θ between 0° and 40°. These values were then

[5] H. U. Sverdrup, M. W. Johnson, and R. H. Fleming, *The Oceans* (Prentice-Hall, New York, 1942), pp. 724–727.

[6] I. Langmuir and W. F. Westendorp, Physics 1, 273 (1939).

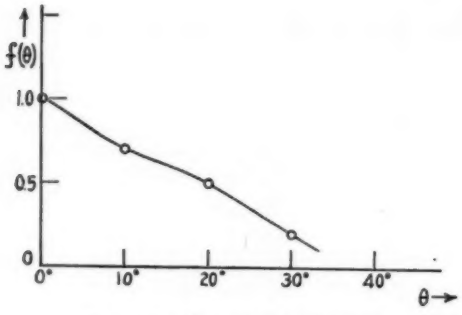

FIG. 2. Angular scattering function.

extrapolated to the distance s, which was 62 meters in the experiment. The resulting curve for $f(\theta)$, shown in Fig. 2, is admittedly not very accurate, but will serve the purpose of relating the brightness B_0 at the center to the total flux of diffuse light.

An attempt was also made to estimate the absolute brightness B_0 of the scattered light when the light source was immersed at the depth s, in this instance 62 meters. Measurements were made with a Luckeish-Taylor brightness meter, and could only be rather rough because of the very low brightness. However, the resulting value, 1.2×10^{-6} candle/cm^2, or one-sixth of moonlight, should represent the correct order of magnitude.

EVALUATION OF ABSORPTION AND SCATTERING

Denoting by α and σ the absorption and scattering coefficients respectively, and by I the candlepower of the source, the illumination at the eye due to unscattered light is, at the distance s,

$$E_d=\frac{I}{s^2}e^{-(\alpha+\sigma)s}. \tag{3}$$

The total illumination, including scattered light, is given to a close approximation by

$$E=\frac{I}{s^2}e^{-\alpha s}. \tag{4}$$

This assumes that all the light is traveling nearly radially. The great preponderance of forward scattering, to be described below, justifies this assumption. The flux density of scattered light then becomes

$$E_s=E-E_d=\frac{I}{s^2}e^{-\alpha s}(1-e^{-\sigma s}). \tag{5}$$

This quantity can also be expressed in terms of the brightness B of the background of scattered light as observed at the surface, namely

$$E_s=2\pi\int_0^{\pi/2}B(\theta)\sin\theta d\theta. \tag{6}$$

Hence, from Eqs. (5) and (6), substituting the value for $B(\theta)$ from Eq. (2), we find

$$\frac{I}{s^2}e^{-\alpha s}(1-e^{-\sigma s})=2\pi B_0\int_0^{\pi/2}f(\theta)\sin\theta d\theta. \tag{7}$$

The integral was evaluated graphically from the experimental curve of Fig. 2, which gave

$$\int_0^{\pi/2}f(\theta)\sin\theta d\theta=0.079. \tag{8}$$

Inserting this value in Eq. (7) we obtain

$$B_0=\frac{6.4}{\pi}\frac{I}{s^2}e^{-\alpha s}(1-e^{-\sigma s}). \tag{9}$$

The quantities E_d and B_0 given by Eqs. (3) and (9) are related by Langmuir and Westendorp's criterion, Eq. (1), so that

$$\frac{I}{s^2}e^{-(\alpha+\sigma)s}=3.5\times10^{-9}\left[\frac{6.4}{\pi}\frac{I}{s^2}e^{-\alpha s}(1-e^{-\sigma s})\right]^{\frac{1}{2}}. \tag{10}$$

For the cases we are considering $e^{-\sigma s}$ is negligible compared to unity, and hence we obtain

$$\frac{I^{\frac{1}{2}}}{s}e^{-\{(\alpha/2)+\sigma\}s}=\left(\frac{6.4}{\pi}\right)^{\frac{1}{2}}\times3.5\times10^{-9}$$
$$=5.5\times10^{-9}\ \text{lumen}^{\frac{1}{2}}\ \text{cm}^{-1}, \tag{11}$$

as the relation between the candlepower I of the source, the visual range s, and the absorption and scattering coefficients α and σ.

The lamp used in the experiments is rated at 30 lumens per watt so that its candlepower in air is approximately 2400. When used under water, which can be regarded, in these thicknesses, as practically opaque for the red and yellow, the lamp will have a smaller effective

intensity, which we estimate from the known absorption curve of water[7] to be about 1000 candles. Its exact value is unimportant, as is seen from Fig. 3, which is a plot of the visual range against candlepower of the source according to Eq. (11), using the absorption and scattering coefficients derived below for water having $s=85$ meters.

As will be seen from Eq. (11), a measurement of s does not allow us to distinguish the separate effects of absorption and scattering, but yields the value of $(\alpha/2)+\sigma$. However, the absorption can be estimated in the following manner with sufficient reliability to give valuable results on the scattering. In the deep water observations the background of diffuse light became invisible at a depth of about 120 meters. This should occur at a brightness of about twice average starlight, or 1.2×10^{-7} candle per sq. cm.[8] Eq. (9) can then be applied, using this value of B_0 and again neglecting $e^{-\sigma s}$ with respect to unity. We obtain $\alpha=0.04$ per meter. A similar, though less accurate, value is obtained by using the measured value of B_0 for $s=62$ meters, namely 1.2×10^{-6} candle/cm². We then obtain $\alpha=0.06$, but the fact that the result is higher does not indicate a real difference between oceanic and coastal water, because of the roughness of the measurement on which the latter value is based. In the following discussion, we shall assume $\alpha=0.04$. The fact that it is very nearly the same as the extinction coefficients determined by oceanographers for the clearest water is rather striking, and indicates that in these cases the attenuation is caused almost entirely by true absorption.

It is of interest to compute the scattering coefficient σ in the case of very clear coastal water.

TABLE II.

s	$\alpha+\sigma$	σ	$\lambda=\frac{1}{\alpha+\sigma}$	E_d	B_0
37	0.41	0.37	2.5 m	21.0×10^{-12} lumen/cm²	35.0×10^{-6} candle/cm²
62	0.24	0.20	4.1	7.5	4.5
72	0.21	0.17	4.8	5.2	2.3
85	0.18	0.14	5.6	3.6	1.0
150	0.10	0.06	10.1	1.6	Assumed zero

[7] Reference 5, Fig. 20, p. 85.

[8] I. Langmuir and W. F. Westendorp. General Electric Company Research Laboratory Publication No. 503 (1932).

Using $s=8500$ cm and $I=1000$ c.p. in Eq. (11), we obtain $(\alpha/2)+\sigma=0.16$ per meter, indicating $\sigma=0.14$. Thus the mean free path for scattering $1/\sigma$ is only 7 meters. Table II shows the results of similar calculations for other values of s, using Eqs. (1), (3), and (11). The values in the last line were computed differently, because of the different conditions during disappearance of the light, namely complete absence of visible background. Here we must assume the threshold

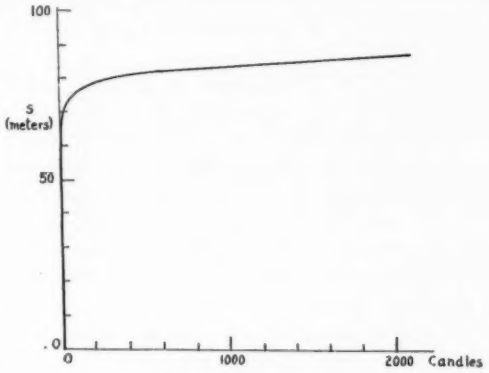

FIG. 3. Visual range *vs.* candlepower of source.

for visibility for a point source in the dark, which may be taken as a 5.5 magnitude star. This gives 1.6×10^{-8} lumen per square meter, which requires that a source 150 meters away have an intensity of 3.5×10^{-4} candle. Since the actual candlepower is taken as 1000, the reduction due to absorption and scattering amounts to a factor of 2.9×10^{6}, or $e^{14.9}$. Thus, we obtain $\alpha+\sigma=14.9/150=0.10$ per meter, for this case.

A check on this figure is afforded by our observations on the difference in visual range when the intensity of the source was changed. An increase in range of 25 meters resulted from raising the intensity at λ5000 by a factor of 10, or $e^{2.3}$. Thus we have $\alpha+\sigma=2.3/25=0.09$, in satisfactory agreement with the above value of 0.10.

OBSERVATIONS ON THE SCATTERING PARTICLES

It is evident from these values of the scattering coefficient that the limitation of visibility in sea water is primarily caused by a haze of scattering particles. The nature of these particles appears

to be not too well understood, and no direct observations of the size and distribution of the particles appear to have been made. Some indirect evidence exists from studies of the angular dependence of scattering[9] as well as of their filterability.[10] The particles, called "debris" by the oceanographers, are much smaller than plankton, and may consist of fragments of organic matter, but are more probably bits of the clay-like materials that often constitute the sediments of ocean bottoms. One author has stated it[11] "that the ocean waters always contain dust."

To get further information on these particles, we constructed the apparatus shown in Fig. 4. It consists essentially of a low power water immersion microscope focused on an intensely illuminated region of the water, and an arrangement for varying the angle between the illuminating beam and the line of sight. The microscope M was inserted in a hole in a vertical cylinder C of four-inch Pyrex, eight inches high. S_1 and S_2 were single-filament 21 c.p. lamps which were imaged in the center of C by the lenses L_1 and L_2, of 5-cm. focal length. Two light sources illuminating the water at different angles were provided in order to detect the presence of fine bubbles by total reflection. No evidence of persistent bubbles was found. The objective had $f=24.7$ mm and N.A. 0.11, giving a resolution of 2.5μ. Oculars from 6.4× to 25× were used,

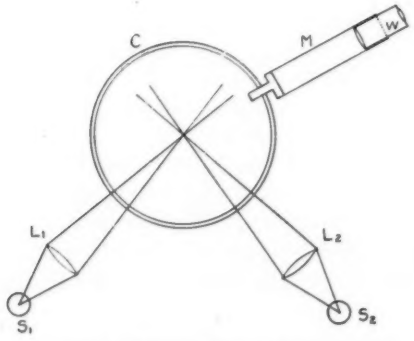

FIG. 4. Microscope for observing scattering particles.

and the over-all magnification was not sufficient to show Brownian motion for particles of the size encountered here.

Samples of various types of water were transferred directly from the ocean to the chamber, and observed visually. The most striking effect is the very pronounced forward scattering, which has been noted in the photometric measurements of various observers.[1,9] Further evidence of this was found in numerous observations of the beam of an underwater searchlight, which preserves its collimation for considerable distances, the beam widening only gradually near the end of its visible path. It is clear from this that the majority of the light cannot be scattered by particles much smaller than the wave-length of light. Furthermore, the color of the beam, which is bluish-white, should be much more intense if this were the case.

The particles were mostly smaller than the limit of resolution, 2.5μ, since only a few showed an observable shape. By using a Whipple micrometer disk (W, Fig. 4) in the eyepiece, counts indicated that in offshore water having $s=85$ m there were in each cubic mm about 4 particles larger than 2.5μ, and 100 that were smaller. The latter, as judged by their brightness, seemed to be rather uniform in size, very few being small enough to be hardly visible. Another indication of this is obtained from a rough computation of the scattering cross section using the above numbers of particles. Assuming that the larger ones have an average cross section of 50 sq. μ and the smaller ones 2 sq. μ, the total area obscured in 1 mm^3 is 4×10^{-4} mm^2. This gives a mean free path for scattering of 2.5 meters, which is one of the same order of magnitude as the values in Table II. All indications therefore point to the fact that particles of size comparable to the wave-length of visible light are responsible for most of the scattering.

DISCUSSION

The distance at which objects may be seen or photographed clearly under ocean water is disappointingly small, since as we have shown, the mean free path for scattering lies in the range 2–10 meters. Although appreciable light will penetrate great distances, as indicated by the

[9] K. R. Ramanathan, Phil. Mag. **46**, 543 (1923). See also other work quoted in reference 5, p. 87.
[10] G. L. Clarke and H. R. James, J. Opt. Soc. Am. **29**, 43 (1939).
[11] Reference 5, p. 88.

attenuation coefficient $k=0.04$ per meter in clear water, it rapidly becomes diffuse, spoiling any sharp outlines. Hazy outlines may be seen at greater distances, thanks to the predominance of forward scattering.

A possible exception to the above statement is brought out by our observations on the disappearance of a light in the true oceanic water more than 225 miles offshore. Here the disappearance seemed to be brought about by true absorption. Although the scattering was about normal in the first hundred meters or so of well-mixed water, there is some evidence that the lower region, with a thermal gradient leading to stability, may be very free from scattering. Further study of water of this type with a scattering meter employing a collimated beam would be very desirable.

Finally, it appears from our measurements of scattering in the ocean that the results on water transported to the laboratory are essentially correct. Thus, Hulbert's recent determinations[1] of σ yielded values in the neighborhood of 0.10 m^{-1} for coastal water, somewhat lower than most of our results for comparable water. However, in this work the larger particles were allowed to settle out before measurements were made. The most satisfactory results would certainly be obtained by instruments directly immersed in the ocean, and it is to be hoped that these preliminary results will stimulate further investigations by more accurate methods.

The authors are indebted to Commander R. Revelle for invaluable assistance in making our apparatus seaworthy, to him and to Dr. B. T. Wright for their help in operating it, and to Dr. F. T. Rogers, Jr. for performing some of the numerical calculations.

JOURNAL OF THE OPTICAL SOCIETY OF AMERICA VOLUME 36, NUMBER 11 NOVEMBER, 1946

Contrast Thresholds of the Human Eye

H. RICHARD BLACKWELL*
Louis Comfort Tiffany Foundation, Oyster Bay, New York
(Received July 12, 1946)

THE L. C. Tiffany Foundation is an art school in peacetime, but its facilities were completely engaged during the war years under a contract with the Office of Scientific Research and Development. The part of the war program upon which this paper is based pertains to the determination of the contrast threshold of the normal human observer under a wide variety of experimental conditions. The typical experimental procedure consisted in projecting a spot of light on a white screen some sixty feet from a group of observers who individually reported whether the stimulus had been seen. A large number of such presentations, made with varying brightness of the stimulus, provided data from which, by statistical analysis, the contrast threshold could be determined. Experiments of this sort were repeated with stimuli of varying sizes and with values of screen brightness covering a range from full daylight to slightly less than the darkest night. In all, more than two million responses to the test stimulus were recorded, some four hundred and fifty thousand of which have been statistically analyzed and reported herein.

I. EXPERIMENTAL PROCEDURE

Laboratory

The laboratory in which experiments were conducted is shown in Figs. 1 and 2. The entire inner surface of the observation room was covered with flat white paint, whose reflectance was approximately 0.89. A ventilation system, details of which are shown in Fig. 2, maintained a moderate temperature and kept the air relatively free from dust particles.

Illumination of the observation room was provided chiefly by a number of special lighting units. The lighting units (troffers) were strategically situated in order to provide maximum

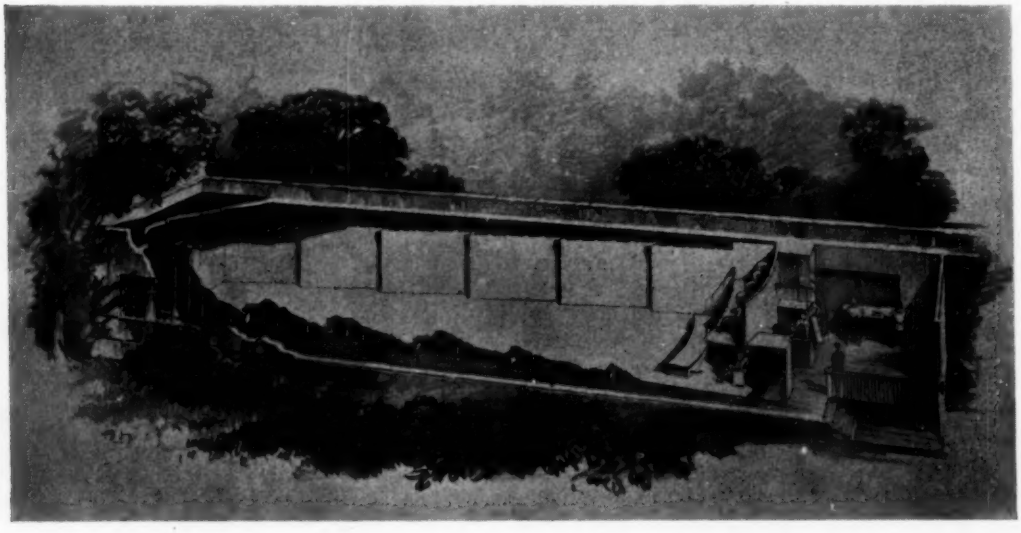

FIG. 1. Sketch of laboratory. A plywood structure was installed within an existing framework. The large plywood room served as a field of standardized brightness (the *observation room*). To the right was located the main control room. To the left was a supplementary control room.

* Now Technical Aide, Army-Navy-NRC Vision Committee, University of Michigan.

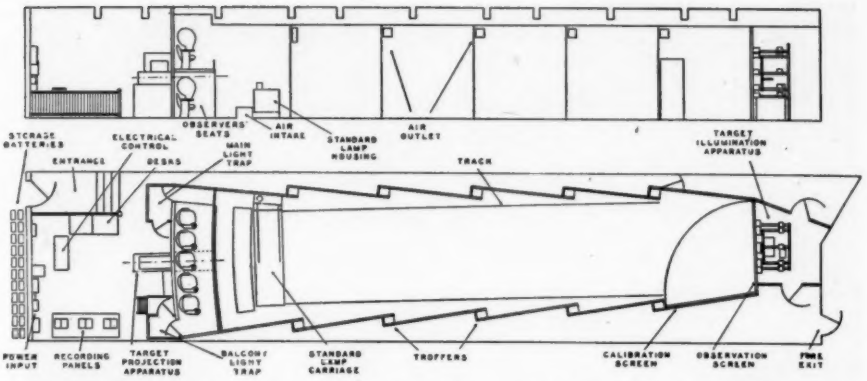

FIG. 2. Floor plan of laboratory. Dimensions of the plywood room (observation room) were: length, 63 feet; height, 10 feet, and width at the narrowest points, 10 feet.

uniformity of illumination. As can be seen in Fig. 2, five troffers were located on each of the left and right walls of the observation room. The brightness of the surfaces of the room could be varied from zero to 1000 footlamberts by adjusting the components of the troffers.

The front wall of the observation room, subtending 10° at the eyes of the observers, served as a screen upon which test stimuli were produced. The use of multiple sources of illumination and walls of high reflectance insured that the brightness of the portion of the screen upon which the stimuli were produced was uniform within the precision of visual photometry. Over the entire surface of the screen, variations in brightness did not exceed ± 3 percent.

It was not possible for all surfaces of the observation room to be made equally bright. Because the troffers were directed forward, the observation screen was always somewhat brighter than other portions of the room. By careful manipulation of the output of the several troffers, surface brightnesses were made to decrease gradually from greatest brightness at the observation screen to least brightness near the rear of the room.

Figure 3 is a view of the observation screen from the rear of the room under typical illumination conditions. It is evident that no portion of the room had a greater brightness than the observation screen and that, in general, the brightness of the room decreased gradually from a maximum at the screen. The irregularities which existed were not distracting.

Preliminary experiments indicated the necessity for control not only of the brightness of the screen, but also of the pattern of brightness of the various surfaces of the observation room. It was shown that the threshold contrast of a stimulus projected onto the observation screen was a function of the pattern of brightness in the visual field surrounding the stimulus. As a consequence, the relative brightnesses of various surfaces of the observation room were rigidly controlled. The pattern of surface brightnesses illustrated by Fig. 3 was standardized. In the few instances in which deviations from this pattern were necessary, it was proved that no significant change in threshold contrast resulted.

The over-all brightness of the observation room was subject to precise control. Whenever possible, the sources of illumination were supplied by storage batteries. When the requisite power could not be produced in this way, a stabilized a.c. supply was employed.

To illuminate the observation screen to a brightness greater than 0.2 footlambert, each troffer was supplied with 120-volt, general service lamps, ranging in wattage from 20 to 300 and in number from 2 to 20. Each troffer extended the entire height of the room, but light emanated only from a flashed opal window 4 inches in width and 40 inches in height.

The output of the troffer units was varied not only by the number and wattage of lamps but also by means of a metal baffle which served to reduce the width of the diffusing window. A wooden reflector extended the full length of the

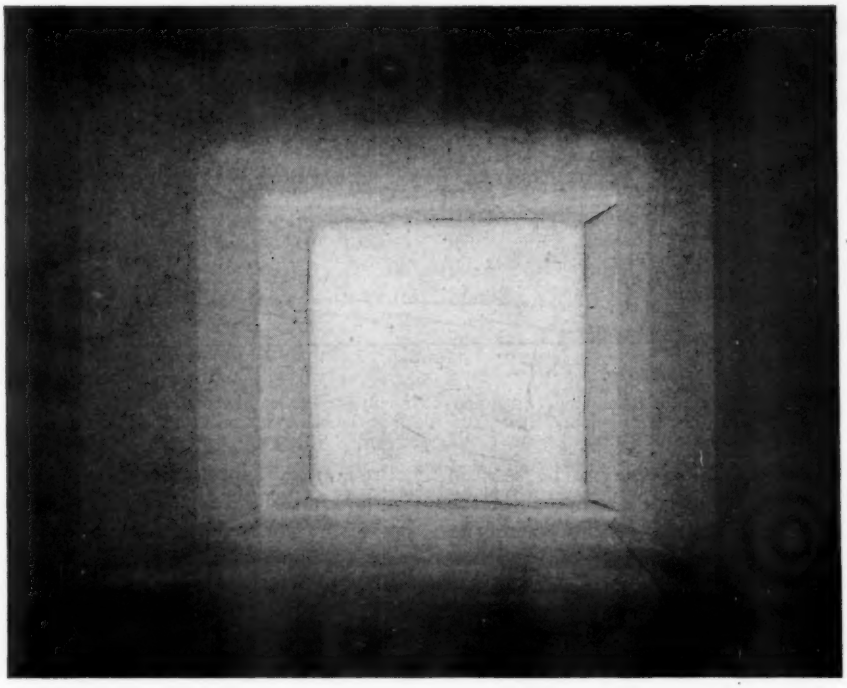

FIG. 3. Observation room with standard illumination, viewed from observers' stations.

troffer which was used to distribute output from the troffer in order to achieve maximum uniformity of illumination.

The lamps were supplied by a three-phase a.c. line, standardized by the Long Island Lighting Company. In order to insure even greater stability, the phase supplying the lamps in the two troffers nearest the observation screen on each side of the room was manually controlled by means of a variable transformer and compensator.

To illuminate the observation screen to a brightness less than 0.2 footlambert, each troffer was provided with from two to four specially designed fixtures. Each fixture was a light-tight brass tube containing an automobile head lamp and ground glass plates, which served as a secondary source. The head lamps were supplied by storage batteries. Reduction in output was obtained by varying the separation between the head lamp and the ground glass plates and by the addition of supplementary ground glass plates and opaque diaphragms. Sufficient ground glass plates were fixed in place to serve as the secondary source so that the addition of supplementary plates did not alter the optical properties of the fixtures. The flashed opal windows of the troffers were removed so that the secondary sources of the fixtures illuminated the observation room directly. Precise control over the spectral quality of the illumination was possible in this way since internal reflection within the troffers was not permitted.

Auxiliary illumination of specific portions of the observation screen was provided by projection equipment located in the control room at the rear of the observation room. Three standard Bausch and Lomb Balopticons were employed, modified somewhat for special purposes. It was sometimes necessary to illuminate extremely small areas of the observation screen. Image definition with the projection apparatus located 65 feet away was unsatisfactory. Accordingly, special techniques were devised by which the observation screen was transilluminated from the small control room shown in Fig. 2.

FIG. 4. View of observers' stations.

Psychophysical Procedure

Observers were seated at the rear of the observation room in upholstered chairs mounted on the floor and on a balcony (Fig. 4). The observers entered the observation room from the large control room through light traps.

A standard experimental session consisted of 320 presentations of a test stimulus. An electrical buzzer served as the signal for a stimulus presentation, remaining activated continuously during the presentation. Breaking the buzzer circuit served as a signal for the observers to indicate whether they had detected the presence of the stimulus.

The duration of the stimulus varied among experiments. In each case, a 6-second rest period followed each stimulus presentation. Additional rests were scheduled so that the observers did not become excessively fatigued.

In preparation for an experimental session, the troffers were adjusted for the desired level of illumination, and projection or transillumination equipment was prepared with a stimulus of selected size. The observers were allowed to adapt to the observation room brightness sufficiently long to insure stable visual performance. At low brightnesses, the period of adaptation was shortened by preliminary adaptation outside the laboratory with standard Polaroid dark adaptation goggles.

Five appropriate stimulus contrasts were selected on the basis of preliminary observations. Both during preliminary observations and during the regular session, each of the stimuli was presented in random sequence an equal number of times. The five stimuli were detectable by the observers with varying probability. The largest stimulus contrast was usually detected with a probability of 95 percent and the smallest stimulus contrast, with a probability of 10 percent. Three additional stimuli were selected so that an adequate function relating probability of detection and stimulus contrast was obtained. Threshold contrast was defined as the contrast which was detected with a probability of 50 percent, due allowance having been made for chance success.

The functions relating probability of detection and stimulus contrast were considered to be normal probability integrals. Graphical analysis

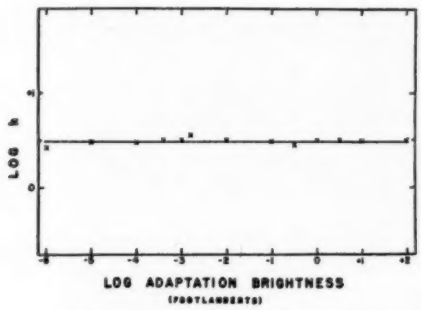

FIG. 5. The arithmetical mean of h values computed from individual probability curves, plotted against adaptation brightness.

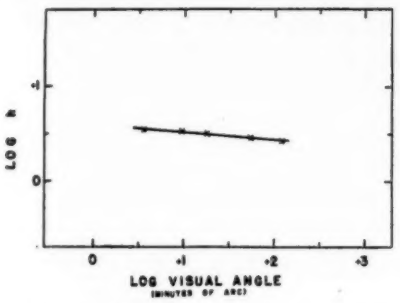

FIG. 6. The arithmetical mean of h values computed from individual probability curves, plotted against stimulus area.

of large numbers of such functions revealed gratifying conformity to the predictions of the Gaussian formula.

Accordingly, solution for the contrast corresponding to 50 percent probability was accomplished by what has been called Urban's constant process.[1] This solution yields M, the stimulus value corresponding to a probability of 50 percent, due allowance having been made for chance success, and h, a constant which is an inverse measure of the steepness of the probability curve. The constant h can be converted into σ, the standard deviation of the normal probability integral.

The adequacy of the Urban solution was investigated for a substantial number of probability functions in the following way: A normal probability curve was generated from values of M and σ and plotted together with the appropriate experimental points. An attempt was made to improve the fit of the normal curve to the experimental points by varying the values of M and σ from those obtained by the Urban process. In no case was an M found which resulted in a better fit of the data, and in only a few cases was a slightly better value of σ found. Since only M values figure in the reported results, this analysis was considered to be an adequate demonstration of the adequacy of the Urban solution. All experimental data reported herein are based upon threshold contrasts computed in this way.

At the outset of experimentation, it was supposed that the five stimulus contrasts would have to vary not only absolutely, but also relatively, among the various experimental sessions. If the steepness of the probability curves varied significantly among the various experimental sessions, in order to include an adequate range of probability values, five stimuli of different relative contrast would have to be selected. Elaborate provisions were made for the production of stimuli with different relative and absolute contrasts.

It soon became evident that an appropriate four to one variation in stimulus contrast corresponded very nearly to a variation in probability from 10 to 95 percent for all experimental sessions. In other words, the shapes of probability curves were very nearly identical in all experimental sessions. Accordingly, five contrasts bearing the same relationship to each other were employed in all experimental sessions.

The five contrast stimuli used in every experimental session were related approximately as the numbers: 1.0, 0.75, 0.55, 0.37, and 0.24. In order to produce contrasts related in this constant fashion, four gelatine filters were obtained whose

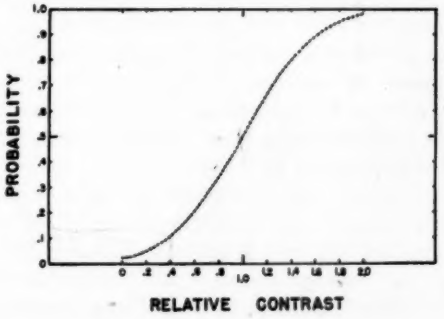

FIG. 7. Average probability curve.

[1] J. P. Guilford, *Psychometric Methods* (McGraw-Hill Book Company, Inc., New York, 1935), p. 170ff.

FIG. 8. Permanent recording of experimental data.

transmittances were identical with the last four numbers in the above series. A mechanism was constructed by which either an empty bracket or a bracket containing one of the four filters could be rotated into the projector beam.

A qualitative estimate of the extent to which the shapes of probability curves were independent of experimental variables such as adaptation brightness and stimulus area can be obtained by comparing h values computed by the Urban method. Data are presented in Figs. 5 and 6, representing a total of 200,000 observations. Values of h were computed by the Urban method from individual probability curves, derived from the body of data reported below in "Results, Part I."

It is apparent that substantial differences in h as a function of either adaptation brightness or stimulus size do not exist.[2]

The definition of "threshold" probability as probability 50 percent greater than chance success was selected primarily because the steepness of the probability curve is greatest at this point, resulting in maximum precision in the determination of thresholds. If the "threshold" be redefined in terms of any probability other than 50 percent, the original threshold data can be converted by means of a simple constant. This procedure is valid because it has been shown that the steepness of probability curves is constant to a first approximation for all experimental conditions.

The average probability curve for all the experimental data reported in this paper was constructed in the following manner: The probability curve for each observer, for each experimental session, was solved by the Urban method for M and σ. The constants M and σ for 1500 individual probability curves were averaged. From the average values of the constants, a normal probability integral was constructed from standard tables. The average probability function can be used in determining the constant which will convert the contrast thresholds presented in this paper to "thresholds" corresponding to other levels of probability.

The average probability curve for 450,000 observations is plotted in Fig. 7. The use of this curve can be illustrated by the following example: If "threshold" contrasts are desired which correspond to a probability of detection, $P=0.90$, thresholds presented in this paper should be multiplied by the constant 1.62.

Interpretation of probability data must be made with care. Trained observers can respond

[2] Although only random differences are present in Fig. 5, the data of Fig. 6 exhibit a consistent trend of smaller h for larger stimuli. The differences in h between the largest stimulus and each of the other stimuli were tested for significance. Value of CR_σ and of P (probability of a difference existing in the direction obtained) are presented:

Stimulus size (ranked with respect to largest stimulus)	CR_σ	P
2	1.83	0.966
3	4.33	0.999992
4	3.90	0.99995
5	5.13	0.999997

TABLE I. Ophthalmological records.

Observer	Visual acuity (20 ft.) O.D.	O.S.	O.U.	Near point (mm) O.D.	O.S.	O.U.	Muscle balance 20 ft.	33 cm
B.B.	20/20−	20/20	20/20+	100	110	110	0.25 Eso.	5 Exo.
I.T.B.	20/25+	20/25+	20/20−	100	110	90	0.5 Eso. 0.25 RH.	1.5 Exo.
M.J.B. (a)	20/15−	20/15−	20/15−	140	140	130	0.5 Eso. 0.25 Hyper.	Normal
(b)*	20/15−	20/15−	20/15−	140	140	130	0.5 Eso.	Normal
E.L.C.	20/15−	20/15−	20/15	130	110	105	1.0 Exo. 0.5 Hyper.	Normal
C.C.C. (a)	20/20−	20/25−	20/20+	120	108	95	0.5 Exo. 0.25 Hyper.	Normal
(b)*	20/20+	20/20+	20/15−	120	110	110	0.25 Exo. 1 Hyper.	Normal
M.C.	20/15−	20/15−	20/15−	70	80	70	2 Eso. 0.5 RH.	1.75 Eso.
L.H.	20/20+	20/20+	20/20+	120	130	120	0.75 Eso.	0.5 Eso.
E.L.H.	20/20	20/20	20/20+	90	90	90	0.5 Eso. 0.25 RH.	Normal
D.H.	20/25+	20/25	20/20−	110	110	100	0.5 Eso.	2 Exo.
L.T.H.	20/20+	20/15−	20/15−	140	140	140	0.5 Eso.	Normal
N.L.H.	20/20	20/20	20/20	120	130	110	0.5 LH.	0.5 Eso.
J.J.	20/15−	20/15	20/15	120	120	100	0.5 Exo. 0.5 RH.	2 Exo.
E.S.K.	20/15−	20/15−	20/15	105	100	100	3 Eso.	3 Exo.
V.R.M.	20/15−	20/15−	20/15−	100	120	100	1.5 Exo.	9 Exo.
M.R.R.	20/15−	20/15−	20/15−	105	115	95	2 Eso. 2 Hyper.	Normal
S.R.	20/20+	20/15−	20/15−	130	120	120	Normal	7 Exo.
M.S.	20/20+	20/20	20/15−	100	110	90	0.37 RH.	2.5 Exo.
J.T.	20/20	20/20	20/20+	110	110	110	0.5 Eso.	3 Exo.
G.H.W.	20/15	20/15−	20/15	90	110	90	2 Eso. 0.5 RH.	2 Exo.

Abbreviations: Eso. Esophoria; Exo. Exophoria; Hyper. Hyperphoria; RH. Right Heterophoria; LH. Left Heterophoria

* Repeat examinations made after three months of intensive observations.

very successfully on the basis of hunches. It was found by interrogation that the observers did not feel confident of having "seen" a stimulus unless the level of probability of detection were greater than 0.90.

Recording of Data

The method used in recording experimental data was rapid and free from error. A large number of electrical circuits were used, each including a neon signal lamp. Master control panels were constructed, at which complete information was at all times available in the form of a constellation of excited neon lamps. Each observer recorded her responses by means of an 8-point selector switch, connected in circuit with eight neon lamps. In this way, each observer had a repertoire of eight possible responses. Projection

or transillumination equipment was equipped with similar switches so that information concerning stimulus presence, stimulus location, and stimulus contrast was represented by appropriate neon signal lamps at the master control panel.

Permanent records were made for each stimulus presentation, which included characteristics of the stimulus and the response of each of the observers. This was accomplished by placing a tissue paper over the master panel and circling with pencil the locations of the excited neon lamps. A record assistant is shown in Fig. 8 recording a typical stimulus presentation. The tissue record sheets were sorted, responses were scored, and probability of detection values were obtained for each observer for each of the five stimulus contrasts. Threshold contrast was then computed for each observer by the Urban method.

Observers

The observers were young women, aged 19–26 years, whose visual acuity in each eye and in both eyes was approximately 20/20 without refractive correction. Table I presents ophthalmological records for the young women whose observations constitute the experimental data of this paper. These and other ophthalmological examinations were made by Dr. Gertrude Rand, Columbia University, and represent a generous personal contribution to the experimental program. The observers were employed full-time for periods varying from six months to two and one-half years. Observing occupied approximately half their time, the remainder being devoted to the statistical analysis of their data. *A priori* objections to this procedure were soon overcome by the obvious stability of individual experimental results.

Observers were never considered "trained" until they had made approximately 6400 observations under varied experimental conditions. In general, the experimental data of this report were obtained with observers who had been occupied from six months to a year in preliminary experiments. Consequently, they were veterans of from 35,000–75,000 observations when the experiments reported here were begun. The exceptional experience of the young women in the task of observing resulted in unusual sensitivity and gratifying stability of response.

Photometric Procedure

Preliminary investigations revealed that under the conditions of these experiments, the precision of ordinary photometric measurements was less than the precision of responses to visual stimulus. As a consequence elaborate photometric determinations were made throughout the experiments reported in this paper. The resulting photometric precision was always at least as good as that of responses to visual stimulus. Measurements were made of brightnesses varying from 100 to 1×10^{-6} footlambert. At least two independent photometric measurements were made of each surface brightness. The two measurements ordinarily agreed within 5 percent, so that brightness values based on two measurements were accurate within less than 5 percent.

All photometric quantities were expressed in footlamberts, defined in terms of the photopic visibility function. Surface brightnesses were evaluated in terms of standard brightnesses by means of null visual photometers. The visual photometers were modifications of the Macbeth illuminometer, chosen for its stability and precision. Standard brightnesses of a special test surface were provided by means of standard lamps, varying in candlepower from 20 to 1000.

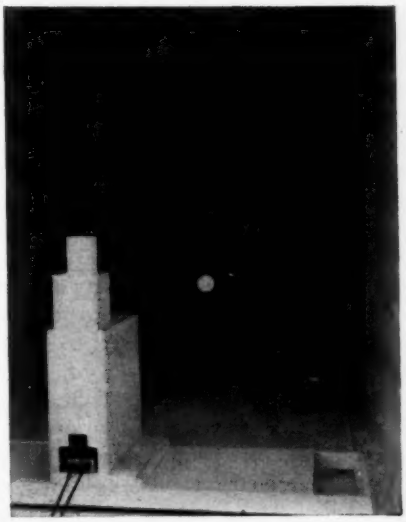

FIG. 9. Apparatus for producing standard brightnesses of a test surface.

Three sets of standard lamps were available. Their reliability was assured by cross-checks and by frequent calibrations at the Electrical Testing Laboratories, New York.

The test surface was always mounted near the observation screen. The standard lamps, in housings mounted on a carriage, could be positioned at distances from the test surface varying from 10 to 50 feet. The carriage moved on the tracks shown in Fig. 2. A black felt calibration screen was mounted before the observation screen when the test surface was illuminated by standard lamps. By preventing re-illumination of the test surface, the calibration screen made it possible for the inverse square law to be used in computing standard brightnesses. A view of the test surface, standard lamp housing, and calibration screen is shown in Fig. 9. The calibration screen was swung into place from its normal position against the right wall as indicated in Fig. 2. Standard brightnesses of the test surface could be varied from 0.006 to 10 footlamberts. When larger or smaller values were needed, gelatine filters were used in the visual photometers, the transmittance of which had been determined for the photopic eye by means of the inverse square law.

In order to fulfill the specification of the photometric unit, it was necessary either to maintain spectral equivalence between surface brightnesses and standard brightnesses, or else to make all brightness evaluations with the photopic eye. It was sometimes possible to obtain spectral equivalence with low intensities by the physical reduction of high intensity sources of known spectral quality. In these instances, evaluations were made at fairly low adaptation brightnesses. More customarily, it was impossible to maintain the spectral quality of surface brightnesses exactly because of the slight selectivity of available materials. In these instances, photometric measurements were made indirectly so that the photopic eye could always be used. Since the selectivity of materials was only slight, direct low level photometry was used occasionally as a check on the indirect photometry. Although the low level photometry exhibited less precision than the indirect photometry, no systematic discrepancy was ever discovered between the two.

The photometric policy adopted insured that surface brightnesses were evaluated correctly in footlamberts. *Apparent* brightnesses always differed somewhat from actual brightnesses because of the slight selectivity of materials, and the variations in luminosity factors of the observers. The question arose whether brightness contrasts were equivalent to *apparent* brightness contrasts. In order to compare actual and *apparent* brightness contrasts, spectrophotometric data for each surface brightness, and luminosity factors for each observer at each brightness level, would be required. Adequate spectrophotometric data were available; no information was available concerning the luminosity factors of the observers. As an approximation, interpolations from average luminosity factors offered by Jones[3] were used. Analysis indicated that significant differences between actual and *apparent* brightness contrasts did not exist.

II. RESULTS AND DISCUSSION

Part I

A comprehensive investigation was made to determine the mutual relationships between adaptation brightness, stimulus area, and threshold contrast. Stimuli, circular in form and brighter than the observation screen, were presented in any of eight possible positions on the screen for an exposure of six seconds. As a consequence, the observers scanned the screen at a rate comparable to that employed by lookouts in the military service in determining the position they thought the stimulus occupied.

General Procedure

Adaptation brightnesses were investigated varying from zero to 100 footlamberts. Circular stimuli varied in diameter from 121.0 to 3.60 minutes of arc. Threshold contrasts were obtained for each of a group of nine observers for each of seventy-seven experimental sessions, consisting of 320 stimulus presentations each. A total of approximately 220,000 observations was made, therefore, under experimental conditions differing only in adaptation brightness, stimulus area, and stimulus contrast.

[3] L. A. Jones, "Summary of American opinion, BS/ARP 18, British standard specification for fluorescent and phosphorescent paint," Great Britain Ministry of Home Security. RC(C) 85 (July, 1942).

Let us set the brightness of the observation screen equal to B_0. When a stimulus was presented, a brightness increment, ΔB, was either added to or subtracted from the prevailing B_0. The stimulus brightness, B_s, equaled $B_0+\Delta B$ or $B_0-\Delta B$. Following standard practice,

$$C \text{ (contrast)} = (B_s-B_0)/B_0 \text{ for stimuli brighter than the observation screen,}$$
$$= (B_0-B_s)/B_0 \text{ for stimuli darker than the observation screen.}$$

Values of C range from 0 to $+\infty$ for stimuli brighter than the screen and from 0 to $+1$ for stimuli darker than the screen. In the experiments of this section, only stimuli brighter than the observation screen were investigated.

Near threshold, the difference between B_s and B_0 is often less than 1 percent. In order to insure sufficient precision, ΔB was produced independently of B_0 by a projection system located in the control room behind the observers. The beam of the projector passed between the observers, as shown in Fig. 4, and struck the observation screen at the opposite end of the observation room.

A small red orientation point was located in the center of the observation screen. The stimulus was projected in one of eight positions on the circumference of a circle generated about the orientation point on a three degree radius. The eight positions used corresponded to the eight major points of a compass. A thin prism, rotated before a standard lantern-slide projector, provided reliable stimulus positioning. At the sound of a signal buzzer, the observers looked toward the screen and instigated a systematic search routine to attempt to locate the stimulus. The six-second exposure permitted only a rapid scanning of the stimulus orbit.

The observers were not given specific scanning instructions. They were told to fixate and to search in the manner they found most efficient. They were instructed that they might find it profitable to use parafoveal vision at low brightnesses. The scanning routine was not identical for all observers, but long experience tended to stabilize the scanning procedures so that reproducible data could be obtained.

At the conclusion of the six-second stimulus exposure, the observers selected the position which they believed the stimulus had occupied. Response consisted of rotating their recording switch until its handle assumed a position analogous to the position of the stimulus. The observers were required to respond to each presentation. They were shown their own data at the conclusion of each experimental session, and soon learned that their hunches were quite often correct. After repeated performance, their responses became semi-automatic.

Response data were recorded from the master control panels as shown in Fig. 8. Each response was scored and the probability of successful detection was computed for each observer for each of the five stimulus contrasts. Threshold contrasts were computed by the Urban method (corresponding to 50 percent probability, due allowance having been made for chance success). Under the experimental conditions, chance success could be expected in one of eight presentations.

Analysis of the response data revealed that there were no systematically favored positions. Further, if an error were made, there was equal probability that the incorrect response would fall in each of the seven positions not occupied by the stimulus. The analysis from which these conclusions were drawn was made with stimuli detected successfully only a few percent better than chance.

Photometric Procedure

Values of B_0 and ΔB were always photometered independently in order to obtain maximum precision in the determination of contrast. When B_0 or ΔB was as great as 0.1 footlambert, a direct measurement was made from the rear of the observation room. A Macbeth illuminometer, fitted with a telescopic attachment, was used as a null instrument in evaluating the unknown surface brightness in terms of the standard brightness of a test surface. For brightnesses less than 0.1 footlambert, special techniques were devised so that brightnesses could legitimately be expressed in footlamberts.

Reduction in the output of the projection system used to provide ΔB was accomplished by the use of gelatine filters, chosen for their lack of selectivity. In addition, when ΔB values less than

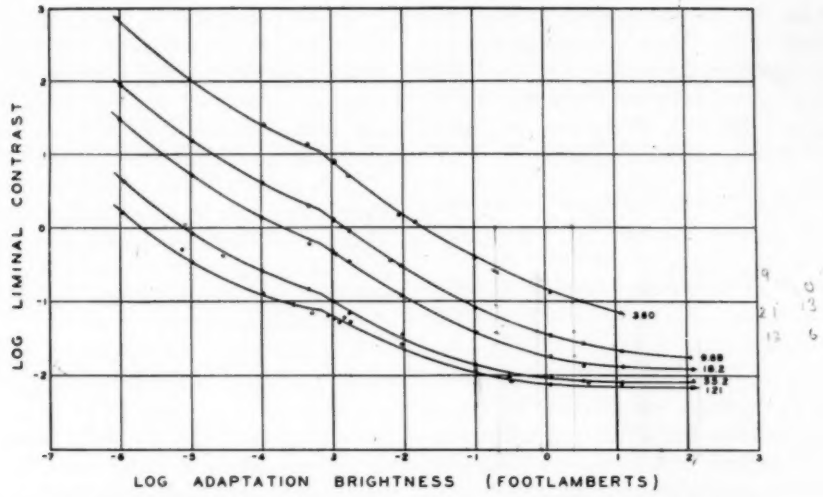

FIG. 10. The arithmetical mean of threshold contrasts, computed from individual probability curves, plotted as a function of adaptation brightness for five stimulus areas.

0.1 footlambert were required, a ground glass plate was inserted in the lantern-slide projector near the aperture. The ground glass became the secondary source of the projection system. Since the absorbing filters were inserted between the ground glass and the projection lamp, reduction in output did not alter the optical properties of the system.

Two independent measurements were made for small values of ΔB:

(1) The gelatine filters were removed and the unattenuated ΔB was measured directly with the Macbeth illuminometer and telescopic attachment. The transmittance of the gelatine filters was then measured in the projection system. Ground glass plates were inserted near the projection lens, on the side away from the projection lamp. The brightness of the foremost ground glass plate was measured with a visual photometer with the gelatine filters in place and with the filters removed. The ratio of the brightnesses was taken as a measure of the visual transmittance of the filters.

(2) A photometric technique was devised in which the gelatine filters were positioned as they had been during experimentation. It was recog-

TABLE II. Arithmetical mean threshold contrast. Stimuli brighter than surround (Part I). Angular subtense of stimulus (minutes of arc).

121.0		55.2		18.2		9.68		3.60	
Log B_0	Log C	Log B_0	Log C	Log B_0	Log C	Log B_0	Log C	Log B_0	Log C
2.080	−2.124	2.084	−2.041	2.081	−1.894	2.053	−1.739	1.072	−1.127
2.061	−2.127	1.083	−2.061	2.078	−1.895	1.077	−1.671	0.523	−0.980
1.074	−2.082	0.605	−2.085	1.086	−1.861	0.533	−1.568	0.075	−0.868
0.076	−2.102	0.531	−2.049	0.542	−1.863	0.076	−1.460	−0.996	−0.401
−0.471	−2.081	0.078	−1.997	0.070	−1.736	−0.994	−1.083	−2.053	0.175
−0.497	−2.065	−0.504	−2.021	−0.975	−1.415	−2.031	−0.505	−2.768	0.703
−0.994	−1.937	−0.504	−1.971	−2.034	−0.918	−2.757	−0.044	−2.951	0.905
−2.029	−1.579	−0.991	−1.858	−2.755	−0.460	−2.979	0.090	−2.978	0.896
−2.756	−1.274	−2.020	−1.438	−2.952	−0.344	−2.984	0.116	−3.341	1.144
−2.907	−1.280	−2.769	−1.150	−2.989	−0.313	−3.346	0.298	−3.964	1.397
−2.987	−1.228	−2.981	−1.012	−3.323	−0.219	−3.982	0.618	−5.016	2.026
−3.065	−1.178	−3.331	−0.831	−4.002	0.151	−4.986	1.179	−6.032	2.868
−3.296	−1.148	−3.995	−0.595	−4.982	0.705	−5.999	1.944		
−3.979	−0.891	−4.989	−0.079	−6.012	1.479				
−4.995	−0.474	−5.948	0.622						
−5.969	0.212								

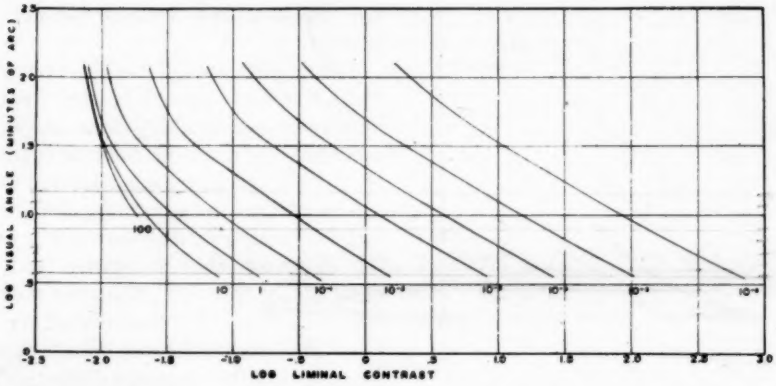

FIG. 11. Interpolations from Fig. 10. Each curve represents the relation between threshold contrast and stimulus area for a given adaptation brightness.

nized that the illumination striking the observation screen bore a constant relation to the brightness of the secondary source of the projection system. The constant factor relating ΔB to the brightness of the secondary source of the projector was established at maximum output. Subsequently, the secondary source brightness was measured and ΔB was computed.

Agreement between the two measurements of ΔB was ordinarily obtained within ± 3 percent.

At low brightnesses, B_0 was provided by the special fixtures described under "Experimental Procedures." Since reduction did not affect the areas of the secondary sources, or in any way alter their optical properties, there was a constant relationship between the brightness of the observation screen and the brightnesses of the secondary sources of the fixtures.

At a screen brightness level of 0.1 footlambert, the constant factor relating B_0 to the brightnesses of the secondary sources of the fixtures was measured. For low brightnesses, B_0 was computed from measurements of the appropriate brightnesses.

The validity of the indirect photometric measurement was established by the following photometric technique: A disk, three feet in diameter, was mounted at the center of the observation screen. Since its surface reflectance was lower than that of the screen, the disk appeared as a large dark circular patch in the center of the observation screen. An increment of illumination could be added to the disk from the projection apparatus located in the control room behind the observers. When the appropriate increment of illumination was added, the disk became indistinguishable from the observation screen.

The group of nine observers used the disk and screen as a huge visual photometer. Increments of illumination were selected, some of which were insufficient to increase the disk brightness to that of the screen, while others made the disk brighter than the screen. The increments were presented randomly to the observers, who judged whether the disk was brighter or darker than the surrounding screen. The increment just sufficient to make the disk indistinguishable from the screen was interpolated from the psychophysical data. The spectral quality of the disk and the observation screen were carefully equated so that

TABLE III. Interpolations from Fig. 10. Log (arithmetical mean threshold contrast).

Angular subtense of stimulus (minutes of arc)	B_0								
	100	10	1	1×10^{-1}	1×10^{-2}	1×10^{-3}	1×10^{-4}	1×10^{-5}	1×10^{-6}
121.0	−2.132	−2.130	−2.114	−1.959	−1.640	−1.198	−0.910	−0.461	0.238
55.2	−2.062	−2.060	−2.020	−1.857	−1.500	−0.996	−0.590	−0.069	0.666
18.2	−1.889	−1.857	−1.738	−1.421	−0.928	−0.325	0.137	0.716	1.467
9.68	−1.730	−1.658	−1.437	−1.070	−0.526	0.124	0.615	1.196	1.950
3.60	—	−1.111	−0.812	−0.385	0.182	0.911	1.410	2.017	2.821

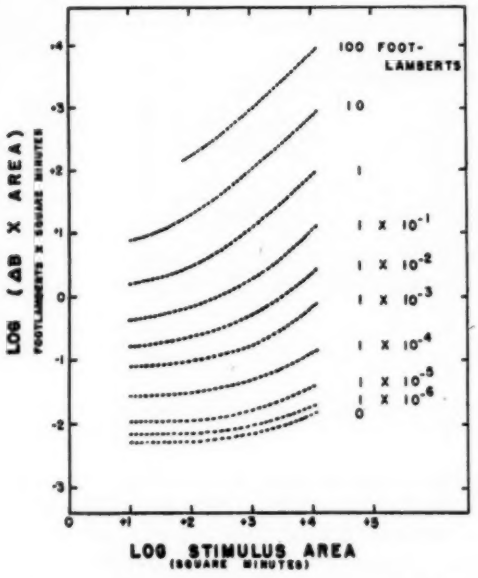

FIG. 12. Interpolations from Fig. 10. The product of ΔB and stimulus area is plotted as a function of stimulus area for various adaptation brightnesses.

evaluation errors were not introduced at low brightnesses.

The value of illumination increments from the projection system was computed in the following manner: A ground glass plate was inserted in the projection system which served as a secondary source. Reduction in the output of the optical system was accomplished by the insertion of gelatine filters between the secondary source and the projection lamp; consequently, the optical properties of the system were not altered. A constant factor related the brightness of the secondary source to the illumination striking the disk.

With B_0 set for 0.1 footlambert, the relation between secondary source brightness and illumination at the disk was measured. The relation between illumination required to render the disk indistinguishable from its surrounds and B_0 was established. Subsequently, critical values of illumination were determined from observer judgments, and B_0 was computed. The direct measurement of B_0 did not vary systematically from the value computed from the indirect photometric measurement. Random differences between the two measurements usually did not exceed ± 4 percent.

The circular stimuli used in the various experimental sessions varied in size from 0.7 to 26 inches in diameter. Measurements were made to determine the exact distribution of energy in each of the stimuli. For each stimulus the diameter was considered to be that of a stimulus of equivalent flux, uniformly distributed. For large stimuli, the diameter thus computed did not differ significantly from the diameter measured with rule and calipers. For the smallest stimulus, there was a 15 percent difference between the computed diameter and the measured diameter. The diameter based upon energy considerations was considered the most adequate measure of size because in the case of a stimulus as small as 3.60 minutes of arc, the eye usually responds on the basis of total physical energy.

The experimental data are presented in Table II and are plotted in Fig. 10, fitted by empirical curves. The data represent approximately 220,000 observations obtained during a period of four months by a group of nine observers. (The open circles represent experimental data obtained under different experimental conditions. Subsequent reference will be made to these points in Part II.)

Two interesting aspects of the contrast sensitivity functions are apparent. At high brightnesses, especially for large stimuli, contrast becomes constant with respect to adaptation brightness. For a 121-minute stimulus, for example, there is no appreciable change in threshold contrast as adaptation brightness is reduced from 100 to 1 footlambert. This relation has been called the Weber-Fechner law.

Each of the curves shows a discontinuity at approximately 7×10^{-4} footlambert. From interrogation, it was clear that this discontinuity

TABLE IV. Arithmetical mean threshold ΔB ($B_0=0$).

Angular subtense of stimulus (minutes of arc)	Log ΔB
121.0	−5.836
	−5.951
55.2	−5.444
18.2	−4.594
9.68	−4.184
	−4.056
3.60	−3.268

TABLE V. Arithmetical mean threshold contrast. Stimuli brighter than surround (Part II). Angular subtense of stimulus (minutes of arc).

121.0		55.2		18.2		9.68		3.60	
Log B_0	Log C	Log B_0	Log C	Log B_0	Log C	Log B_0	Log C	Log B_0	Log C
−2.831	−1.208	−4.505	−0.372	−2.994	−0.308	−2.117	−0.434	−1.823	0.078
−3.551	−1.031								
−5.134	−0.297								

corresponded to a change in the nature of scanning. Since the observers were allowed to fixate where they chose, they used foveal vision at high brightnesses and parafoveal vision at low brightnesses.

Interpolations from Fig. 10 are presented in Table III and in Fig. 11.

Figure 12 is presented in order to compare the data of Fig. 10 with data obtained at zero adaptation brightness. The basic data for zero adaptation brightness are presented in Table IV. It is apparent that the performance of the eye is very similar for adaptation brightnesses smaller than 1×10^{-5} footlambert.

Precision

Analysis of photometric measurements revealed that each surface brightness was accurately measured within ±4 percent. Estimates of the repeatibility of the observer's response data were obtained by computing the probable errors of group probability functions constructed from all the observer data in each of the experimental sessions. The average P.E. obtained indicated that in 99 percent of repeat experiments the same response data would be obtained within ±8 percent; in 50 percent of repeat experiments, within ±2 percent.

Inspection of Fig. 10 indicates that the experimental points fall on the smoothed curve within ±5 percent on the average, with an occasional point deviating as much as 16 percent. The precision of experimental data measured in this way is in agreement, therefore, with the precision predicted from standard statistical measures. The over-all precision of the experimental procedure was approximately ±5 percent. The precision of the smoothed curve is approximately ±0.6 percent.

Examination of the data for individual observers revealed that the average deviation from a smoothed curve was ±12 percent, with an occasional deviation of 40 percent.

Part II

An experimental program was conducted to determine whether stimuli darker than the observation screen are equivalent to stimuli brighter than the screen of equivalent contrast. For convenience, stimuli brighter than the screen will be considered *positive* and stimuli darker than the screen will be considered *negative*. (It must be emphasized that the definition of contrast results in positive values of contrast for both *negative* and *positive* stimuli.)

In almost all particulars, the experimental procedure duplicated that of Part I. Special projection apparatus was devised to permit the presentation of negative stimuli. A transparent slide containing an opaque spot was placed in an ordinary lantern-slide projector. When the entire observation screen was illuminated, a negative stimulus could be produced in any of eight locations. The negative stimulus was positioned by means of a special mechanism designed to change the position of the opaque spot in the projector beam. In order to reduce the contrast of the negative stimulus, additional illumination of the screen was provided by a second projector, adjusted to illuminate exactly the same area as the first. Additional reduction of contrast was accomplished by illuminating the screen and the remainder of the observation room with the troffer units.

It was necessary to produce five values of contrast related in a constant fashion, to be used in obtaining probability curves in each experimental session. This was accomplished by inserting one of a pair of filters of complementary transmittances in the beam of each of a pair of projectors. The initial output of the projectors was equated; as a consequence, their combined output was

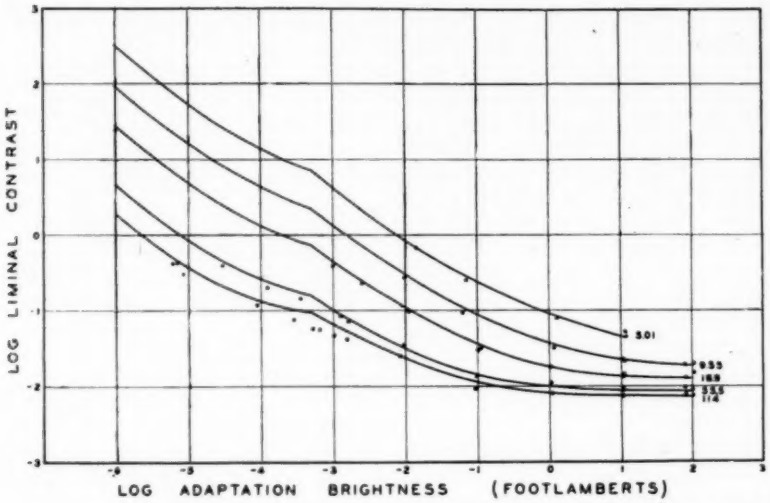

FIG. 13. The arithmetical mean of threshold contrasts computed from individual probability curves, plotted as a function of adaptation brightness for five stimulus areas. The solid curves represent interpolations from Fig. 11.

maintained constant as the relative contribution from each was varied. The transparent slide and opaque spot were included in only one of the projectors. Consequently, as the different combinations of filters were used, stimulus contrast varied in a systematic fashion. For a given experimental session, the proportions of screen brightness provided by the troffer units and the pair of projectors were adjusted so that the contrasts approximated those used in the corresponding experiment of Part I.

In order to change the position of the stimulus, it was necessary to remove the stimulus from the observation screen. Accordingly, a shutter interrupted the beams of the pair of projectors at the end of each six-second stimulus presentation. Removal of the stimulus reduced the brightness of the observation screen and affected the brightness adaptation of the observers. Accordingly, a third projector was used to compensate for the reduction in screen brightness resulting from stimulus removal. The output of the third projector equaled the combined output of the pair of projectors. A single shutter arm uncovered the

TABLE VI. Arithmetical mean threshold contrast. Stimuli darker than surround (Part II). Angular subtense of stimulus (minutes of arc).

114.0		55.5		18.9		9.55		5.01	
Log B_0	Log C	Log B_0	Log C	Log B_0	Log C	Log B_0	Log C	Log B_0	Log C
2.022	−2.119	2.012	−2.033	2.022	−1.821	2.024	−1.699	1.073	−1.344
1.914	−2.103	1.894	−2.018	1.911	−1.881	1.901	−1.712	1.066	−1.278
1.035	−2.122	1.039	−2.037	1.041	−1.835	1.047	−1.667	0.115	−1.096
1.027	−2.143	1.029	−2.046	1.029	−1.869	1.024	−1.641	−1.152	−0.590
0.040	−2.096	0.027	−1.950	0.019	−1.740	0.070	−1.490	−1.826	−0.173
−1.029	−2.033	−1.012	−1.867	−0.949	−1.494	−1.200	−1.033		
−2.068	−1.611	−2.024	−1.452	−0.999	−1.520	−2.004	−0.554		
−2.807	−1.382	−2.798	−1.140	−1.952	−1.012				
−2.970	−1.325	−2.900	−1.072	−2.603	−0.636				
−3.190	−1.256	−3.457	−0.842	−3.042	−0.403				
−3.287	−1.250	−3.920	−0.696						
−3.546	−1.112	−4.532	−0.402						
−4.055	−0.932								
−5.073	−0.520								
−5.156	−0.366								
−5.224	−0.375								

projection lens of the compensating projector as it covered the projection lenses of the pair of projectors. In this way, the brightness of the observation screen was unchanged during the removal and production of the stimulus.

The production of contrasts approaching the upper limit of negative stimuli (+1.0) necessitated that only the pair of projectors illuminate the observation screen. Illumination from the troffer units always served to reduce the stimulus contrast. It is apparent, therefore, that production of large stimulus contrasts was possible only by reduction in the relative amount of illumination of the screen produced by the troffers. The pattern of surface brightnesses in the observation room was somewhat different for illumination by troffers and illumination by projectors. When troffer illumination was used, the standardized distribution of brightness shown in Fig. 3 resulted. The use of projectors illuminating the observation screen alone resulted in greater brightness of the screen relative to the other brightnesses of the room. With troffer illumination, the brightness of the areas immediately adjoining the screen were 95 percent as bright as the screen. With projected illumination, the corresponding value was 44 percent.

Experiments were conducted to determine whether this variation in the pattern of brightnesses in the visual field influenced threshold contrast. The observation screen was illuminated solely by a projector. A positive stimulus increment was added by a second projector. Conditions duplicated corresponding experiments in Part I except for the difference in the pattern of brightness in the visual field. Seven experimental sessions were conducted, corresponding to the instances in which the maximum variations in the pattern of brightness were required with negative stimuli. The results are presented in Table V, and are plotted as open circles in Fig. 10. It is apparent that the maximum variation from the standardized brightness pattern encountered in the experiments of this section did not influence the threshold contrasts of positive stimuli. As a first approximation, it can be assumed that the same variation in the pattern of brightnesses did not influence the threshold contrasts of negative stimuli.

The experimental data of this section are presented in Table VI and in Fig. 13, representing a total of approximately 125,000 observations by a group of eight observers. It is apparent that in most instances there is evidence that negative stimuli are equivalent to positive stimuli of equivalent area and contrast. In the case of large stimuli and low adaptation brightnesses, however, a consistent discrepancy exists. Comparison of the threshold contrasts of the same observers in corresponding experiments of Parts I and II indicates 20 percent lower thresholds for negative stimuli.

Part III

Preliminary experiments indicated that the six-second exposure used in the experiments of Part I and Part II did not represent sufficient time for minimal thresholds. A supplementary program was conducted to determine threshold contrasts when an indefinitely long exposure was used. In general, the experimental procedures of Parts I and II were followed very closely.

It was found that if the stimuli were presented in any of eight positions as in Parts I and II, extremely long exposures were necessary for minimal thresholds. An exposure as long as 60 seconds was not clearly sufficient for minimal thresholds under all circumstances. Accordingly, the method of experimentation was modified so that substantially shorter exposures could be used. The stimulus was always presented in the same position, in the center of the observation screen. Orientation points were provided at the four edges of the target at a distance of approximately 2 degrees from each edge. The customary five stimulus contrasts were used, interspersed with trials in which no stimulus was presented. The observers were required to respond whether they believed a stimulus had been shown. Their response consisted of rotating the handle of their recording switch to one position for "yes," another for "no." The number of positive responses obtained when no stimulus was presented was used as the "chance" score in interpreting the resulting probability curves.

In each experimental session, it was proved that doubling the exposure did not increase the frequency of correct judgments. In general, exposures of 15 seconds were adequate for minimum thresholds.

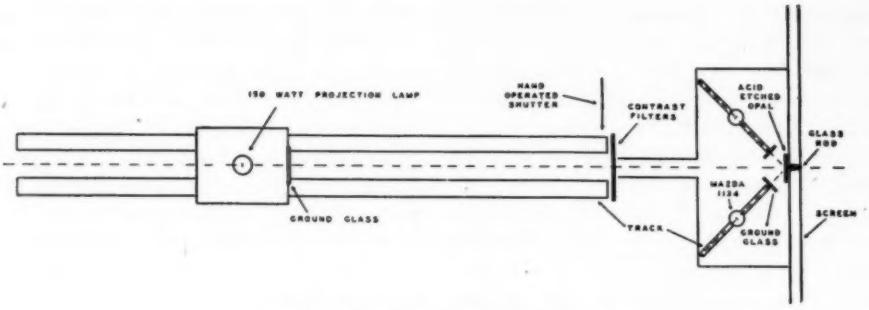

FIG. 14. Stimulus illuminating system.

Analysis of the data of Part I indicated that certain profitable changes in emphasis could be made in a supplementary program. It was apparent from the data of Fig. 10 that targets both larger and smaller than those of Part I should be investigated. The data of Fig. 12 indicated that experimentation at screen brightnesses less than 1×10^{-5} footlambert was not very necessary. In Part I, large numbers of observations were made to determine the exact nature of the discontinuities in the visual functions. Sufficient information was obtained so that less emphasis was necessary in the supplementary experimental program.

In order to produce an extremely small stimulus, it was necessary to develop a new apparatus. Since it was impossible to obtain satisfactory image definition by projection, a small stimulus was produced by transilluminating the observation screen. A section of glass rod, optically polished on each end, was inserted in the exact center of the observation screen. The front face of the rod was mounted flush with the front surface of the screen. An acid-etched opal plate was mounted 0.01 inch from the rear face of the rod. The opal plate served as the stimulus, baffled by means of the glass rod to a known diameter.

The optical system used to illuminate the opal plate is shown in Fig. 14. A balanced pair of automobile head lamps served to illuminate the opal so that its brightness equaled that of the observation screen. Additional illumination, producing a brightness increment, was provided by a lamphouse mounted on an optical bench. Preceding stimulus presentations, one of five gelatine filters was inserted (corresponding to one of five fixed stimulus contrasts) and a shutter was removed from the beam. The absolute level of the five contrasts was varied by means of the inverse square law and the addition of ground glass plates and opaque diaphragms to the face of the lamphouse.

The brightness of the opal plate through the glass rod was always measured with a Macbeth illuminometer, fitted with a lens to focus the opal plate in the cube of the photometer. It was recognized that a more adequate photometric procedure would involve the computation of stimulus brightness from a measurement of its candlepower. A test was made which indicated excellent agreement between measurements made with the alternative photometric techniques.

Investigation was made to ascertain whether a shadow around the glass rod existed, which would serve to reduce the effective candlepower of the

TABLE VII. Arithmetical mean threshold contrast. Stimuli brighter than surround (Part III). Angular subtense of stimuli (minutes of arc).

360.0		121.0		55.2	
Log B_0	Log C	Log B_0	Log C	Log B_0	Log C
1.857	−2.519	1.850	−2.596	−0.053	−2.436
1.024	−2.455	1.044	−2.510	−0.994	−2.174
−0.051	−2.603	−0.052	−2.441	−1.859	−1.688
−1.041	−2.296	−1.005	−2.209	−2.924	−1.149
−1.883	−2.033	−1.878	−1.799		
−2.948	−1.558	−2.939	−1.361		
−3.997	−1.221	−3.969	−1.029		
−5.052	−0.847	−4.974	−0.569		

18.2		9.68		3.60		0.595	
Log B_0	Log C	Log B_0	Log C	Log B_0	Log C	Log B_0	Log C
1.853	−2.462	1.874	−2.063	1.044	−1.559	1.854	−0.323
0.070	−2.294	−1.023	−1.672	0.039	−1.324	1.034	−0.051
−0.984	−1.971	−1.900	−1.075	−1.887	−0.384	0.039	0.264
−1.871	−1.322	−2.953	−0.157	−2.965	0.593	−1.019	0.643
−2.923	−0.655	−3.932	0.425			−1.894	1.136
−4.982	0.584					−2.941	2.104
						−3.957	2.756
						−4.999	3.397

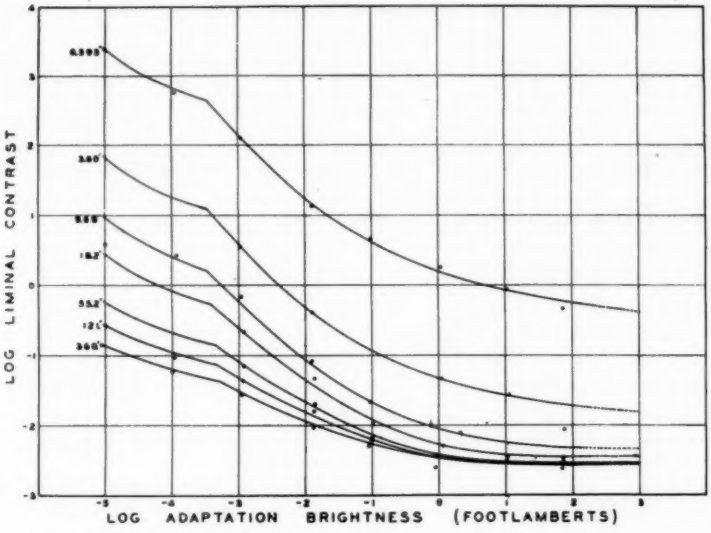

FIG. 15. The arithmetical mean of threshold contrasts computed from individual probability curves, plotted as a function of adaptation brightness for seven stimulus areas.

opal source. Measurements made with an integrating sphere and visual photometer revealed that there was no such effect.

The experimental data of this section are presented in Table VII and in Fig. 15, summarizing approximately 90,000 observations by a group of seven observers. It is evident that the precision of results is significantly less than in Part I and Part II. The lower precision is attributed to the fact that the observers were required to search for the stimulus repeatedly over a very small area. Under these conditions, the motivation and fatigue of the observers became extremely important. The curves fitted to the experimental data of Fig. 15 were empirically determined as the best-fitting curves consistent with characteristics of the contrast sensitivity functions established in Part I.

Interpolations from the smoothed curves are presented in Table VIII and in Fig. 16.

Each curve in Fig. 16 consists partially of a linear portion representing the fact that the product of area and stimulus brightness, ΔB, is a constant. Stimuli whose areas place them on the linear position of these curves are effectively "point sources." The point at which each curve departs from linearity corresponds to a fundamental property of the human eye. "Critical visual angle" is defined as the angle at which the relationship: area $\times$ brightness = a constant ceases to exist. "Critical visual angle" is plotted as a function of adaptation brightness in Fig. 17. The shape of this function is similar to that of the function relating threshold contrast and adaptation brightness.

Interpolations from Fig. 16 are presented in Fig. 18. The curves for most contrasts show discontinuities, indicating the change from foveal to parafoveal vision. For high contrasts, the curves are parallel, indicating that area $\times$ brightness = a constant.

ACKNOWLEDGMENTS

The dependence of the success of the experimental program upon Professor Arthur C. Hardy can scarcely be overemphasized. As Chief, Section 16.3, NDRC, he was responsible for appreciating the need for the research, for initiating both administrative and technical aspects of the program, and for maintaining close contact with experimental results and with laboratory problems encountered in obtaining them. Because he was willing to concern himself with the bothersome details of the research more completely than

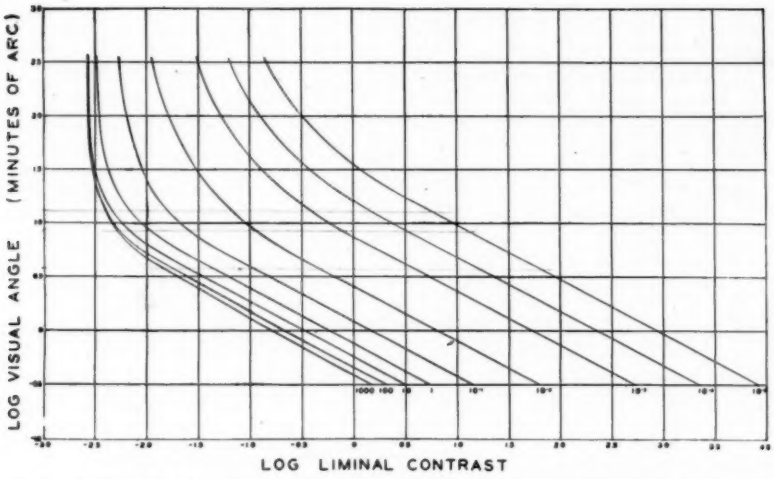

FIG. 16. Interpolations from Fig. 15. Each curve represents the relation between threshold contrast and stimulus area for a given adaptation brightness.

TABLE VIII. Log (arithmetical mean threshold contrast). Interpolations from Fig. 15.

Angular subtense of stimuli (minutes of arc)	B_0 1000	100	10	1	1×10^{-1}	1×10^{-2}	1×10^{-3}	1×10^{-4}	1×10^{-5}
360.0	−2.566	−2.566	−2.558	−2.478	−2.272	−1.959	−1.519	−1.205	−0.866
121.0	−2.561	−2.561	−2.553	−2.464	−2.212	−1.818	−1.324	−0.967	−0.562
55.2	−2.547	−2.547	−2.538	−2.428	−2.131	−1.666	−1.096	−0.686	−0.239
18.2	−2.460	−2.460	−2.428	−2.276	−1.914	−1.341	−0.614	−0.094	0.444
9.68	−2.339	−2.328	−2.241	−2.051	−1.672	−1.041	−0.208	0.396	0.978
3.60	−1.812	−1.721	−1.569	−1.322	−0.924	−0.300	0.622	1.253	1.837
0.595	−0.383	−0.248	−0.060	0.196	0.607	1.246	2.179	2.813	3.397

could have been reasonably expected, many of the unusual features of the research technique can be attributed to him.

Dr. S. Q. Duntley, Section Technical Aide, and the members of the Section, especially Professor Edwin G. Boring, contributed invaluable professional advice to the general conduct of the research.

The professional staff employed temporarily by the Tiffany Foundation to conduct the research program varied considerably during the period of experimentation. Without exception, members of the staff devoted themselves diligently to the progress of the program. Special acknowledgment must be made to Dr. Helen M. Richardson for her earnest and often inspired work with the psychophysical aspects of the program, and to Mr. William F. Little of the Electrical Testing Laboratories, New York, with whose aid the photometric procedures were developed.

Of the many assistants, without whom the program would have been impossible, special mention should be made of Mr. B. S. Pritchard,

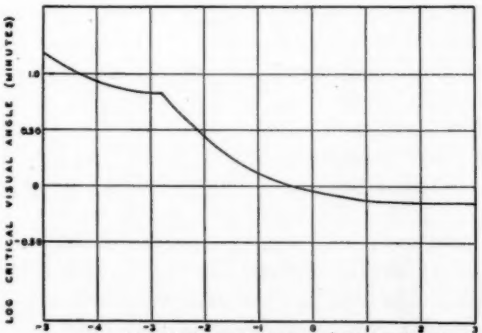

FIG. 17. "Critical visual angle" as a function of adaptation brightness. The area under the curve represents "point sources."

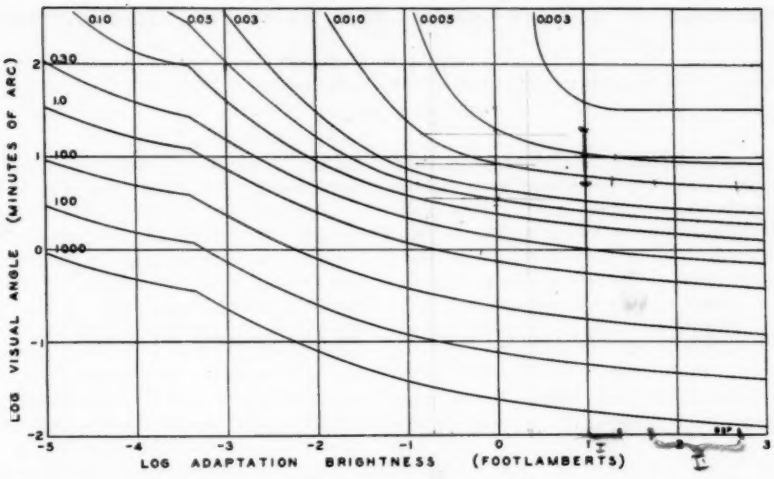

FIG. 18. Interpolations from Figs. 15 and 16. The relation between stimulus area and adaptation brightness for stimuli of various contrasts.

Mrs. S. C. Taplin, Miss M. J. Bernstein, Miss I. T. Bell, and Miss Jane Tapley.

Although not present during the conduct of the experiments reported herein, Dr. Helen Peak, Mr. Carl Foss, and Dr. Parry Moon were instrumental in designing the experimental apparatus and procedures for the earliest experiments. Some of the original apparatus and procedures were utilized in the reported experiments, whereas others were adapted.

SUMMARY

Experimental data are presented representing approximately 450,000 responses made by trained observers under laboratory conditions. Contrast thresholds are presented for stimuli brighter and darker than their background, and for two values of stimulus exposure. In each case, wide variations were studied in the parameters: stimulus contrast, stimulus area, and adaptation brightness.

JOURNAL OF THE OPTICAL SOCIETY OF AMERICA VOLUME 36, NUMBER 11 NOVEMBER, 1946

Direct Determination of Wave-Lengths from Fabry-Perot Interferometer Patterns

GEORGE R. HARRISON
George Eastman Research Laboratory of Physics, Massachusetts Institute of Technology, Cambridge, Massachusetts
(Received August 19, 1946)

A new type of measuring and computing engine has been constructed which determines wave-lengths and wave numbers directly from spectrograms made by crossing the dispersion of a Fabry-Perot interferometer with that of a concave diffraction grating. The wave-length of a spectrum line is first determined to six figures from the grating dispersion by the method used in the author's automatic comparator, and this wave-length is then converted to wave number by a mechanical continuous-function computing arrangement. The thickness of the etalon separator used having been pre-set into the machine, all wave-lengths are automatically divided into twice this thickness to give on dials the order of interference corresponding to the instantaneous wave-length setting of the comparator. The interference pattern of each spectrum line is projected on a screen in front of the operator with a magnification proportional to the square root of the order of interference, and falls on a set of parabolic fiducial lines drawn to fit the optical system used to project the interference fringes on the slit of the grating spectrograph. The operator moves the screen carrying these parabolic lines up or down until they coincide with the density maxima of the interference pattern; the partial order of interference ϵ in the center of the pattern can then be read to three figures from a dial. By turning the plate control handle of the machine slightly the operator then makes the ϵ reading of the machine coincide with that of this dial; cams having introduced corrections for the dispersion of air and the variation of phase change with wave-length, the dials then give the wave-length and wave number of the line correctly to seven or eight figures, depending on its sharpness. The speed of reduction of Fabry-Perot patterns is by this means increased at least 20-fold over that of previous methods, and the precision of setting appears to be considerably improved also. Repeat readings on sharp lines are found consistent to within a few ten-thousandths of an angstrom. The precision of the wave-length values obtained is limited principally by the diffuseness of the interference pattern arising from the breadth of a line.

Improvements now under development include automatic photoelectric scanning of interferometer patterns, and the direct recording by an electric typewriter of eight-figure wave-length and wave-number values for each line. The new device is being used to determine standard wave-lengths needed for the more effective utilization of the original automatic comparator.

1. INTRODUCTION

ALL wave-lengths in the ultraviolet, visible, and infra-red regions are measured in terms of the international primary standard, the cadmium red line whose wave-length is defined as 6438.4696A. As an intermediate step in the determination of wave-lengths with a diffraction grating, international secondary wave-length standards, measured with the Fabry-Perot interferometer, are commonly used. To be eligible for status as an international secondary standard a spectrum line must have been measured independently in at least three laboratories, with an uncertainty in the final mean not greater than 0.001A.

Since the adoption of the international wave-length scale fewer than 400 spectrum lines have been defined as international secondary standards, most of these being in the spectrum of the international iron arc or those of discharge tubes containing neon or krypton. The gas lines, while sharp, are few in number, and the iron standard lines are inadequate for the purposes of present day spectroscopy, for they are diffuse and distributed unevenly through the spectrum.

In the extensive series of wave-length measurements made with the automatic comparator,[1] which resulted in the publication of the *Massachusetts Institute of Technology Wavelength Tables*,[2] the most serious limitation on precision was found to arise from the lack of satisfactory standard lines. Measurements on lines in such complex spectra as cerium and thorium, for example, showed much better internal consistency than did those on the iron standards themselves.

The paucity of wave-length standards has resulted principally from the difficulty of making measurements with the Fabry-Perot interferometer, not so much because of the delicacy of adjustment and control required for its proper use, as because of the tedious and involved computations needed to determine wave-length val-

[1] G. R. Harrison, J. Opt. Soc. Am. **25**, 6 (1935); Rev. Sci. Inst. **9**, 15 (1938); G. R. Harrison and J. P. Molnar, J. Opt. Soc. Am. **30**, 343 (1940).
[2] *M.I.T. Wavelength Tables* edited by G. R. Harrison (John Wiley and Sons, Inc., New York, 1939).

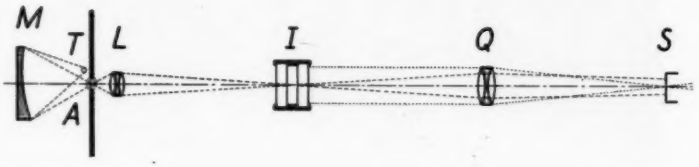

FIG. 1. Optical system used for projecting Fabry-Perot etalon fringes on the slit of a stigmatic grating spectrograph. Quartz-fluorite achromat Q focuses on the slit the fringes formed at infinity, and at the same time focuses the interferometer aperture on the collimator mirror of the spectrograph.

ues once the interferometer patterns have been measured.

To assist in remedying this situation a machine has been designed which makes possible the rapid determination of wave-lengths for use as standards in complex spectra. While it is not yet complete in the fully automatic form which it is expected to attain ultimately, in its present form it completely eliminates the necessity of making computations when determining wave-lengths from Fabry-Perot patterns, once the etalon thickness and the phase-change variation have been determined and set into the machine. Several settings can be made on an interferometer pattern in less than one minute, and the machine then gives a direct reading of wave-length in air and wave number in vacuum, corresponding to the average setting. The system of setting used appears more reproducible than that involved in ordinary comparator setting. Errors in computation are eliminated, while those due to improper setting are immediately made apparent to the operator because the relationships among the various factors in the interference formula are obvious while he is operating the machine.

2. PREPARATION OF FABRY-PEROT SPECTROGRAMS

The theory of the adjustment and use of the Fabry-Perot interferometer has recently been discussed by Meissner.[3] Interference patterns are produced by splitting an incoming beam of light into a dozen or more beams by means of two partially reflecting surfaces held parallel and a fixed distance apart by means of an etalon spacer. The thicker the spacer the greater the order of interference between the beams, and if an etalon having a thickness t lying between 5 mm and 25 mm is used, orders of intereference of not less than 14,000 and not more than 125,000 are obtained in the visible spectrum. By proper control of the reflectivities of the interferometer surfaces resolving powers in excess of one million are readily obtained.

Since it was desired to measure spectrum lines lying anywhere in the range 2000 to 10,000A, quartz interferometer plates were used. Several sets of these were available in diameters of 25 mm, 37 mm, and 60 mm. Several fused quartz plates were tried but were found insufficiently homogeneous for interferometer use, and all plates finally selected were made of crystal quartz, cut perpendicular to the axis with at least one surface on each plane to 1/25th wave. All plates were coated with aluminum by evaporation, until each showed transmission in the visible of about 11 percent.

Fused quartz ring separators were used, made according to the design of Meissner, with optically flat rather than rounded bosses at the contact points. It was found that an interferometer provided with this sort of separator would remain in constant adjustment for many days when held in a mount of the type recommended by Meissner.

Since the orders of interference are very close together in a Fabry-Perot pattern, it is customary to cross the dispersion of this interferometer with that of a prism or grating spectrograph, usually by focusing the interferometer patterns on the entrance slit of the spectrograph. The optical system used in preparing the spectrograms discussed in the present paper is shown in Fig. 1.

Light from a standard source T, consisting usually of a neon or krypton discharge tube, was focused with an aluminized concave mirror

[3] K. W. Meissner, J. Opt. Soc. Am. **31**, 405 (1941).

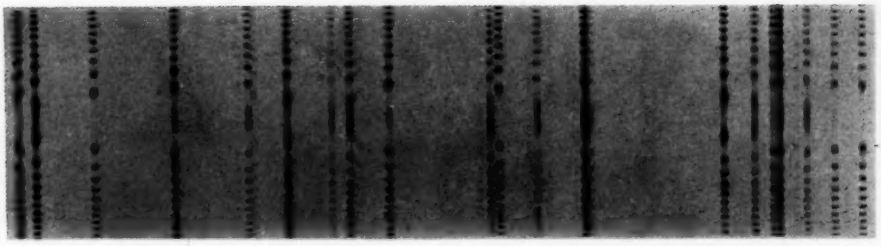

FIG. 2. Portion of a typical interference spectrogram of iron and neon.

M of 10-cm diameter and 20-cm radius of curvature on the center of the arc stream of a Pfund-type arc A. Light from both sources was then focused on the interferometer by means of the fairly achromatic lens L, and was again focused on the collimator of the spectrograph by the quartz-fluorite achromat Q. This lens of 50-mm diameter and 500-mm focal length also focused the rings of the interference pattern on the slit S of the spectrograph. The variation in focal length of Q was found to be less than 2 mm between 2000 and 7000A, and it was refocused for each 1500A region covered on a single 20-inch plate. The grating spectrograph was refocused in each region to improve the sharpness of horizontal lines as compared with the usual vertical spectrum lines.

The Fabry-Perot interferometer was fitted into an evacuated thermostated chamber which could be filled to any desired low pressure with purified gases. In the routine determination of wave-lengths it is planned to work usually with the interferometer in vacuum, since the vacuum wave number of each line is what is desired in theoretical investigations.

Figure 2 shows a portion of a typical interference spectrogram, the horizontal dispersion of 3.2A/mm having been produced by a 35-ft. 15,000 line-per-inch aluminum-on-glass concave grating in a Wadsworth mounting, and the vertical dispersion being that of a Fabry-Perot interferometer with 10-mm etalon separation.

3. REDUCTION OF INTERFEROMETER PATTERNS

The usual methods of determining wave-lengths from Fabry-Perot interferometer patterns involve determining the order of interference of the center of the ring system, of which only a diametral portion passes through the spectrograph slit. The formula commonly used is

$$P = P_0 + \epsilon = \frac{2t}{\lambda} + \frac{2t \cdot d^2}{\lambda \cdot 8f^2},$$

where P is the order of interference at the center of the pattern, t is the thickness of the etalon separator, λ is the wave-length of the line, d is the diameter of an interference ring maximum, and f is the focal length of the lens used to form the image of the interference pattern on the slit of the spectrograph. $P_0 = 2t/\lambda$ is the integral order of interference at the position of the first maximum measured by d.

The usual method of reducing such patterns is to measure with a comparator the diameters d of three or more successive rings and then calculate the squares of these diameters and the differences between these squares.[4] Root mean square methods are than used to determine the value of ϵ, the partial order of interference at the center. Meissner[3] discusses the various methods of calculating wave-lengths from such patterns, all of which involve somewhat laborious calculations. The thickness t of the etalon is determined from the primary standard line, or from well-known and sharp secondary standards.

It is found that the wave-lengths for a given line obtained with different etalon spacers will vary with t, and it is necessary to introduce a small correction for phase change on reflection which varies with wave-length by amounts which depend on the character of the reflecting surface used. The variation of this correction for silvered or aluminized plates may be as great as

[4] For a special comparator which reads directly the squares of fringe diameters, see K. Burns, J. Opt. Soc. Am. and R.S.I., 19, 250 (1929).

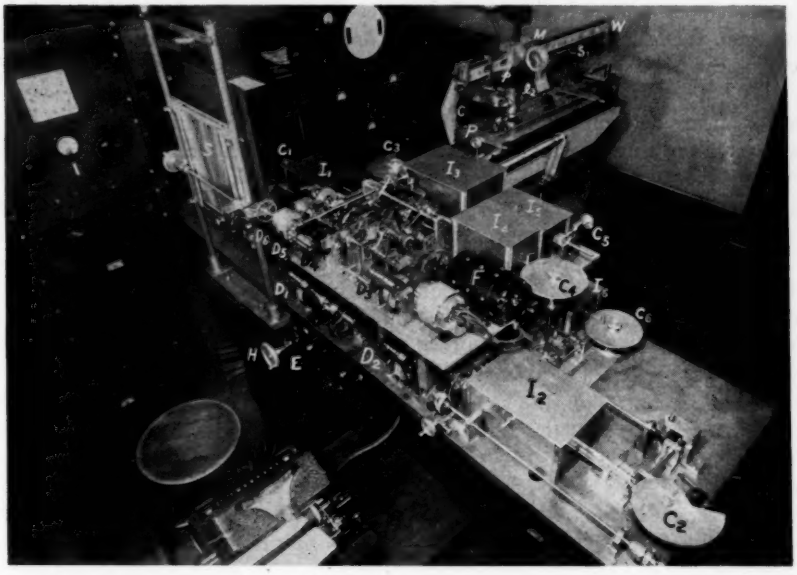

FIG. 3. Oblique photograph of the machine, known as WINMAC (wave-length interferometric measurement and computation), with which wave-lengths and wave numbers can be determined directly from Fabry-Perot spectrograms.

0.010A per 1000A. Corrections depending on the pressure and temperature of the air in the interferometer at the time the exposure was made may also be needed. When orthodox methods of reduction are used, numerous routine calculations are required before a single correct wave-length value can be determined, and it was with the purpose of improving this situation that the machine to be described was devised.

4. DIRECT DETERMINATION OF WAVE-LENGTHS

A photograph of the machine in its present form is shown in Fig. 3.* The comparator carriage will hold two plates of length up to 25 in., either of which can be racked into scanning position. The plates are held with their emulsion sides up, against a fixed stop. One end of the plate to be measured is accurately centered on fiducial marks on the projection screen, and the other end is centered by means of a fixed microscope m, set on "absorption" marks impressed on each plate during exposure in the spectrograph by means of a quartz fiber stretched across the slit. By means of gears, variable speed units, and appropriate wave-length cams cut for each of the spectral regions covered by a single plate setting (1500A), the wave-length dial D_1 is made to read λ to eight figures when a line is set on a fiducial mark, though only the first six figures are likely to be correct at this stage of the measurement. This precision is sufficient, however, to determine the wave number σ to six figures on dial D_2, and in turn, by multiplying σ by $2t$ (set into decimal gears G and an integrator unit I_5 to eight figures) to obtain P_0, the integral order of interference, on dial D_4, to the five figures needed to determine it uniquely.

The comparator screw is turned by motor E or handle H until a standard spectrum line is centered on a fixed horizontal cross line on screen S, and the wave-length λ, wave number σ, and integral order number P_0 dials are set to give correct readings for this line. The plate is then advanced until the image of the next line

* To distinguish this apparatus from the automatic comparator which measures grating wave-lengths directly, the latter is called in the laboratory the WAMAC (wave-length automatic measurement and computation, pronounced waymac), while the new device is called WINMAC (wave-length interferometric measurement and computation).

pattern is accurately set on the horizontal cross line on the screeen. Wave-length, wave number, and order values can then be read correctly to five figures.

The operator next determines the partial order of interference ϵ to three figures by turning a handle which raises or lowers screen S, on which is plotted a group of parabolic reference lines, until these coincide with the maxima of the interference pattern which is projected on it with suitable magnification. This magnification is controlled automatically to three figure precision. ϵ appears on dial D_6 which is next to a similar dial D_5 also reading ϵ, but driven from the main wave-length control of the machine. The operator now need only turn the main control handle H slightly to adjust the two ϵ readings to coincidence, and the wave-length and wave-number counters will then read λ and σ correct to eight figures if the precision of setting of ϵ has justified this. Five figures have come from the grating dispersion, and three figures more from the interferometer pattern.

5. THE DETERMINATION OF ϵ

A typical interference pattern for a spectrum line, as projected on a set of parabolic fiducial lines, is shown in Fig. 4. It is desired to determine the value of ϵ, the partial order of interference at the center of the pattern, with precision as close as possible to 1 part in 1000. Since we need determine ϵ to only three digits, mechano-optical computation methods can readily be used.

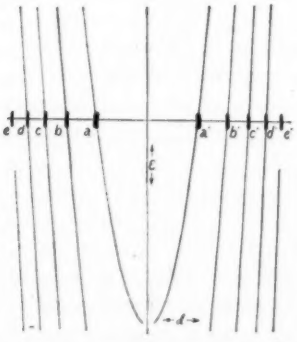

FIG. 4. Appearance of a set of interference fringes (Ne λ6217) on the screen in front of the operator, after he has made a setting of the parabolic fiducial lines on fringes a, b, c', and d'. Owing to distortion of the image produced by an unsatisfactory projecting lens the other fringes are improperly located. A lens was later procured and tested which showed less distortion than 0.1 percent.

The optical system used for projecting the interferometer pattern on the parabola screen is shown in Fig. 5. Light from a 6-volt lamp L operated from a storage battery is collimated by a condensing lens l_1, through the plate P being measured, and lens l_2 of 6-in. focal length images the interference pattern on the screen S in front of the operator. The light is doubly reflected by a triple mirror M, which displaces the return beam to avoid interference with the right-angle prism p, and renders the projected beam insensitive to small amounts of tilting of M. In order to provide variation of magnification between 10 and 20 diameters, mirror M is moved a distance of 30 in. along carefully smoothed ways W. The projection lens l_2 is moved with a cam so as to give a sharply focused image at any setting of M. During the entire excursion of mirror M the center of the interferometer pattern imaged on the screen should move not more than a few thousandths of an inch in any direction. The mirror carriage is mounted on ball-bearing rollers and is moved by a screw having 24 threads per inch (S_1 in Fig. 3).

To facilitate centering of the patterns at all magnifications, mirror M can be moved from one end of its track to another in a few seconds by electric motor. Thus the point of invariant projection can quickly be located on the screen, and the parabola system centered on it. The screw which moves mirror M is then connected to the P_0 shaft on the machine by flexible cable C, through a cam-integrator combination which keeps the mirror at the proper position to give the correct magnification at any plate setting. Thus all patterns are projected on the screen to the same dimensions to within 0.001 order.

The projection screen was prepared by first determining the constants in the formula, thrown into the form

$$\epsilon/D^2 = P_0/8f^2m^2.$$

Here D is the diameter of a ring on the screen projected with magnification m from its original diameter d on the slit of the spectrograph. If m is made to vary with $(P_0)^{\frac{1}{2}}$, the fraction remains constant, and one set of parabolic lines will serve for all patterns on the plate, or on any

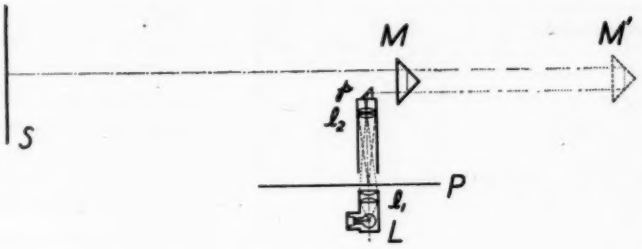

FIG. 5. Variable-magnification projection system used to form on the screen an enlarged image of the interference patterns so that they are always on the same scale of ϵ *vs.* d, no matter by what wave-length produced.

other plate photographed under identical conditions. The broken parabola results from plotting D as abscissa against ϵ as a periodic ordinate ranging from 0 to 1 across each of 4 or 5 successive rings.

Correction for the deviation of magnification, and hence of mirror motion, from linearity with P_0, owing (1) to the square root relationship, (2) to the motion of lens l_2, and (3) to the variation with wave-length of the magnification of the grating spectrograph and of the "achromatic" lens Q, is introduced by properly shaping the cam which controls the variable-speed drive of the mirror screw from the P_0 shaft.

Since the triple mirror M is arranged to permit magnifications of between 10 and 20, and $m \propto (P_0)^{\frac{1}{2}}$, it is possible with one set of parabolic lines to cover a fourfold range of orders. With the gears now used the machine will reduce spectra involving orders from the 22,000th to the 88,000th, but this range can readily be extended in either direction by provision of new gears or a new parabola system.

The parabolic lines were carefully plotted on a 10×12-in. sheet of glass coated thinly with an opaque lacquer, using a small comparator to move the engraving tool horizontally with D, and the actual rack and pinion vertical motion of the machine for varying ϵ in accordance with the reading of its dial. Every precaution was taken to insure that the parabola system was correct to one-thousandth of an order. It was copied photographically by contact printing on contrast process plates, and a black line copy was mounted face inward against a sheet of waxed drafting paper to serve as a screen, which was then covered on the reverse side with a piece of clear glass. The whole was then mounted, with adjusting screws to permit accurate alignment, in the screen frame F of the measuring engine.

This frame could be moved ten inches vertically between accurate ways by turning the handle controlling ϵ, and its motion was communicated through gears to dial D_6, which was engraved with 100 divisions, so that ϵ could be readily estimated to one part in a thousand. If desired, settings can be made independently on each of ten interference maxima projected on the screen, and the resulting ten ϵ values can be averaged, or all settings can be made more or less simultaneously and an average value of ϵ determined.

The use of parabolic fiducial lines not only eliminates the necessity of calculating ϵ, but makes more nearly equivalent the results obtained from the broad central maxima and the outer narrower but closer maxima, since with the broad inner orders the slope of the parabola changes more rapidly than with the outer. Extensive measurements show that extremely sharp interference maxima, as obtained with krypton lines, can be set on repeatedly with a consistency of ± 0.001 order.

6. MECHANICAL COMPUTATION OF WAVE-LENGTHS AND WAVE NUMBERS

Various methods of mechanical and electrical computation were considered. Since eight-figure precision at high speed was desired, the use of electronic digital computation seemed indicated. The measuring function of the engine involves continuous motion, however, and since the necessary transfer from mechanical measurement to electrical computation would involve additional complexity, it was decided to adopt a continuous-function computing system in which the necessary precision was attained by periodically using automatic justification. Thus eight-figure precision was to be attained by combining two steps, each capable of better

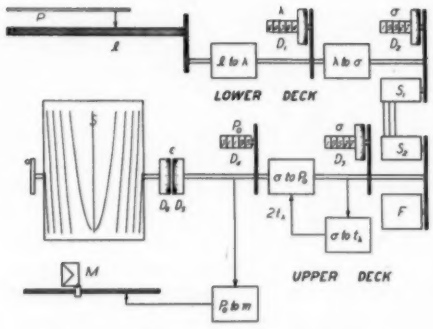

FIG. 6. Block diagram of the mechanical parts of WINMAC. The various rectangles marked with conversions indicate units of which a simplified version is shown in Fig. 7.

than four-figure precision, and suitably linking these.

The mechanical system, shown in block diagram in Fig. 6, contains the following parts, all basically similar, one of which is depicted in simplified form in Fig. 7:

(1) The connection between distance l along the plate, and wave-length λ. On account of the slowly varying dispersion of the grating this is conveniently made up of a linear portion obtained by setting the first two figures of dispersion by means of decimal gears, and a variable portion obtained by means of an integrator unit, controlled by a cam suitably cut for each of the spectral regions covered by a single plate, and feeding in through a differential d. Six-figure precision in λ is desired.

(2) The connection between wave-length λ and wave number σ. This relationship is hyperbolic, with a small additional term to introduce the correction of wave number from air to vacuum. This too was divided into a linear portion (see Figs. 7 and 8) given directly by gears, and a non-linear remainder. Since this relationship sets the most difficult mechanical problem presented in the design of the engine, it is discussed further below. Eight-figure precision is needed.

(3) The connection between wave number σ and order of interference P. Eight-figure precision is needed here, but can easily be obtained, as the deviations from linearity are very small. Four banks of decimal gears give the first four figures of t, the etalon thickness, and an integrator unit I_5 on the upper deck gives the last four figures. These can be altered continuously with wave-length by means of cam C_5 to introduce the phase-change variation, which can be treated as a small change in t, which is therefore labeled t_λ in Fig. 6.

The spectrum to be covered was divided into regions 1500A long, each of which could be photographed on a 20-in. plate. Since it was desired to have some overlap, standard regions were set up as follows: 2000 to 3500A, 3000 to 4500A, etc. All cams with the exception of the magnification cam were cut to cover a 1500A region; cam C_3 covers the entire range of P_0 from 22,000 to 88,000.

Because of the limited torque load which can be put on an integrator it was necessary to introduce torque amplification between σ and P_0, and a General Electric selsyn transmitter and receiver with amplidyne control were used. Selsyn transmitter S_1 is driven at the σ_1 dial D_2 at a speed of 2σ, and its receiver S_2 is geared to another σ dial D_3 on the upper deck, so that the entire later load is driven by a selsyn-controlled motor F. The two σ dials are found to remain in step at all accelerations needed, and to hold together accurately to 1/700 revolution, which corresponds to 0.0014 cm^{-1}.

All rotating parts of the machine are mounted on ball bearings. Integrator and differential units are of the type built by the Ford Instrument Company for Navy computers. Backlash was kept to a minimum by using maximum allowable shaft speeds, but is not compensated for, since in its full-automatic form all parts of the machine will move continuously forward, and in

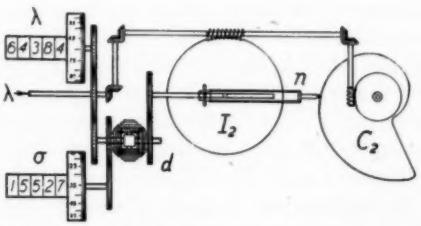

FIG. 7. Simplified sketch of non-linear conversion unit (in this case from wave-length λ to wave number σ). A linear portion of the $\lambda-\sigma$ relation goes directly through gears; the non-linear remainder is controlled by a cam which provides the proper instantaneous speed ratio from an integrator unit through a differential.

hand operation backlash can readily be taken care of.

The connection between the dials which read wave-length and wave number afforded the most difficult mechanical problem, since it was desired to have the σ dial read continuously in terms of λ to 1 part in 10^8. This would not be difficult with an almost linear system, but where the relationship is hyperbolic great difficulties arise. The variable-ratio integrator unit I_2 was provided with a cam C_2 to give the hyperbolic relationship, but the best such units available cannot be relied upon to more than four figures. The method adopted was to divide the relation between λ and σ into: (1) a linear portion for each spectrum range, marked A in Fig. 8, which could be controlled by means of gears to eight-figure precision; (2) a non-linear remainder, B, which was usually not more than one-third of the total variation, fed through integrator I_2 and controlled by cam C_2. An integrator unit of the type which can pass through zero without undue error or wear was used, and was found to repeat in either of the two directions to one part in 20,000. Thus by the combination of A and B, integrator readings reliable to at least one part in 60,000 could be obtained. The remaining precision is introduced by a justifying system which comes into action periodically before the maximum tolerable error has been accumulated.

It was desired to have all measurements reliable to better than 0.001A, and the natural limit of mechanical precision of the machine as now constructed is found to be about 0.0003A. The 1500A interval of any region can be thought of as consisting of 5,000,000 units each 0.0003A long. The integrator can then be run uncorrected over a wave-length range of $60{,}000 \times 0.0003$A, or 18A. To give a large factor of safety it was decided to justify the machine every 3A, or 500 times per plate.

In the final form of the machine it is planned that the λ and σ dials will be compared automatically by photoelectric means every 3A, any necessary correction then being automatically put in without stopping the machine. A small mirror on the λ shaft, reflecting light from a lamp flashed on by a contactor which closes a circuit once every 3A, will throw a beam of light on the slit of a photo-cell whenever the λ dial reads an integral multiple of 3.0000A. A disk on the σ shaft is pierced with small holes through which a beam of light falls on another photo-cell. A second disk close to the first, running at 1 revolution per 1500A, has in it 500 pairs of holes whose positions give the correct last digits of the wave number values for the 500 λ values at which automatic checking is to be made. Thus a σ pulse is obtained for each λ pulse; if the former arrives before the latter, a positive correction of the necessary magnitude will be put in by a small motor operating from a time expander circuit; when the opposite is true, a negative correction will be made.

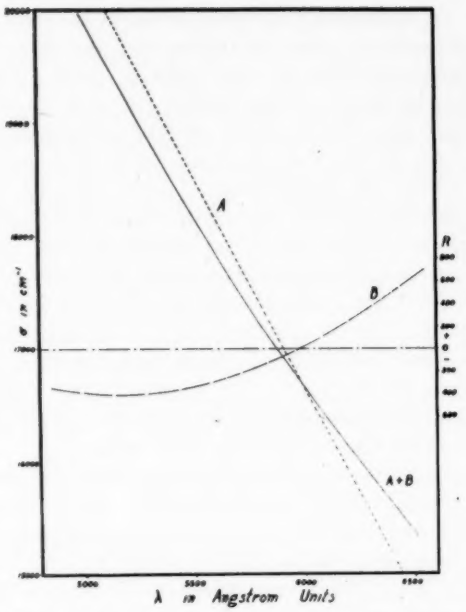

FIG. 8. Curve $A+B$ gives the relation between wave-length λ and wave number σ in the range 6500–5000A. Curve A shows a linear approximation to this, obtained through a gear train and chosen so as to leave a minimum non-linear residue involving only one change in sign. Curve B shows the remainder, fed in through a unit of the type shown in Fig. 7.

In the absence of this refinement, the operator merely makes an extra setting just before reaching the center of each line at some λ reading whose last three digits are 0, and adjusts the last σ dial to the proper digit as given by Kayser's *Tabelle*,[5] if this proves necessary.

[5] H. Kayser, *Tabelle der Schwingunszahlen* (S. Hirzel, Leipzig, 1925; revised edition J. W. Edwards, Ann Arbor, 1944).

In determining the gear ratios to be used in designing a machine of this sort it is necessary to compromise between the desire to obtain precision by using a large number of turns of each shaft per unit measured, and the limitations on speed of rotation consistent with reasonable rapidity of measurement. Care must also be taken to see that the accelerations used do not impose undue torques on the integrators, and that the upper deck drive motor can follow.

The λ and σ dials D_1, D_2, and D_3 each consist of five counter dials connected to 4-in. dials engraved with 100 divisions, which turn with the drive shafts. One thousandth of a revolution can be estimated quite readily, which corresponds to 0.0001A in λ, and 0.001 cm^{-1} in σ.

Though the wave-length and wave number dials can be read to eight figures, variable friction and elasticity give rise to variations in setting which cannot now readily be kept to less than 0.0003A. Improvements in the selsyn controls, and increases in certain shaft speeds relative to the output dials, would make greater precision possible if needed.

Whether the spectrograms being measured are made with the interferometer operated in air or in vacuum, the end products desired are wave numbers in vacuum and wave-lengths in air. The former is the more fundamental of the two quantities, and to subject the wave-lengths rather than the wave numbers to the uncertainties in the index of refraction of air it seemed desirable to operate the interferometer in vacuum whenever possible.

When the interferometer is operated in vacuum, P_{vac} is obtained directly on the machine, and when in air P_{air}. To three figures these two are identical, so either will serve to operate the magnification control. To obtain σ_{vac} and λ_{air}, which are the quantities wanted, however, it is necessary to be able to convert from either P_{vac} or P_{air}. Therefore cam C_2 is made to convert λ_{air} into σ_{vac}. A special integrator I_4 with cam C_4 is then provided for σ_{vac} to σ_{air}. When plates taken with the interferometer in vacuum are being measured, C_4 is circular. When plates taken in air are measured, the conversion is $P_{air} \rightarrow \sigma_{air} \rightarrow \sigma_{vac} \rightarrow \lambda_{air}$, while for vacuum plates it is $P_{vac} \rightarrow \sigma_{vac} \rightarrow \lambda_{air}$. The fact that the spectrograph is operated in air affects only cam C_1, which need only give λ_{air}.

TABLE I. Plate 43.
$2t = 2.00851596 \pm .00000005$ cm.

Wave-length	ϵ_S	ϵ_M	ϵ_N	ϵ_H	ϵ_1	ϵ_2
6382.9914	.688	.679	.687	.693	.691	.693
6334.4279	.930	.930	.930	.930	.930	.922
6304.7892	.988	.993	.990	.986	.977	.988
6266.4950	.665	—	—	.668	.670	.662
6217.2813	.374	.371	.373	.374	.374	.366
6163.5939	.767	—	—	.766	.760	.770
6096.1630	.215	.234	.224	.224	.226	.223
6074.3377	.596	.592	.596	.600	.588	.597
6029.9971	.738	—	—	.739	.749	.731
5975.5340	.326	—	—	.326	.318	.330
5944.8342	.904	.910	.906	.904	.916	.905
5881.8950	.430	.425	.427	.429	.432	.424
5852.4878	.011	.002	.006	.016	.026	.015

7. PRECISION OF SETTING

Professor K. W. Meissner kindly spent several weeks in our laboratory giving us the benefit of his technical skill in the adjustment of interferometers and in taking spectrograms with them. Many exposures were made by him with our apparatus, using his own interferometers and ours, and a number of the resulting spectrograms have been measured, both in the orthodox manner and by means of the new machine.

An indication of the precision of determining ϵ by various methods is given in Table I. The first column gives the accepted wave-lengths of the neon international secondary standard lines used for testing. The etalon thickness $2t$ was carefully determined by two independent observers from the same plate, one using repeated measurements on a single sharp line, and the other using all the lines listed and averaging the results, which were very consistent with the first determination. The second column gives ϵ, the fractional order, as calculated from the accepted wave-length with the value of $2t$ given. The third column gives ϵ as found by Meissner on measuring the plate in the usual way. The fourth column gives ϵ as determined by an inexperienced observer using the machine, setting on each of ten maxima and averaging for each line. The fifth column gives similar determinations by another observer, after the plate had been taken from the machine and set up again some weeks later. The sixth column gives the

results of a single setting on each pattern, eight or ten maxima being encompassed simultaneously. The last column gives the results of settings made by grouping four or five maxima on one side of the pattern in one setting, then setting on the opposite equivalent group, and averaging the two settings. The values in the last four columns involve single settings; Meissner's values, on the other hand, involve four settings on each maximum.

Experience indicates that the most consistent results are obtained by making settings on eight or ten maxima and averaging these. Such values require a total of about 50 seconds to determine. On the other hand, values of the type listed in column ϵ_2 are a close second in precision, and these require only twenty seconds each. Values obtained by orthodox methods require at least 30 minutes each, and even when made by an observer of unsurpassed skill and experience show no superiority to values obtained with the machine.

Such results indicate the desirability of including several maxima in one parabola setting, but of making at least one setting on each side of the pattern to take care of imperfect centering of the plate. Three sets of such settings on one pattern can readily be made in one minute, and give results more precise than those obtained by any other type of setting made in an equal time. An ϵ value obtained in this way is ordinarily good to within 0.002 order, except for the broadest lines. In the spectral region included in Table I, under the conditions used, 0.002 order corresponds to 1 part in 15 million, or about 0.0004A. Nearly twice this precision of wave-length setting was obtained by using a 16-mm etalon and the same neon lines.

The precision of the remainder of the machine can be made to match this. Some difficulties have arisen from irregular commutator motion in the drive motor on the upper deck when slow settings are made, but this can be improved by substituting a motor of higher speed and gearing it down further, and can be expected to diminish greatly when automatic settings are made without stopping the machine.

8. PLANNED IMPROVEMENTS

The precision of wave-length measurements with the computing engine is at present limited in most cases by the diffuseness of the interference maxima resulting from the breadth of the spectrum lines studied. It appears probable that electrical scanning with a "maximum-picker" similar to that used for narrow spectrum lines in the original automatic comparator[1] would improve the precision of setting considerably. A scanning mirror has been designed which moves the pattern with variable speed across a slit in such a way as to scan a constant number of fringes per second, except in the center of the pattern, and preliminary tests show excellent reproducibility. Such scanning appears to eliminate the effect of the varying widths and separations of the different orders and their asymmetry, since the pattern is scanned at a rate proportional to the dispersion at a given point. Ten maxima per second can be located in this manner, the results appearing as flashes of a stroboscopically illuminated revolving slit on a phosphorescent screen, so that 20 or 30 ϵ values for a given pattern should pile up on the screen while a reading is being made. The average value of ϵ should then be obtainable directly from the screen by selecting the center of gravity of the phosphorescent spot. Other scanning methods have been suggested and will be investigated.

A second contemplated improvement is the use of an electromatic typewriter to record the readings of the λ- and σ-dials. A memory system is being arranged for the output of these dials so that the comparator carriage can continue to the next line while the typewriter is recording the wave-length and wave number of a preceding line. It seems probable that the machine can be made entirely automatic in its operation, so as to scan each line without pausing, while recording data on the previous line.

It is planned with the present hand-operated model of the machine to determine working standards in the spectra of a number of elements having complex spectra. These standards can then be used in making spectrograms directly with concave gratings, of the type to be reduced with the original automatic comparator.

It is a pleasure to acknowledge the able assistance of Dr. Karl W. Meissner in improving the adjustment and use of our Fabry-Perot interferometers; of Mr. Frederick Bates and Dr. I. C. Gardner of the National Bureau of Standards in the procurement of suitable interferometer plates; of Dr. J. Rand McNally, Jr., in laying out and checking cams; and of Kenneth B. Newbound, Thomas C. Furnas, and James C. Anderson in making numerous tests of the engine and in setting up its electrical system. Its excellent mechanical performance results from the careful workmanship of Carl G. Selig and William Conly.

JOURNAL OF THE OPTICAL SOCIETY OF AMERICA VOLUME 36, NUMBER 11 NOVEMBER, 1946

Interference in Thin Parallel Surfaced Transparent Plates as a Source of Error in Spectroquantitative Analysis

JOSHUA STERN
U. S. Naval Engineering Experiment Station, Annapolis, Maryland
(Received August 30, 1946)

INTRODUCTION

MANY commercial spectrographs, both grating and prism instruments, use flat quartz windows to protect the delicate slit mechanism from dust and mechanical injury. Flat plates are also used in spectroscopy in the form of ruled fixed slits and neutral absorbing films. Although interference effects in thin plates are well known, the writer has been unable to find any reference to the possibility of error in spectrochemical analysis from this source and the manufacturers of instruments using plane protective windows seem to be unaware of the phenomena. It therefore seems desirable to describe these interference effects and to analyze the errors derivable therefrom, especially, since, once aware of the presence of interference, the elimination or avoidance of the errors becomes a simple matter.

ORIGIN AND NATURE OF THE INTERFERENCE EFFECTS

General Application

If light is normally incident upon a transparent plate bounded by plane surfaces, a percentage of the incident light will be reflected from each surface. Under certain conditions, the phase relationships between the two reflected rays will be such that destructive interference will take place. Since the interference is to take place between a ray reflected from the front surface and another which has traversed twice the thickness of the plate, the conditions for interference will be:

$$x\lambda = 2nd \qquad (1)$$

in which equation:

x = an integer,
λ = wave-length,
n = refractive index (which will vary with wave-length),
d = thickness of the plate.

It is seen from the equation that a quarter wave-length change in the thickness, d, of the plate will produce the conditions necessary for reinforcement of the reflected rays. When conditions are right for interference, the resulting total reflectance will be a minimum and the transmittance, therefore, a maximum. When conditions are right for reinforcement of the reflected rays, the total reflectance will be a maximum and the reflected light will be lost, resulting in minimum transmittance. It is clear that the transmittance of the thin plate for light of any wave-length will be a function of the wave-length.

In order to determine the maximum variation in transmittance which can occur, it is necessary to determine the intensities of the reflected rays from the front and back surfaces. The following is a demonstration, by the method of Stokes,[1] that the intensity of the ray reflected from the

[1] Wood, *Physical Optics*, p. 193.

front surface is equivalent to the total intensity of the rays reflected from the back surface (account being taken of the multiple internal reflections).

In the diagram, Fig. 1, AB represents the ray incident on the front surface, BC the ray reflected from the front surface, and BD the ray refracted into the transparent plate.

If the intensity of the incident ray is designated: (a), the intensity of the reflected ray will be ab; (b), being the fraction reflected, and the intensity of the refracted ray will be ac; (c), being the fraction refracted.

The principle of optics that reversing the rays must produce the original ray is applied with the following results.

BC reversed will produce a reflected ray along AB of intensity ab^2 and a refracted ray along BE of intensity abc.

BD reversed will produce a reflected ray along BE of intensity eac; and a refracted ray along AB of intensity acf; e, and f, being, respectively, the fraction reflected and the fraction refracted at the back surface.

Since the ray BE does not actually exist, the sum of the rays along BE must be zero, so that:

$$ace+abc=0. \tag{2}$$

Similarly, the rays along AB must add up to produce the initial ray of intensity a, so that:

$$acf+ab^2=a \tag{3}$$

and,

$$cf=1-b^2. \tag{4}$$

From Eq. (2) it follows that

$$b=-e, \tag{5}$$

so that the reflectance from the front surface is equal to the reflectance at the back surface.

The intensities of the rays emerging from the front surface of the plate after multiple internal reflections will be:

$$abcf+ab^3cf+ab^5cf+\cdots, \text{ etc.} \tag{6}$$

$$=abcf(1+b^2+b^4+\cdots, \text{ etc.}) \tag{7}$$

$$=abcf(1/1-b^2)=ab(cf/1-b^2) \tag{8}$$

which from Eq. (4)

$$=ab,$$

proving that the emerging rays sum up to the intensity of the ray reflected from the front surface.

If conditions are correct for destructive interference, (Eq. (1)), the reflected rays will completely destroy each other so that the transmittance of the plate for light of that wave-length will be 100 percent (neglecting the usually insignificant amount of absorption).

Since, as has been shown, the reflectance at

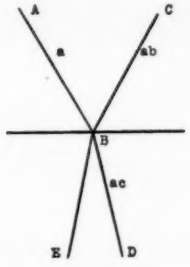

FIG. 1.

the back surface is equal to that at the front surface, the system becomes analogous to the Fabry-Perot interferometer[2] and the equations derived by those authors to relate the intensity of the light transmitted to the reflectance and the phase relationships between the reflected rays are applicable if modified to take account of the fact that in the present case:

1. The medium between the reflecting surfaces is not air.
2. The absorption by the reflecting surfaces is zero.
3. A reversal of phase takes place when internal reflection occurs.

When so modified the equation becomes,

$$T=1\Big/\left[1+\frac{4R}{(1-R)^2}\cos^2\pi\frac{2dn}{\lambda}\right], \tag{9}$$

in which,

T = transmittance,
R = reflectance for a single surface,
n = refractive index at the wave-length in question,
λ = wave-length,
d = thickness of the plate,
π = its customary value.

This equation can be used to calculate the transmittance of the plate for all phase relationships.

[2] Ann. Chim. Phys. **12**, 459 (1897).

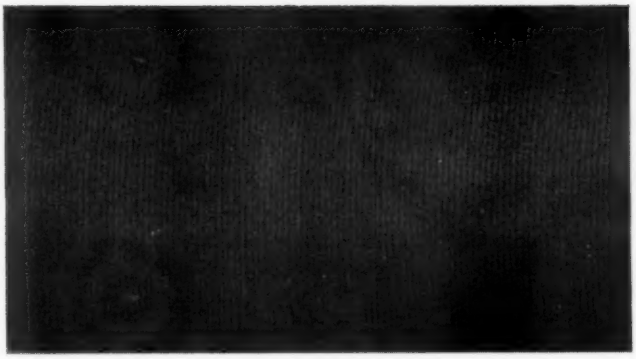

FIG. 2. Interference fringes obtained with quartz slit cover 1 mm thick on a stigmatic grating spectrograph. Wave-length region 5500A. Incandescent tungsten light source. Five times enlarged.

When $2dn/\lambda$ has an integral value the transmittance is a minimum; when $2dn/\lambda$ has a value 0.5 less than integral, the transmittance becomes unity.

Application to quartz

Quartz is the material which is generally used in spectro-chemical work for slit covers and in making ruled fixed slits and neutral absorbing step weakeners. Table I gives the transmittance of a plane parallel quartz plate for light of such wave-length that reinforcement of the reflected rays occurs. The transmittances were calculated from Eq. (9). The reflectance values were calculated for a number of wave-lengths from the equation:

$$R=(n-1)^2/(n+1)^2, \qquad (10)$$

in which:

R = reflectance at normal incidence,
n = refractive index.

The values of refractive index used are for the ordinary ray in crystalline quartz as given by Gifford.[3]

TABLE I. Minimum transmittance, T, of quartz plate.

λ	n	R	$T\%$
7950A	1.5385	0.04501	83.51
5461	1.5462	0.04601	83.20
3962	1.5582	0.04761	82.40
2446	1.6046	0.05388	80.65

[3] J. W. Gifford, Proc. Roy. Soc. **70**, 329 (1902); **84**, 193 (1910).

As the tabulation shows, a change in thickness of the quartz plate, amounting to one quarter of a wave-length of the light used, may result in a change of approximately 20 percent in the intensity of the transmitted light.

OBSERVED INTERFERENCE EFFECTS

The interference effects are most easily observed by examining the spectrum of an incandescent source. Figure 2 is a five-times enlargement of interference fringes obtained with a stigmatic grating spectrograph and an incandescent tungsten source. The flat quartz plate was 1 mm thick. The region shown is 5500A. The curvature of the lines is caused by deviation from parallelism of the plate faces and deviation from normal incidence. If a source of discontinuous spectra is used, the interference is very difficult to observe but the magnitude of the effects is even greater because of the absence of overlapping slit images.

ERRORS INTRODUCED BY INTERFERENCE

The interference effects described can cause errors in spectrochemical analysis in a variety of ways. In the following, the introduction of errors into particular techniques and applications will be discussed. It should be noted that the magnitude of the errors will be derived on the basis of idealized conditions. All deviations from idealized conditions such as astigmatism, variation from normal incidence, deviations from parallelism of plate faces, etc., will operate in the direction of reducing the magnitude of the errors by averaging out the effects of the interference. A discussion of particular errors follows:

1. Plate calibration with step sector: If the step sector method of plate calibration is used with a spectrograph which has a flat slit cover, difficulties will be encountered whose magnitude will depend on the deviation of the faces of the slit cover from parallelism. If the faces are perfectly flat and parallel, and the slit is illuminated along its whole length by parallel rays normal to the surface of the slit cover, no effect on the plate calibration will result since the interference fringes will be parallel to the direction of the spectral lines and the effect on the darkness of the line will be uniform over the entire length of the line. However, this degree of parallelism is rarely obtained and a change in the thickness of the slit cover of only one-quarter of the wave-length of the light used can cause a discrepancy of 20 percent in the intensity of light in a given step of the step sector. A vertical line drawn in Fig. 2 to correspond to a spectral line will give an indication of the variation from uniform line illumination to be expected in an ordinary case. Similar difficulties will be encountered in any technique which requires uniform slit illumination.

2. Measurement of wave-length: The position of a spectral line is generally measured as the position of the intensity peak. In the case of a fairly wide line the interference effect superimposed on the energy distribution along the width of the spectral line will result in a shift in the position of the peak of intensity which may result in error in measurement of position. This is more likely to occur with thick plates since the fringes are then closer together.

3. Intensity ratios: Reference to Fig. 3 will show how errors are introduced into the measurement of intensity ratios. For a given plate thickness, the absolute intensity ratio of two lines may be in error by approximately 20 percent in the case of quartz. However, a change in thickness of the plate, such as will result if the plate is removed and replaced in a slightly different position, may result in variations of as much as 40 percent in the value of the intensity ratio if the lines being compared happen to fall in the positions indicated by λ_1, and λ_2 in the figure. If the slit cover is permanently fixed in position, the values of the intensity ratio will be erroneous but constant.

4. Plate calibration by standard spectral lines: The considerations outlined under "Intensity Ratios" above apply with equal force to the use of standard intensity ratios, obtained from the

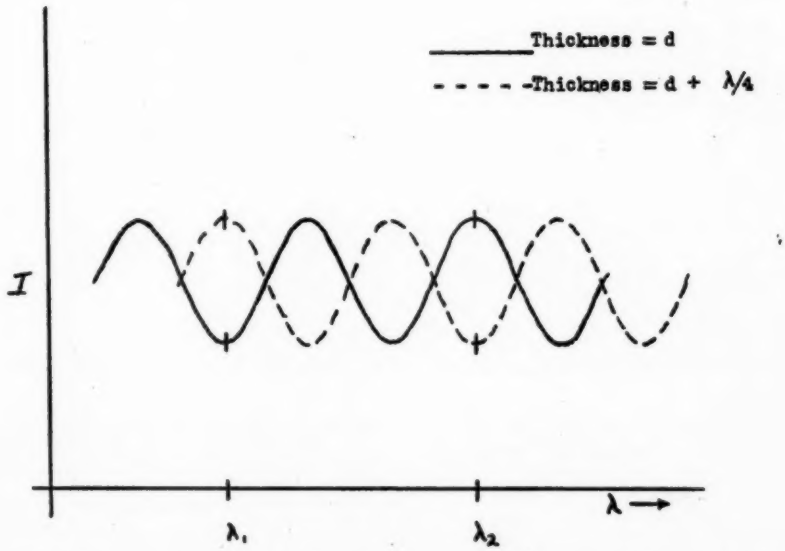

FIG. 3. Diagram showing relationships between wave-length of light, thickness of plate, and intensity of transmitted light.

measurement of selected lines of a reproducible spectrum, for the calibration of photographic plates. If a flat slit cover is used, measurements made on one spectrograph will not be transferable to another and any change in thickness of plate will necessitate the remeasurement of the standard intensity ratios.

5. Ruled fixed slits: The use of ruled fixed slits will introduce all the errors discussed above, with the exception that no change in plate thickness is possible. This will eliminate the most serious error which is that introduced into the measurement of intensity ratio. The intensity ratios, while not correct will be constant.

6. Neutral absorbing step filters: Since the use of stepped film devices for plate calibration depends on uniformity of illumination of the various steps, the same considerations will apply as in the case of the use of the stepped sector. In addition, since the effect of the change in plate thickness on the step ratio depends on wavelength, the absorption cannot be considered neutral.

ELIMINATION AND AVOIDANCE OF ERRORS

The simplest and most practicable method of eliminating the errors discussed above is to avoid the use of parallel-faced plates. This can easily be done in the case of slit covers, without losing the protection provided, by using a lens instead of a flat plate as the cover. The large angle between the lens faces causes the fringes to be squeezed together in the vertical direction so that the variation in intensity is averaged out in the length of line usually measured. Where flat plates are unavoidable, as in the case of fixed ruled slits and neutral absorbing films, consideration of the factors outlined above makes it possible to use these devices without introducing any appreciable error.

ACKNOWLEDGMENT

The writer wishes to express his appreciation to Mr. J. G. O'Neill, Superintendent of the Chemical Laboratory of the U. S. Naval Engineering Experiment Station, for authorizing and encouraging the present work.

JOURNAL OF THE OPTICAL SOCIETY OF AMERICA VOLUME 36, NUMBER 11 NOVEMBER, 1946

The Kinetics of Visual Dark Adaptation[1]

THEODORE LOUIS JAHN
Zoological Laboratories, State University of Iowa, Iowa City, Iowa
(Received September 9, 1946)

AT present there is available a considerable amount of precise information concerning the course of dark adaptation of human rods following various degrees of light adaptation.[2–7] The course of regeneration of visual purple during dark adaptation has also been studied by several investigators.[8–10] However, it has been pointed out repeatedly that there is no adequate theoretical basis for relating the data on visual dark adaptation to those on visual purple regeneration.[2, 6, 10–13] The present paper[14] is an attempt to provide such a basis.

I. THE DARK ADAPTATION DATA

Data concerning the course of dark adaptation are usually presented as tables and graphs showing the logarithm of the threshold intensity as a function of time in the dark.[2–5] This is a convenient way of presenting the data, but it is also one which makes it difficult to compare these data with those for the regeneration of visual purple.

On the assumption that for brief constant exposures the same quantity of photo-product must be formed by a threshold flash of light at

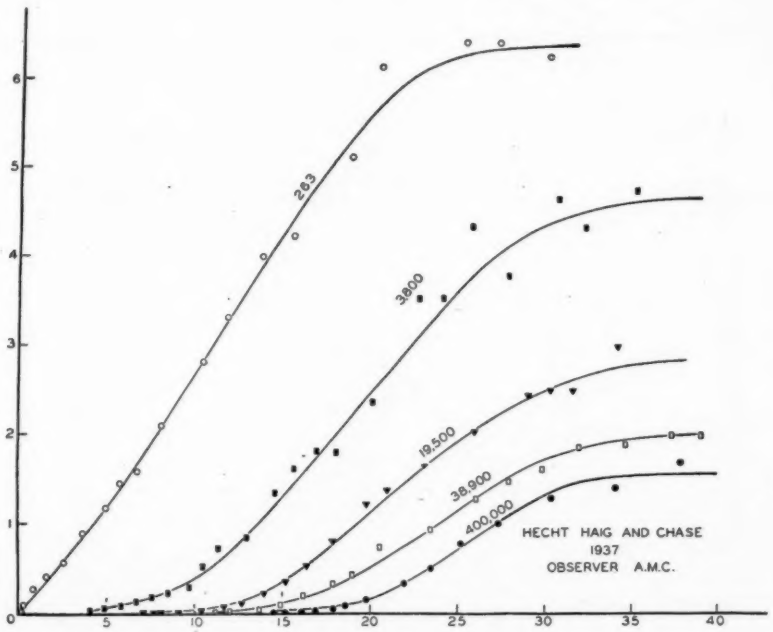

FIG. 1.

[1] Aided by a grant from the Rockefeller Foundation for research on the physiology of the normal cell.
[2] C. P. Winsor and A. B. Clark, Proc. Nat. Acad. Sci. **22**, 400 (1936).
[3] S. Hecht, C. Haig, and A. M. Chase, J. Gen. Physiol. **20**, 831 (1937).
[4] G. Wald and A. B. Clark, J. Gen. Physiol. **21**, 93 (1937).
[5] C. Haig, J. Gen. Physiol. **24**, 735 (1931).
[6] G. Wald, *Medical Physics*, edited by Otto Glaser (The Year Book Publishers, Chicago, 1944), p. 1663.
[7] C. Sheard, J. Opt. Soc. Am. **34**, 464 (1944).
[8] K. Tansley, J. Physiol. **71**, 442 (1931).
[9] M. Zewi, Acta Soc. Scient. fenn. **2**, No. 4 (1939).
[10] J. C. Peskin, J. Gen. Physiol. **26**, 27 (1942).
[11] R. Granit, Doc. Ophthalmologica **1**, 7 (1938).
[12] S. Hecht, Ann. Rev. Biochem. **9**, 465 (1942).
[13] P. Moon and D. E. Spencer, J. Opt. Soc. Am. **35**, 43 (1935); J. Math. and Phys. **24**, 65 (1945).
[14] T. L. Jahn, Fed. Proc. **5**, 52 (1946).

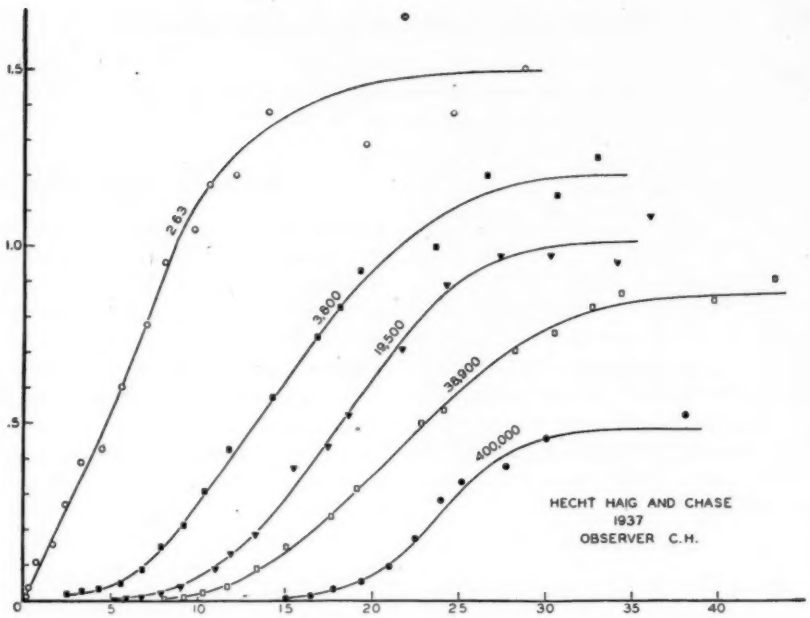

FIG. 2.

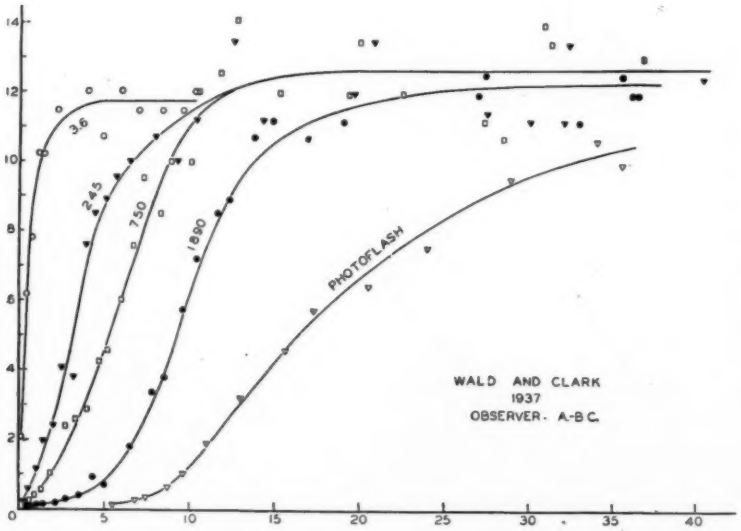

FIG. 3.

any time during the course of dark adaptation the threshold intensity should vary inversely with the concentration of photo-sensitive material. Therefore, it is convenient to compare the curves for the reciprocal of the threshold intensity, otherwise known as the sensitivity, with those for the regeneration of visual purple, either theoretical or experimental.

Figures 1–5 show representative rod data from Hecht, Haig, and Chase,[3] Wald and Clark,[4] and Haig[5] plotted in terms of sensitivity as a function of time (in minutes). The figures on the curves

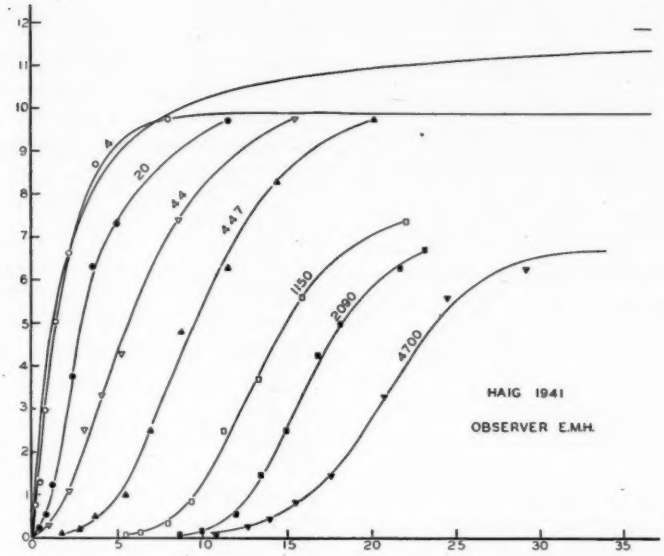

FIG 4.

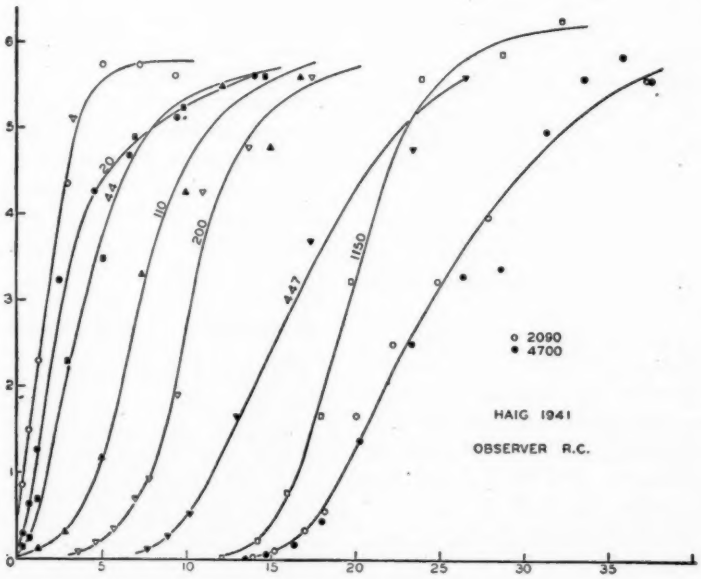

FIG. 5.

denote the intensity of the adapting light, measured in photons for Figs. 1 and 2 and in millilamberts for Figs. 3–5. Following intense light adaptation the curves are sigmoid, and in Figs. 1, 2, and 4 the data for the highest adapting intensity have been fitted with the monomolecular autocatalytic equation. The data for the lowest adapting intensity in all four figures obviously cannot be fitted by the same equation. However, the data for the lowest intensity in Figs. 3 and 4 can be approximated by either a mono- or a bimolecular equation. Intermediate data of these figures and the low intensity data of Figs. 1 and 2 presumably could be approximated by

some combination of autocatalytic and of either mono- or bimolecular equations.

II. THE REGENERATION OF VISUAL PURPLE

It has been demonstrated by Wald[15] that during dark adaptation there are two chemical reactions by which visual purple is regenerated. They are shown in Fig. 6. Regeneration from visual yellow is much more rapid than the reaction chain which involves visual white. As the degree of light adaptation is increased the amount of pigment in the form of visual white is increased. Therefore, it is possible for the apparent regeneration curve subsequent to a small amount of light adaptation to be quite different in form from that subsequent to a large amount.

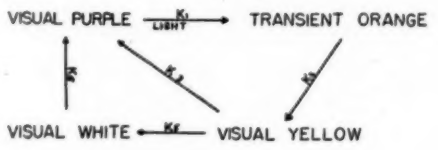

FIG. 6.

Several investigators have made direct quantitative studies of the rate of visual purple regeneration in the intact animal by chemical and spectroscopic methods. Tansley[8] found the regeneration of rhodopsin in the eye of the rat could be described approximately as a monomolecular reaction with a low velocity. Zewi[9] found a rapid regeneration during dark adaptation but was unable to find a satisfactory theoretical description of the course of the reaction. Peskin[10] performed many analyses of retinae during dark adaptation and found that in much of his data the course of the reaction could be described as autocatalytic. Some of the curves, however, were definitely asymmetrical, the rate of increase during the first half of the curve being much greater than during the latter half. The shape of the first part of the curve could be changed by the amount of light used for adaptation, the more light the lower the initial position *and slope* of the curve.

III. THE NEED OF A NEW SOLUTION

It is apparent that on the basis of both chemical and threshold measurements the dark adaptation curves are of various types. It seems possible that simultaneous solutions for the two courses of the chemical reaction could be used to explain both the increase in sensitivity and the increase in visual purple as a function of time. Although the necessity for some such analysis was pointed out by Winsor and Clark[2] no simultaneous solutions for the equations of kinetics have ever been applied to dark adaptation phenomena. On the contrary, in the most recent treatment of dark adaptation by Moon and Spencer[13] the reaction involving visual white has been completely ignored because of its slowness. This is not a valid reason because during the course of adaptation the slower of two simultaneous reactions should have a greater effect on the time course of the adaptation process, especially under conditions that cause most of the material to pass through the slower reaction chain. The effect of the slower reaction is detectable for a half-hour in man and for two hours in the frog; the faster reaction seems to be essentially over in less than ten minutes in man and twenty minutes in the frog.

It is the purpose of the present note to show that all of the valid adaptation data can be explained as the result of two simultaneous chemical reactions: (1) a mono- or bimolecular conversion of visual yellow to visual purple, and (2) an autocatalytic conversion of visual white to visual purple.

IV. KINETICS OF THE CHEMICAL REACTIONS

The three known chemical reactions, which we shall call reactions 3, 5, and 6, and which occur during dark adaptation, are denoted in Fig. 6 by their three velocity constants, k_3, k_5, and k_6. (The particular subscripts are used to avoid confusion with those for other reactions.[16]) Let us denote the amounts of visual yellow, visual white, and visual purple by x, y, and z, respectively. Then $x+y+z=$a constant which may be placed equal to 1. If regeneration from visual yellow is bimolecular and that from visual white is autocatalytic then the rate of formation of visual purple by means of these reactions can be denoted by Eqs. (1) and (2) below, where t is

[15] G. Wald, J. Gen. Physiol. **19**, 351 (1935).

[16] T. L. Jahn, J. Opt. Soc. Am. **36**, 76, 83 (1946).

time in the dark.

$$(dz/dt)_3 = k_3x^2, \quad (1)$$

$$(dz/dt)_6 = k_6yz. \quad (2)$$

The combined rates of the simultaneous reactions will then be

$$(dz/dt)_{3+6} = k_3x^2 + k_6yz. \quad (3)$$

Since reaction 5 is probably monomolecular the value of y is determined by its initial value at the end of light adaptation and also by that of x and of k_5. At present it seems wise to ignore this reaction for three reasons. (1) The computed course of the total regeneration of rhodopsin if reaction 5 is included would probably be almost the same as if it were ignored and a slightly higher initial value of y were assumed. The only way of distinguishing between these two possibilities would be to obtain very accurate data during the first few minutes of adaptation. Because of the rapid rate of change this is the time when measurements seem to be least accurate. (2) As measured by changes in the concentration of retinine[10] in the frog at 25°C, the major portion of reaction 3 (and also of reaction 5 because they use the same substrate) is essentially over within ten minutes whereas the course of adaptation continues for two hours. Therefore, omission of reaction 5 should not have much effect on the computed curves after the first few minutes. (3) One should expect the same amount of light delivered over different periods of time during light adaptation to result in different initial ratios of x and y, a low intensity over a long period of time yielding a relatively larger value of y, and a high intensity over a short period of time giving the higher relative value of x. Experimental data on this point are at variance. The data of Haig[5] indicate that the course of dark adaptation is determined within wide limits by the amount (i.e., intensity times the exposure time) of the adapting light. This means that for a given quantity of light most of the conversion of visual yellow to visual white takes place quickly (certainly within the time that the k_3 reaction is important) and that this adjustment in the ratio of x to y does not significantly affect the course of the total increase of z. The data of Wald and Clark[4] and Wald,[6] however, are contradictory to those of Haig[5] and indicate that the initial ratio of x to y is important. Quite aside from this divergence of viewpoints it should be pointed out that one of the most important items in determining the course of the regeneration reaction from visual white is the initial value of z, especially for small values of x.

For the above reasons it seems permissible to omit consideration of reaction 5 until more accurate data become available, especially since the inclusion of this reaction would greatly complicate the present essentially simple theory.

By integration of Eq. (3) it is possible to obtain an expression for z as a function of time in the dark (t). This equation may be solved if the integral of the first term

$$[x = 1/(k_3t+a), \quad \text{where } a = 1/x_0]$$

and the value for z, $[z = 1-x-y]$ are substituted into the second term which becomes

$$dy/dt = -k_6y\left(1 - \frac{1}{k_3t+a} - y\right). \quad (4)$$

This expression may then be solved for y by means of the Bernoulli equation which reduces the solution to that of the type form

$$\int w^m e^{-bw} dw.$$

If $k_3 = k_6$, then $m = 1$ and the solution for y is

$$y = \frac{t+a}{t+a+1+Ke^t}. \quad (5)$$

When this is combined with the solution for x in the equation $z = 1-x-y$, the solution for z becomes

$$z = 1 - \frac{1}{t+a} - \frac{t+a}{t+a+1+Ke^t}. \quad (6)$$

If k_3 is not equal to k_6 the solution of Eq. (4) may be much more complex, becoming an infinite series if m is not an integer.[17]

Figure 7 shows a family of curves computed from Eq. (6) together with three bimolecular

[17] The author is greatly indebted to Professor Nelson B. Conkwright of the Department of Mathematics, State University of Iowa, for assistance in the solution of this equation.

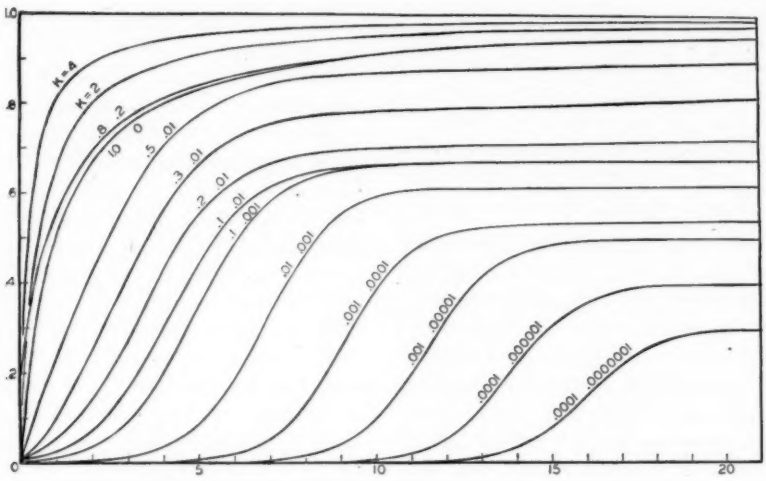

FIG. 7.

curves with various velocity constants ($K=1$, 2, and 4). On all curves except the first two ($K=2$ and 4) there are two decimal numbers marked on each curve. The first of these two numbers denotes the assumed value of x at the beginning of dark adaptation, i.e., x_0. The second number is the assumed value of z at the beginning of dark adaptation, i.e., z_0. All of the assumed values of z_0 are small except in the third curve where y_0 was assumed to be zero and z_0 was assumed to be 0.2. This would correspond to the theoretical condition following a very slight degree of light adaptation where 80 percent of the visual purple was converted into visual yellow but none had yet been converted into visual white. Reaction 5 would probably prevent any such curve from being obtained in the eye, and it is shown only for the purpose of comparison. In all curves except the first three on the left it can be seen that decreasing x_0 tends to make the curves sigmoid and that decreasing z_0 tends to shift the sigmoid curves to the right.

V. COMPARISON OF THEORY AND DATA

If the family of theoretical curves shown in Fig. 7 is compared with the experimental data of Figs. 1–5, it is readily seen that the progressive change in form with increasing light adaptation is the same for all series both theoretical and experimental. There is a tendency for the points on the curves of Figs. 1–5 to scatter wherever the sensitivity is high. This scattering is inherent in the method of plotting, and is not noticeable when the same data are plotted in the usual manner.[2–5]

In Fig. 6 some of the maxima have been arbitrarily decreased, i.e., $x+y+z$ has been assumed to equal less than 1. The maxima assumed were, left to right, 1.0, 1.0, .95, .95, .90, .85, .75, .65, .65, .61, .52, .50, .49, and .30. This decrease is comparable to that seen in Figs. 1–4 where the curves obtained after intense light adaptation rise to a lower maximum than those obtained after slight light adaptation.

The most reasonable explanation of the decrease in the maxima of the data seems to be that after visual purple is converted into visual white (vitamin A and protein) the vitamin A is free to diffuse into the blood stream from which it can be absorbed and stored by other body organs, principally by the liver. Apparently in the eyes of normal individuals several hours are necessary for complete recovery (which involves the complete return of visual purple to the retina) to occur. This explanation is in agreement with the observation of Wald[6,15,18] that during light adaptation of frog eyes between two-thirds and four-fifths of the vitamin A may leave the

[18] G. Wald, J. Gen. Physiol. **19**, 781 (1936).

eye if the eye is *in situ* with normal blood supply but not if the eyes are excised.

The data of Fig. 5 are especially interesting in that there is no decrease in the maximum following intense light adaptation. The observer, R. C., was suffering from a liver cirrhosis which apparently prevented storage of vitamin A. This necessitated his daily ingestion of large quantities of the material in order to keep his visual sensitivity higher than one-fifth normal.[5] In these data the sensitivity is one-half normal and his blood stream therefore was probably high in vitamin A and consequently any loss from the retina was readily replaced.

There are a few exceptional data published in which the maxima are not arranged exactly in accordance with the quantity of adapting light, e.g., the left curve of Fig. 3. If such an experiment were performed immediately after one in which a high degree of light adaptation was used, the data become readily understandable. However, since the authors have not always stated the order in which the experiments were performed judgment on this matter must be reserved.

It is possible to produce an approximate fit of all of the data of Figs. 1–5 by means of Eq. (6). However, this has not been presented for two reasons: (1) the scattering of the experimental points whenever the sensitivity is high, and (2) the fact that the available data do not represent the whole course of dark adaptation. Any fitting of curves must therefore be only approximate. Furthermore, if data for the complete recovery were available it would then be necessary to introduce factors into the equation for the diffusion of visual purple out of and then back into the retina. Since actual data concerning that process is unavailable such a detailed comparison is considered to be beyond the scope of the present paper.

One assumption of the present interpretation is that during even moderate light adaptation most of the visual purple is converted into visual yellow and visual white (95 percent or more in all data in Figs. 1–5). This is contradictory to the assumption made by Jahn[16] in deriving equations for flicker as a function of intensity, and in order to have a uniform explanation of these visual phenomena it seems necessary to change the assumption made for the flicker equations. This will not change the general form of the flicker equation (Eq. (15) in paper on flicker[16]) but will prohibit a simple substitution (Eq. (16)) which greatly simplified the calculations. Therefore, the mathematical difficulties temporarily avoided in the previous paper must eventually be overcome in order to provide a uniform interpretation.

VI. CONCLUSION

An attempt to provide a theoretical basis for the interpretation of the data for dark adaptation in terms of the photochemical cycle is presented. If we assume that visual purple may be regenerated by two simultaneous reactions, one autocatalytic and one mono- or bimolecular, an equation may be derived for the regeneration of visual purple as a function of time. Curves calculated on this basis have a time course that is very similar to that of the data for dark adaptation calculated in terms of sensitivity. It is concluded that the theory provides an explanation of the available data in terms of the photochemical cycle and that within the variability inherent in the data this explanation seems to be adequate.

JOURNAL OF THE OPTICAL SOCIETY OF AMERICA VOLUME 36, NUMBER 11 NOVEMBER, 1946

A Study of Photometric Nomenclature

PARRY MOON
Massachusetts Institute of Technology, Cambridge, Massachusetts
AND
DOMINA EBERLE SPENCER
Tufts College, Medford, Massachusetts

(Received August 1, 1946)

1. INTRODUCTION

IN the teaching of illuminating engineering and related subjects over a period of years, the authors have been forced to consider the concepts dealing with light. Inconsistencies in the established definitions and nomenclature have been pointed out repeatedly by bright students, and in self-defense we have had to try to improve matters. The principal results of this study are given in the following pages, and it is hoped that these results will be of help to others who are dealing quantitatively with light and color.

We shall consider concepts of radiometry, photometry, and colorimetry. In general, four systems will be compared: the C.I.E. system of 1938 (Commission Internationale de l'Eclairage[1]), the I.E.S. system of 1941 (Illuminating Engineering Society[2]), the O.S.A. system of 1944 (Colorimetry Committee of the Optical Society of America[3]), and the system proposed in this paper.[4]

To be satisfactory, a concept (with name and definition) should satisfy the following criteria:

(1) Exactness,
(2) Generality,
(3) Simplicity,
(4) Internationality.

Some of the existing concepts are satisfactory on all four counts. Other concepts obviously violate one or all of the requirements.

The study is expedited by the use of dimensions. We have found it convenient to employ the unit of power as dimension $[P]$, time $[T]$, wave-length $[\Lambda]$, luminous flux $[F]$, tangential length $[L_t]$, and radial length $[L_r]$. According to this set of dimensions, a unit designating plane angle is not dimensionless[5] but has dimensions $[L_tL_r^{-1}]$ and a unit of solid angle has dimensions $[L_t^2L_r^{-2}]$. Unless these two space dimensions (or an equivalent)[6] are used, it is impossible to distinguish dimensionally between *candlepower* and *luminous flux* or between *brightness* and *flux density*.

2. ACTIVE RADIOMETRIC CONCEPTS

Table I lists the active radiometric concepts advocated by the I.E.S. and O.S.A., also the new proposed set. The C.I.E. has no complete radiometric system,[1] so there is no C.I.E. column. One may regard *radiant power* $[P]$ as the fundamental quantity, all the other concepts being associated by simple spacial and temporal relations. One might logically expect to find the

TABLE I. Comparison of systems of nomenclature. Active radiometric concepts.

Dimensions	m.k.s. unit	I.E.S. (1941)		O.S.A. (1944)		Proposed (1946)	
$[P]$	watt	Φ, P	radiant flux	P	radiant flux	F_r	radiant pharos
$[PL_t^{-2}]$	watt m^{-2}	W	radiant flux density	—	——	D_r	radiant pharosage
$[PL_t^{-2}]$	watt m^{-2} (radiated)	W	radiancy	W	radiant emittance	—	——
$[PL_t^{-2}]$	watt m^{-2} (incident)	H, $\mathfrak{E}$	irradiancy	H	irradiance	—	——
$[PT]$	watt sec.	U	radiant energy	U	radiant energy	Q_r	radiant phos
$[PTL_t^{-2}]$	watt sec. m^{-2}	—	——	—	——	U_r	radiant phosage
$[PTL^{-3}]$	watt sec. m^{-3}	u	radiant energy density	u	radiant density	—	——
$[PL_t^{-2}L_r^{-2}]$	watt steradian^{-1}	J	radiant intensity	J	radiant intensity	—	——
$[PL_t^{-1}L_r^{-2}]$	watt m^{-2} ster^{-1}, herschel	N, $\mathfrak{B}$	steradiancy	N	radiance	—	——
		—	——	—	——	H_r	radiant helios
$[PL_t^{-1}L_r]$	herschel m^{-1}	—	——	—	——	G_r	radiant heliosent
$[PL_t^{-2}\Lambda^{-1}]$	watt m^{-2} micron^{-1}	—	——	H_λ	spectral irradiance	$J(\lambda)$	phengosage
$[P\Lambda^{-1}]$	watt micron^{-1}	—	——	P_λ	spectral radiant flux	—	——
$[PT\Lambda^{-1}]$	watt sec. micron^{-1}	U_λ	spectral radiant energy	—	——	—	——
$[PL_r^{-2}L_r^2\Lambda^{-1}]$	watt steradian^{-1} micron^{-1}	J_λ	spectral radiant intensity	—	——	—	——

following quantities: power per unit length, power per unit area, power per unit volume, energy per unit length, energy per unit area, energy per unit volume, power per unit solid angle, energy per unit solid angle, energy per unit wave-length band, and all other combinations. In practice, however, no one has advocated the standardization of all these concepts, even though all of them may be needed occasionally.

Experience of physicists and engineers has shown that there is a very definite need for units with dimensions $[P]$, $[PL_i^{-2}]$, $[PT]$, $[PTL_i^{-2}]$, $[PL_i^{-4}L_r^2]$ (power per unit area, per unit solid angle), and $[PL_i^{-2}\Lambda^{-1}]$. A previous analysis[6] of the various types of calculation that must be made in dealing with scattering and absorbing media showed the desirability of adding $[PL_i^{-4}L_r]$. This makes a total of 7 radiometric concepts, which seems to be the minimum for handling all possible calculations. In most engineering practice, of course, a smaller number will suffice.

Comparing the foregoing list with the I.E.S. concepts of Table I, one finds in the table three separate flux densities instead of a single flux density. Since all three have the same dimensions $[PL_i^{-2}]$, it seems a violation of simplicity to consider them as different concepts with different names and symbols. Actually, there is but a single concept here; and when the necessity arises for distinguishing radiated flux density from incident flux density, it is done very easily by use of these two adjectives and by employing the subscripts *i* and *e* (Latin *in* and *ex*). The same procedure can be used to simplify the O.S.A. system.

Another unnecessary concept is *radiant intensity J*. This quantity was borrowed by analogy from the antiquated photometric concept of *candlepower* or *luminous intensity*. In the days of candlelight, the concept was helpful, since sources were of such small dimensions that the inverse-square relation could be used to calculate flux density. With modern sources, such as fluorescent lamps, luminous panels, and troffers, however, the inverse-square relation is ordinarily inapplicable. Thus the concept of *intensity* loses most of its value and tends to become merely an incitement to error. In the few places where it is still desirable, it may be written F/ω and called by no particular name.

Another reason for omitting radiant intensity is that it is ordinarily used to define "radiant brightness" $[PL_i^{-4}L_r^2]$. There are two systems of units for this quantity, differing by a factor of π. Radiant intensity leads to the "unrationalized" system, but experience by engineers throughout the world has shown definitely that the "rationalized" or Lambert system is vastly superior. This subject will be considered in Section 3.

There remain the quantities whose dimensional formulas contain $[\Lambda^{-1}]$. Evidently we could have a list of twenty or thirty of such concepts, but simplicity suggests that we limit ourselves to one quantity. The concept whose units are designated by $[PL_i^{-2}\Lambda^{-1}]$ appears to be the most useful.

Considering now the names of the concepts, one notes considerable differences in the I.E.S. and O.S.A. columns. At the time of writing this paper, the reconciliation of these differences by the committees does not seem very hopeful. The worst offender against internationality is the -ANCY ending of the I.E.S. The suffixes -ANCY and -ANCE are from the same Latin ending, and there appears to be no way of distinguishing the two except in English. If both endings were standardized, as advocated by the I.E.S., it would create a troublesome problem in translation and would tend to increase the ambiguity already existing in scientific nomenclature.

The ending -ANCE is an established scientific ending. It indicates a *passive property of an entity*. For example, one speaks of the *resistance*, *inductance*, *impedance*, and *reactance* of a coil, the *capacitance* of a capacitor, or the *transmittance* of a filter. To apply -ANCE also to the *active* concepts of Table I destroys one of the few precious examples of international systematization that exists in modern languages. Both -ANCY and -ANCE, as used in Table I, are therefore definitely reprehensible. The *density* and *intensity* of Table I are also non-international and ambiguous.

To summarize on the basis of the four criteria of Section 1,

(1) Exactness is violated by such words as *density* and *intensity*, which may mean almost anything; and by the endings -ANCY and -ANCE,

TABLE II. Comparison of systems of nomenclature. Active photometric concepts.

Dimensions	m.k.s. unit	C.I.E. (1938)		I.E.S. (1941)		O.S.A. (1944)		Proposed (1946)	
$[F]$	lumen	F, φ	luminous flux	F	luminous flux	F	luminous flux	F_l	luminous pharos
$[FL_i^{-2}]$	lumen m^{-2}	—	surface density of luminous flux	—	——	—	——	D_l	luminous pharosage
$[FL_i^{-2}]$	lumen m^{-2} (radiated)	R	radiance	—	——	L	luminous emittance	—	——
$[FL_i^{-2}]$	lumen m^{-2} (incident)	E	illumination	E	illumination	E	illuminance	—	——
$[FT]$	lumen sec.	L	quantity of light	Q	quantity of light	Q	"luminous energy"	Q_l	luminous phos
$[FTL_i^{-2}]$	lumen sec. m^{-2}	—	exposure	—	——	—	——	U_l	luminous phosage
$[FTL^{-3}]$	lumen sec. m^{-3}	→	——	—	——	q	luminous density	—	——
$[FL_i^{-2}L_r^{-2}]$	lumen steradian^{-1} =candle	I	luminous intensity	I	luminous intensity	I	luminous intensity	—	——
$[FL_i^{-2}L_r^{-2}]$	candle m^{-2}	B	brightness	B	brightness (unrationalized)	B	luminance	—	——
	lambert, blondel	—	——	B'	brightness (rationalized)	—	——	H_l	luminous helios
$[FL_i^{-2}L_r]$	blondel m^{-1}	—	——	—	——	—	——	G_l	luminous heliosent

which should be reserved for *passive* properties if precision of nomenclature is to be established.

(2) Generality is violated by the definitions of J and N, which are supposed to apply strictly only to point sources but which are somehow applied to everything else.

(3) Simplicity is violated by the use of three flux densities where one suffices, and by the inclusion of the antiquated concept of *radiant intensity* and the unnecessary P_λ, U_λ, and J_λ.

(4) Internationality is violated by all the I.E.S. and O.S.A. names.

All of these objections are eliminated by the proposed system of Table I. The definitions[7] are more general and more precise than the usual definitions, all unnecessary concepts have been eliminated, and the new words are international, requiring no translation into the languages of Europe or the Western hemisphere. Of course, the proposed system is not a *unique* solution of the problem; but it is a *possible* solution, and the foregoing analysis should at least indicate some of the ideas to be kept in mind in any revision of the radiometric concepts.

3. ACTIVE PHOTOMETRIC CONCEPTS

One of the advances that has been made in the past decade is the general realization that the active radiometric and photometric concepts should be considered simultaneously in parallel columns. Every quantity of Table II should be obtainable from a corresponding quantity of Table I by weighting the latter by means of the standard lamprosity (visibility) function.[8] Thus an ideal photometric system should contain an analog of each quantity in the radiometric system, with the exception of the concepts "per unit wave-length band."

A consideration of the older systems of Table II shows that greater simplicity should be possible:

(a) The concept of *luminous flux density* is divided into three parts, which is unnecessary.

(b) The concept of *luminous intensity* should be eliminated.

(c) There are two systems of brightness units, causing a great deal of confusion and constituting a real stumbling block to the uninitiated.

The C.I.E. definition[1] of luminous intensity is

> "The luminous intensity (candlepower) of a point source in any direction is the flux per unit solid angle emitted by that source in that direction."

The I.E.S. definition[2] is similar. Note the lack of generality: the concept is specifically restricted to a mathematical point. Practically, this restriction may be of little importance; but it does constitute a logical weakness of the definition.

Brightness is then defined on the basis of the foregoing definition of intensity. According to the C.I.E.,[1]

> "The brightness of a surface in a given direction is the quotient of the luminous intensity in that direction by the projected area."

Since intensity was definitely restricted to a *point*, an inquisitive reader may wonder how it is suddenly applied to a surface. An element of surface, no matter how small, never becomes a point.

Of greater importance is the fact that, by definition, brightness is restricted to *surfaces*. Perhaps the concept can be applied to the sky or to a radiating vapor, but the definition says nothing about it and thus lacks generality. Of wider generality is *helios*,[9] which applies to any point in space in any medium.

The helios at the point P and in a given direction PQ is defined as π times the flux density at P, divided by the solid angle ω, for a lightcone having its axis in the direction PQ, or

$$H=\pi \lim_{\omega\to 0}(D/\omega). \qquad (1)$$

The π is introduced to keep the unit in the rationalized system. If D in Eq. (1) is in lumen m^{-2} and ω is in steradian, then H is in the rationalized m.k.s. unit called the *blondel*. Another way of writing Eq. (1) is

$$H=dD/d\omega, \qquad (2)$$

where ω must be expressed in quarter spheres instead of steradians to obtain a rationalized unit. In either Eq. (1) or (2), we are defining the concept of *flux density per unit solid angle*. The units obviously have the same dimensions as brightness, but in the idea of *helios* we have attempted to circumvent some of the narrowness, complexity, and ambiguity associated with the older term.

For the special case of a perfect medium and a surface source, the brightness of the source (rationalized system) is identical with helios.

This brings up the question of the rationalized and unrationalized brightness units mentioned in Section 2. The unrationalized units are those obtained by the C.I.E. definition and include the candle per square millimeter, candle per square meter, candle per square foot, stilb. The rationalized units are smaller by a factor π and include the lambert, millilambert, footlambert, and apostilb. Helios,[8] as defined by Eq. (1), is rationalized, the unit being the *blondel* if D is in lumen m^{-2} and ω is in steradian.

Table III shows how equations behave in the two systems. The flux density produced by a uniform plane source of infinite extent is πB in the unrationalized and H (or B') in the rationalized. The simplicity of the rationalized formula is of practical advantage. Of greater importance, however, are the two pairs of equations at the bottom of Table III. To obtain the helios of a perfectly diffusing surface having reflectance ρ and incident flux density D_i, one merely multiplies D_i by ρ. In the unrationalized system, on the other hand, a factor π must be introduced. This slight difference may not seem like a vital matter; but to one who must continually change from incident to reflected quantities, the constant multiplication and division by π becomes very annoying and is a potent source of error.

We believe, therefore, that the unrationalized system of brightness units should be abandoned. This can be done if the concept is defined by Eq. (1) rather than in the antiquated and illogical manner based on intensity. In this way, one complete set of brightness units is eliminated, as well as some very confusing definitions, and the subject becomes much simpler. One may then use any symbol he wishes in Eq. (1) and may even call the concept *brightness*, though there are many disadvantages to employing this much overworked word.[9]

Regarding the words of Table II, one notes the ambiguous terms "density," "intensity," and "quantity" and the incorrect use of the suffix -ANCE.

4. PASSIVE CONCEPTS

Forming a bridge between the radiometric and photometric quantities, we have the *connectives* of Table IV. In the older systems, there seems to have been no realization that the spectral lamprosity ("luminosity") has the same dimensions and is the same kind of an entity as the quantity that is erroneously called "luminous efficiency." The only difference is that the former applies to homogeneous radiation and the latter to any radiation. This relation is clearly realized in the O.S.A. system,[3] which therefore constitutes a logical advance. As pointed out elsewhere,[10] however, the word "luminosity" is an unfortunate choice.

TABLE III. Unrationalized and rationalized brightness units.

	Unrationalized (C.I.E. brightness)	Rationalized (as in helios)
Unit-sphere method	$E=B\sigma''$	$D=\frac{H}{\pi}\sigma''$
Unit-cylinder method	$E=\frac{B\pi}{2}s''$	$D=\frac{H}{2}\sigma''$
Infinite uniform plane source	$E=\pi B$	$D=H$
Reflected from perfectly diffusing surface	$B=\rho E/\pi$	$H=\rho D_i$
Transmitted by perfectly diffusing body	$B=\tau E/\pi$	$H=\tau D_i$

TABLE IV. Comparison of systems of nomenclature. Connective concepts.

Unit	C.I.E. (1938)		I.E.S. (1941)		O.S.A. (1944)		Proposed (1946)	
lumen watt^{-1} (for homogeneous radiation)	K	luminosity factor of radiation	K	luminosity factor	K_λ	absolute spectral luminosity	$v(\lambda)$	spectral lamprosity
young watt^{-1} (for homogeneous radiation)	K	relative luminosity factor	K	relative luminosity factor	$\bar{y}_\lambda$	relative spectral luminosity	$\bar{y}(\lambda)$	spectral lamprosity
lumen watt^{-1} (for total radiation)	—	——	—	luminous "efficiency" of radiant energy	K	absolute luminosity	v_t	total lamprosity
young watt^{-1} (for total radiation)	—	——	—	luminous "efficiency" of radiant energy	$\bar{y}$	relative luminosity	$\bar{y}_t$	total lamprosity
lumen per input watt	—	"efficiency" of a luminous source	—	"efficiency" of a source of light	—	——	η	actance
Conversion factors								
lumen young^{-1}	—	——	—	——	K_m	maximum luminosity	c	conversion factor
young lumen^{-1}	—	"mechanical equivalent of light"	—	minimum "mechanical equivalent of light"	—	——	—	——

TABLE V. Comparison of systems of nomenclature. Passive properties of entities and materials.

Recommended symbol	C.I.E. (1938)		I.E.S. (1941)		O.S.A. (1944)		Proposed (1946)	
$\rho(\lambda)$	ρ	spectral reflection factor	ρ	reflection factor	r_λ	spectral reflectance	$\rho(\lambda)$	spectral reflectance
$\tau(\lambda)$	τ	spectral transmission factor	τ	transmission factor	t_λ	spectral transmittance	$\tau(\lambda)$	spectral transmittance
ρ_r	—	——	—	——	r	radiant reflectance	ρ_r	radiant reflectance
τ_r	—	——	—	——	t	radiant transmittance	τ_r	radiant transmittance
α_r	—	——	—	——	A	radiant absorptance	α_r	radiant absorptance
ρ_l	ρ	reflection factor	ρ	reflection factor	R	luminous reflectance	ρ_l	luminous reflectance
τ_l	τ	transmission factor	τ	transmission factor	T	luminous transmittance	τ_l	luminous transmittance
α_l	α	absorption factor	α	absorption factor	—	——	α_l	luminous absorptance
κ	—	——	—	——	k	absorption coefficient	κ	afantivity
$\epsilon(\lambda)$	—	——	ϵ_λ	spectral emissivity	e_λ	spectral emissivity	$\epsilon(\lambda)$	spectral stilbance
ϵ_t	—	——	ϵ_t	total emissivity	e	total emissivity	ϵ_t	total stilbance

TABLE VI. Comparison of systems of nomenclature. Colorimetric concepts.

Recommended symbol	C.I.E. (1938)		I.E.S. (1941)		O.S.A. (1944)		Proposed (1946)	
$\bar{x}(\lambda), \bar{y}(\lambda), \bar{z}(\lambda)$	$\bar{x}, \bar{y}, \bar{z}$	distribution coefficients of the equi-energy spectrum	$\bar{x}, \bar{y}, \bar{z}$	stimuli	$\bar{x}, \bar{y}, \bar{z}$	color mixture data	$\bar{x}(\lambda), \bar{y}(\lambda), \bar{z}(\lambda)$	trichromatic weighting function
X, Y, Z	—	——	X, Y, Z	tristimulus values	X, Y, Z	tristimulus values	X, Y, Z	trichromatic coordinates
(X, Y, Z)	—	——	—	color	—	color	(X, Y, Z)	trichros
x, y, z	x, y, z	trichromatic coefficients of the equi-energy spectrum	x, y, z	trichromatic coefficients	x, y, z	trichromatic coefficients	x, y, z	homogeneous coordinates
(x, y)	—	——	—	chromaticity	—	chromaticity	(x, y)	chros
λ_d	—	hue wave-length	—	——	—	dominant wave-length	λ_d	dominant wave-length
λ_c	—	——	—	——	—	complementary wave-length	λ_c	complementary wave-length
p	—	purity or saturation	—	——	p	purity	p	akratos
T_c	—	color temperature	—	color temperature	—	color temperature	—	——

TABLE VII. Usual names of photometric concepts.

Symbol	Unit	English	French	Italian	Spanish	Portuguese	German	Russian
F	lumen	luminous flux	flux lumineux	flusso luminoso	flujo luminoso	fluxo luminoso	Lichtstrom	svetovoĭ potok
D	lumen m^{-2}	luminous flux density	densité de flux lumineux	densità superficiale del flusso luminoso	densidad del flujo luminoso	densidade do fluxo luminoso	Flächen-lichstromdichte	plotnost potoka
E	lumen m^{-2}	illumination	éclairement	illuminamento	iluminación	iluminação	Beleuchtungsstärke	osveshchennost
L	lumen m^{-2}	radiance, luminosity	radiance	luminosità	radiancia	luminosidade	spezifische Lichtausstrahlung	svetImost
Q	lumen-sec.	quantity of light	quantité de lumière	quantità di luce	cantidad de luz	quantidade de luz	Lichtmenge	kolichIestvo sveta
U	lumen sec. m^{-2}	exposure	excitation	eccitazione	exposición	exposição	Belichtung	ekspozItsselIâ
I	candle	luminous intensity	intensité lumineuse	intensità luminosa	intensidad luminosa	intensidade luminoso	Lichtstärke	sIla sveta
B	candle m^{-2}	brightness	brillance	splendore luminoso	bril'o	brilho intrínseco	Leuchtdichte	Iârkost

TABLE VIII. Present names of some other concepts.

Symbol	English	French	Italian	Spanish	Portuguese	German	Russian
λ	wave-length	longueur d'onde	lunghezza d'onda	longitud de onda	longura de ondas	Wellenlänge	dlIna
$v(\lambda)$	luminosity factor	coefficient de visibilité d'une radiation	coefficiente di visibilità	coeficiente de visibilidad	coeficiente de visibilidade	photometrisches Strahlungsäquivalent	vIdnost radIatsIIâ
v_l	luminous efficacy of radiant energy	efficacité lumineuse d'une radiation	efficacia di una radiazione	eficacia luminosa de radiación	eficacia luminosa de iradiação	spezifische Lichtausbeute	tsvetovaIâ otdacha
η	over-all efficacy of a source	coefficient d'efficacité d'une source	efficienza di una sorgente luminosa	eficacia luminosa de la fuente	eficacia luminosa de fonte	Lichtausbeute einer Lichtquelle	tsvetovaIâ otdacha Istochnika
ρ	reflection factor	facteur de réflexion d'une corps	fattore di riflessione di un corpo	factor de reflexión	factor de reflexão	Reflexion eines Körpers	koèfItsient otrazhenIâ tela
τ	transmission factor	facteur de transmission d'une corps	fattore di trasmissione di un corpo	factor de transmisión	factor de transmissão	Durchlässigkeit eines Körpers	koèfItsient propuskanIâ tela
α	absorption factor	facteur d'absorption d'une corps	fattore di assorbimento di un corpo	factor de absorción	factor de absorção	Absorption eines Körpers	koèfItsient poglosh-chenIâ tela
ϵ	emissivity	pouvoir émissif	potere emissivo	fuerza emisora	força emisora	Emissionsvermögen	luchelspuskatelnaIâ sposobnost
g	"efficiency" of a luminaire	rendement	rendimento	rendimiento	rendimento	Wirkungsgrad	koèfItsient poleznogo
k_r	room index	indice du local	indice di sala	indice de cuarto	indice de sala	Raumindex	Indeks pomeshchenIâ
k_u	coefficient of utilization	facteur d'utilisation	fattore di utilizzazione	factor de útilización	factor de utilização	Wirkungsgrad der Beleuchtung	koèfItsient Ispolzovanlâ
$\bar{x}(\lambda)$, $\bar{y}(\lambda)$, $\bar{z}(\lambda)$	trichromatic weighting functions	coefficients de distribution pour des excitations de même énergie	funzioni tricromátice	funciónes tricromáticas	funçãos tricromáticas	dreichromatische Funktionen	trikhromatIcheskIe funktsII
X, Y, Z	trichromatic coordinates	coordonées trichromatiques	coordinati tricromátice	coordenadas tricromáticas	coordenadas tricromaticas	dreichromatische Koordinaten	trikhromatIcheskIe koordInaty
(X, Y, Z)	color	couleur	colore	color	color	Farbe	tsvet
x, y, z	homogeneous coordinates	coefficients trIchromatiques	coordinati omogene	coordenadas homogéneas	coordenadas homogéneas	Farbenkoefizienten	gomogennye koordInaty
(x, y)	chromaticity	chromaticité	qualità di colore	calidad de color	qualidade de color	Chromatizität	tsvetnost
λ_d	dominant wave-length	longueur d'onde dominante	lunghezza d'onda dominante	longitud de onda dominante	longura de ondas dominante	farbtongleiche Wellenlänge	preobladaIûshchaIâ dlIna volny
p	purity	facteur de pureté	fattore di purezza	pureza de color	pureza de color	Reinheitsgrad	chIstota tsveta
T_c	color temperature	température de couleur	temperatura di colore	temperatura de color	temperatura de color	Farbtemperatur	tsvetovaIâ temperatura

Table V lists various passive properties of entities and of materials. The international endings are

-ANCE = passive property of an entity,
-ITY = passive property of a substance.

Except for the older terms, such as *reflection factor* (which is being supplented by *reflectance*), the established names are fairly satisfactory. An exception is *emissivity*, which refers to the property of a radiator, not a substance. Thus the international ending should be -ANCE, as in the proposed word *stilbance*.

The Greek symbols ρ, τ, α, and ϵ have been so thoroughly standardized internationally for these quantities that it seems unfortunate for the O.S.A. to attempt to replace them by Roman symbols. Note also the use of capital A (a photometric symbol) for a radiometric quantity and the inconsistent use of subscript λ. In Table I, the O.S.A. used the subscript λ to indicate "per unit wave-length band." For example, U indicates radiant energy, having dimensions $[PT]$, while U_λ is radiant energy per unit wave-length band—a completely different quantity having dimensions $[PT\Lambda^{-1}]$. In Table V, on the other hand, the use of the subscript λ does not change the dimensions but merely indicates that the quantity is measured at wave-length λ. The way out of this difficulty is to use a new symbol and name for the spectral quantity in Table I.

5. COLORIMETRIC CONCEPTS

The principal concepts of colorimetry are indicated in Table VI. The symbols are well standardized. The words *chromaticity* and *purity*, however, may be criticized because they are not international and because they do not use -ITY in its international sense. Both of these quantities indicate active characteristics of radiation, not passive properties of a material. Thus the -OS ending would be preferable, as in *chros* and *akratos*.

Three numbers X, Y, and Z represent a point in the 3-dimensional colorspace. Frequently the colorimetrist wishes to speak of the complete entity specified by these three numbers. Mathematically, this entity is a hypernumber (X, Y, Z) having these three coordinates; or geometrically it may be thought of as an affine vector from the origin to the point under consideration. The complete entity[11] has been called *color* or *color-point* but these terms are very ambiguous. We propose the word *trichros*.[7]

Similarly, in the color 2-space one needs a name for the hypernumber (x, y) having coordinates x and y. We suggest the word *chros*.[7]

6. PRESENT NAMES

It is interesting to see how the familiar names of photometry are translated into other languages. Table VII shows how these words[12] appear in seven languages. In view of the large number of Latin words in English and in the Romance languages, one might expect that most photometric terms would be very similar in these languages, even though they differ markedly in German and Russian. Even here, however, there are confusing differences, as *illumination, éclairment; radiance, luminosità; exposure, excitation*. As for German and Russian, even linguistic experts cannot tell which of the words to use unless they have happened to specialize in this particular field, while most writers of technical dictionaries have not even reached the stage where they realize that a distinction exists between *luminous flux, intensity*, and *brightness*. The established words are thoroughly non-international, and there is a very real difficulty in translating photometric information from one language to another.[13]

Table VIII gives corresponding names for some passive concepts and some colorimetric concepts. Again there is almost complete lack of internationality. The reader will note also the extraordinarily cumbersome expression employed in many cases.[14]

7. PROPOSED INTERNATIONAL NAMES

There is no need for the exasperating translational difficulty that now exists[13] in technical writing. By choosing scientific words from classical Greek instead of from popular speech, one automatically obtains[4]

(a) Exactness in English. The new word is specifically defined with one precise meaning. There is no vague popular meaning to confuse the issue.

(b) Internationality. No one is foolish enough to try to translate the new word. It is accepted

TABLE IX. Proposed word endings.

Meaning	International	English	French	Italian	Spanish	Portuguese	German	Dutch	Russian
Basic concept	-oso	-os	-osse	-oso	-oso	-oso	-os	-os	-os
Per unit length	-ento	-ent	-ent	-ento	-ento	-ento	-ent	-ent	-ent
Per unit area	-ago	-age	-age	-aggio	-ago	-ago	-ag	-ag	-azh
Per unit volume	-omo	-um	-um	-umo	-umo	-umo	-um	-um	-um
A device	-oro	-or	-eur	-ore	-or	-or	-or	-or	-or
A process	-cio	-tion	-tion	-zione	-ción	-ção	-tion	-tie	-tsiĝ
Passive property of an entity	-anco	-ance	-ance	-anza	-ancia	-ância	-anz	-antie	-ants
Passive property of a substance	-ito	-ity	-ité	-ità	-idad	-idade	-ität	-iteit	-ito

TABLE X. Proposed international names for radiometric and photometric concepts.

Symbol	International	English	French	Italian	Spanish	Portuguese	German	Dutch	Russian
	Active concepts								
F	faroso	pharos	pharosse	faroso	faroso	faroso	Pharos	pharos	faros
D	farosago	pharosage	pharossage	farosaggio	farosago	farosago	Pharosag	pharosag	farosazh
Q	foso	phos	phosse	foso	foso	foso	Phos	phos	fos
U	fosago	phosage	phossage	fosaggio	fosago	fosago	Phosag	phosag	fosazh
H	helioso	helios	héliosse	elioso	helioso	helioso	Helios	helios	ĥlios
G	heliosento	heliosent	héliossent	eliosento	heliosento	heliosento	Heliosent	heliosent	ĥliosent
$J(\lambda)$	fengosago	phengosage	phengossage	fengosaggio	fengosago	fengosago	Phengosag	phengosag	fengosazh
	Connectives								
$\bar{y}(\lambda), \bar{y}_t$	lamprosito	lamprosity	lamprosité	lamprosità	lamprosidad	lamprosidade	Lamprosität	lamprositeit	lamprosĭti
η	aktanco	actance	actance	attanza	actancia	actância	Aktanz	aktantie	aktants
	Ratios expressing passive properties								
ρ	reflektanco	reflectance	réflectance	riflettenza	reflectancia	reflectância	Reflektanz	reflektantie	riflektants
τ	transmitanco	transmittance	transmittance	transmittenza	transmitancia	transmitância	Transmittanz	transmittantie	transmitants
α	absorbtanco	absorptance	absorptance	assorbenza	absortancia	absortância	Absorptanz	absorptantie	absorbtants
κ	afantito	afantivity	afantivité	afantità	afantividad	afantividade	Afantivität	afantiviteit	afantivĭti
ϵ	stilbanco	stilbance	stilbance	stilbanza	estilbancia	estilbância	Stilbanz	stilbantie	stilbants
	Dimensionless ratios used in room lighting								
f	interflektanco	interflectance	interflectance	interflettenza	interflectancia	interflectância	Interflektanz	interflektantie	interflektants
g	loganco	logance	logance	loganza	logancia	logância	Loganz	logantie	logants
k_r	domanco	domance	domance	domanza	domancia	domância	Domanz	domantie	domants
k_m	luanco	luance	luance	luanza	luancia	luância	Luanz	luantie	luants
T	deloso	delos	delosse	deloso	deloso	deloso	Delos	delos	delos
	Colorimetric terms								
(X, Y, Z)	trikroso	trichros	trichrosse	tricroso	tricroso	tricroso	Trikros	trikros	trĭkros
(x, y)	kroso	chros	chrosse	croso	croso	croso	Kros	kros	kros
p	akratoso	akratos	akratosse	acratoso	acratoso	acratoso	Akratos	akratos	akratos

(with, at most, slight changes in orthography) by all the languages in which appreciable scientific publication occurs.

A study of several hundred scientific words[4] shows that those taken from Greek are nearly always accepted without translation. For instance, *dynamo*, *electricity*, *energy*, *ion*, *mathematics*, *micron*, *photograph*, *solenoid*, *telephone*, *thermometer* are international words taken from Greek. But when a word is taken from popular speech, it is translated into each language, giving the translator's headache indicated by Tables VII and VIII.

It is also advantageous to employ international word endings to reduce the number of distinct Greek roots that must be learned. A list of endings is given in Table IX. The meaning is entered in the first column and the English ending is in the third column. The suffixes -ANCE and -ITY were mentioned previously. The ending -OR for a device (*motor*, *reflector*) and -TION for a process (*activation*, *integration*) are likewise international. Endings -ENT, -AGE, and -UM were introduced several years ago[6] and seem to be acceptable. Slight changes in spelling are advisable to make the new words seem more

TABLE XI. Proposed concepts and their names.

Symbol	Dimensions	Unit	Name (English)
Active radiometric concepts.			
F_r	$[P]$	watt	radiant pharos
D_r	$[PL_t^{-2}]$	watt m^{-2}	radiant pharosage
Q_r	$[PT]$	watt sec.	radiant phos
U_r	$[PTL_t^{-2}]$	watt sec. m^{-2}	radiant phosage
H_r	$[PL_t^{-4}L_r^2]$	herschel	radiant helios
G_r	$[PL_t^{-4}L_r]$	herschel m^{-1}	radiant heliosent
$J(\lambda)$	$[PL_t^{-2}A^{-1}]$	watt m^{-2} micron^{-1}	phengosage
Connectives			
$v(\lambda)$	$[FP^{-1}]$		
v_l	$[FP^{-1}]$		
v_r	$[FP^{-1}]$		
Ratios expressing passive properties (*radiometric*)			
$\rho(\lambda)$	None	Numeric	reflectance (spectral)
$\tau(\lambda)$	None	Numeric	transmittance (spectral)
ρ_r	None	Numeric	reflectance (radiant)
τ_r	None	Numeric	transmittance (radiant)
α_r	None	Numeric	absorptance (radiant)
$\kappa(\lambda)$	$[L_r^{-1}]$	m^{-1}	afantivity (spectral)
κ_r	$[L_r^{-1}]$	m^{-1}	afantivity (radiant)
$\epsilon(\lambda)$	None	Numeric	stilbance (spectral)
ϵ_t	None	Numeric	stilbance (total)

Symbol	Dimensions	Unit	Name (English)
Active photometric concepts			
F_l	$[F]$	lumen, young	luminous pharos
D_l	$[FL_t^{-2}]$	lumen m^{-2}	luminous pharosage
Q_l	$[FT]$	lumen sec.	luminous phos
U_l	$[FTL_t^{-2}]$	lumen sec. m^{-2}	luminous phosage
H_l	$[FL_t^{-4}L_r^2]$	blondel	luminous helios
G_l	$[FL_t^{-4}L_r]$	blondel m^{-1}	luminous heliosent
Connectives			
lumen watt^{-1}		lamprosity (spectral)	
lumen watt^{-1}		lamprosity (total)	
lumen watt^{-1}		actance	
Ratios expressing passive properties (*photometric*)			
ρ_l	None	Numeric	reflectance (luminous)
τ_l	None	Numeric	transmittance
α_l	None	Numeric	absorptance
κ_l	$[L_r^{-1}]$	m^{-1}	afantivity
Dimensionless ratios occurring in room lighting			
	None	Numeric	interflectance
g	None	Numeric	logance
k_u	None	Numeric	coefficient of utilization*
k_r	None	Numeric	domance
k_m	None	Numeric	luance
T	None	Numeric	delos
Colorimetric terms (C.I.E. system)			
Symbol	Dimensions	Unit	Name
$\bar{x}(\lambda)$	$[F_x P^{-1}]$	könig watt^{-1}	trichromatic weighting functions*
$\bar{y}(\lambda)$	$[FP^{-1}]$	young watt^{-1}	
$\bar{z}(\lambda)$	$[F_z P^{-1}]$	priest watt^{-1}	
X	$[F_x L_t^{-2}]$	könig m^{-2}	trichromatic coordinates*
Y	$[FL_t^{-2}]$	young m^{-2}	
Z	$[F_z L_t^{-2}]$	priest m^{-2}	
(X, Y, Z)			*trichros*, a hypernumber having the coordinates X, Y, Z.
$x, y, \mathfrak{C}$	None	Numeric	homogeneous coordinates*
(x, y)			*chros*, a hypernumber having the coordinates x and y.
λ_d	[A]	micron	dominant wave-length*
λ_c	[A]	micron	complementary wave-length*
p	None	Numeric	*akratos*

* Noninternational names. Must be translated into each language.

natural to various ethnic languages. These changes are indicated in Table IX. The column marked "international" is for the international auxiliary languages such as Esperanto,[15] Ido,[16] and Iala.[17]

The endings of Table IX have been employed in forming the proposed international photometric words of Table X. These words, most of which were used in the previous tables, are assembled with symbols in the complete system of Table XI. This system is believed to satisfy all four criteria of Section 1. It provides a complete set of names and symbols,[18] designed to give maximum precision and generality with minimum complexity. International endings are employed in a consistent manner, and the words are international rather than local.

In conclusion, it is a pleasure to acknowledge the help received from Elliot Q. Adams, H. E. Blair, Erich Berger, Salvador Castro, G. Alan Connor, E. C. Crittenden, F. Cuétara, F. M. Currier, Oswaldo P. Doria, Roberto M. Fano, I. H. Godlove, J. P. Den Hartog, International Auxiliary Language Association, H. Jacob, Deane B. Judd, Waldemar Kaempffert, R. F. Koch, W. M. Locke, D. L. MacAdam, Sanford A. Moss, W. B. Nottingham, Mario A. Pei, Duane Roller, Pieter Schoonhoven, Lewis L. Sell, Dirk J. Struik, Gregory Timoshenko, and George A. Znamensky.

8. BIBLIOGRAPHY

1. *International Lighting Vocabulary* (C.I.E., Teddington, England, 1938).
2. "Illuminating engineering nomenclature and photometric standards," Illum. Eng. **36**, 815 (1941).
3. "Report of the Colorimetry Committee," J. Opt. Soc. Am. **34**, 246 (1944).
4. Parry Moon and D. E. Spencer, "Internationality in the names of scientific concepts: A method of naming concepts," Am. J. Phys. **14**, 285 (1946); "Proposed international photometric system" and "Comparison of photometric systems," Am. J. Phys. (1946) (to be published).
5. W. Williams, "On the relation of the dimensions of physical quantities to directions in space," Phil. Mag. **34**, 234 (1892); J. B. Brinsmade, "Plane and solid angles," Am. Phys. T. **4**, 175 (1936).
6. Parry Moon, "A system of photometric concepts," J. Opt. Soc. Am. **32**, 348 (1942); "The names of physical concepts," Am. J. Phys. **10**, 134 (1942).
7. Parry Moon and D. E. Spencer, *An Unofficial Guide to Photometric Nomenclature* (to be published).
8. Parry Moon, "Basic principles in illumination calculations," J. Opt. Soc. Am. **29**, 108 (1939); "New methods of calculating illumination," *ibid.* **33**, 115 (1943).
9. Parry Moon and D. E. Spencer, "Brightness and helios," Illum. Eng. **39**, 507 (1944); "Photometrics in general physics," Am. J. Phys. **11**, 200 (1943).
10. Parry Moon and D. E. Spencer, "International names in colorimetry," J. Opt. Soc. Am. **36**, 427 (1946).
11. H. E. Ives, "The transformation of color-mixture equations from one system to another," J. Frank. Inst. **180**, 673 (1915); J. Guild, "The transformation of trichromatic mixture data," Opt. Soc. Trans. (London) **26**, 95 (1924–1925); T. Smith and J. Guild, "The C.I.E. colorimetric standards and their use," Opt. Soc. Trans. **33**, 73 (1931–1932); T. Smith, "A reading of elementary colorimetric theory," *ibid.* **33**, 214 (1931–1932).
12. Based on reference 1 and on *International Electrotechnical Vocabulary* (Commission Electrotechnique Internationale, London, 1938); L. D. Belkind, *Dictionary of Lighting Terminology* (Moscow, 1939).
13. L. L. Sell, *Syllabus for the Formation of the Professional Polyglot Technician* (International Dictionary Company, New York, 1945). See also L. L. Sell, *English-Spanish Comprehensive Technical Dictionary* (McGraw-Hill Book Company, Inc., New York, 1944), preface; A. S. Litvineko, *Dictionary of Radio Terminology in English, German, French, and Russian* (Moscow, 1937), preface.
14. Parry Moon and D. E. Spencer, "Photometric nomenclature for the post-war world," Illum. Eng. (1946).
15. See, for instance, C. A. Connor and D. T. Connor, *Esperanto* (S. F. Vanni, New York, 1944); W. S. Benson, *Universala Esperanto metodo* (Newark, New Jersey, 1932); M. C. Butler, *Step by Step in Esperanto* (Esperanto Publishing Company, London, 1943); Marcel Rodd, **10** *in* **1** *Dictionary* (Bernard Ackerman, New York, 1945).
16. L. de Beaufront, *Complete Manual of the Auxiliary language* IDO (Pitman and Sons, London, 1919).
17. *General report* (International Auxiliary Language Association, 420 Lexington Avenue, New York, 1945).
18. See also Parry Moon and D. E. Spencer, "Units in the trichromatic system," J. Opt. Soc. Am. **36**, 120 (1946); "Trichromatic units," *ibid.* **36**, 306 (1946); "Analytic representation of trichromatic data," *ibid.* **35**, 399 (1945); "Analytic expressions in photometry and colorimetry," J. Math. Phys. **25**, 111 (1946); "Maintenance factors," Illum. Eng. **41**, 211 (1946).

A New Light Balancing Circuit for the Non-Recording Densitometer*

R. O'B. CARPENTER
Baird Associates, Cambridge, Massachusetts

A description is given of the application of the electron-multiplier photo-tube and the light-chopping method to the design of a densitometer. The techniques discussed are generally applicable to the measurement of very low light intensities.

DENSITOMETERS may be divided into two classes according as the intensity of light is indicated by the direct response of a light sensitive receiver (the deflection method) or is compared with a standard light beam in a null method. Deflection densitometers using photocells have shown considerable popularity in emission spectrographic analysis because of their rapidity of reading. The null method, however, is susceptible to greater stability and reproducibility, the absolute accuracy being dependent on the accuracy of the comparison standard.

Null photo-cell bridge densitometers were reported by Rosenberg[1] and Baird.[2] Dobson[3] reported a balanced beam null instrument in which only a single receiver was used, but the shutter for alternating the beams was manually operated, making for tedious operation. Harrison[4] suggested that the two beams could be mechanically alternated at a fast rate and an alternating-current null detector used. Hardy[5] used such a system in a recording spectrophotometer.

The Baird Associates Non-Recording Densitometer[2] is of the projection type. The light from a ten times magnified image of the plate or film is passed through a suitable selection slit to a photo-tube light receiver. Density is measured by obtaining null balance with a second beam

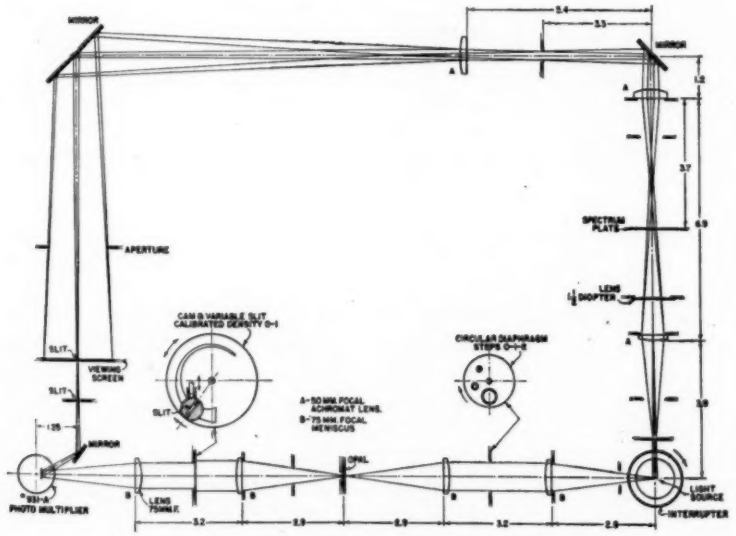

FIG. 1. Optical diagram of the Model 2 densitometer.

* Presented at the 30th meeting of the Optical Society of America, October 18–20, 1945, New York, New York.

[1] H. Rosenberg, Zeits. f. Instrumentenkunde **45**, 313 (1925).
[2] W. S. Baird, "A new non-recording densitometer," J. Opt. Soc. Am. **31**, 179–180 (Feb. 1941).
[3] G. M. B. Dobson, Proc. Roy. Soc. **104**, 248 (1923).
[4] G. R. Harrison, in Chapter IX of W. E. Forsythe's *Measurement of Radiant Energy* (McGraw-Hill Book Company, Inc., New York, 1937), p. 291.
[5] A. C. Hardy, "A recording photoelectric color analyzer," J. Opt. Soc. Am. **18**, 96 (1929).

which has passed through accurately calibrated apertures. See optical diagram of the Model 2 densitometer in Fig. 1.

In the original design (Model 1) the electronic null detector consisted of two high vacuum photo-tubes (RCA 917 or 919) in a bridge circuit, with a d.c. amplifier and indicator for the null detection. See Fig. 2.

In the Model 2 design, which is discussed here, the two light beams are mechanically alternated onto a single light receiver. The electronic circuit consists of a RCA 931-A electron-multiplier photo-tube for the light receiver, a tuned amplifier, a rectifier, and a visual electron-ray indicator (6E5). See Figs. 3 and 4.

The mechanical interrupter is a $1\frac{5}{8}$-inch outside diameter brass cylinder with six $\frac{7}{16}$-inch holes drilled at equal spacing around the circumference. The interrupter is driven by a 1500 r.p.m. induction motor. Ideally we should desire this alternator to place square pulses of light intensity of exactly 180° duration onto the photo-tube. In this case if the intensities of the beams are equal, the pulses will overlap to produce a constant light level on the receiver. Otherwise there will be "pips" at the alternation points. But with proper geometrical alignment of equal light beams, the resulting photo-tube output will not contain any component of the fundamental frequency. With care in mechanical design, the "overlap" or "underlap" between pulses was kept within 3 percent of the light level for equal beams. However, these harmonic components at balance, in addition to the statistical noises in the photo-tube output, prevent the null signal from the tuned amplifier from reaching zero. Hence a manual bias control is provided on the indicator tube in order to bring

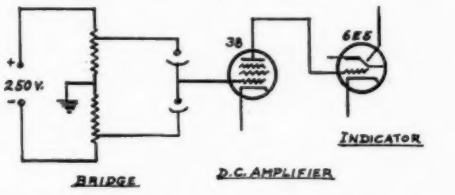

FIG. 2. Block schematic of the Model 1 electronics.

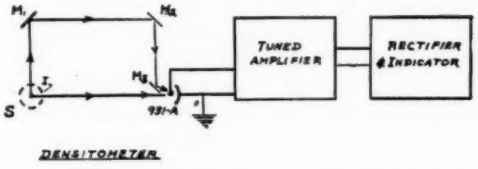

FIG. 3. Block schematic of the Model 2 electronics.

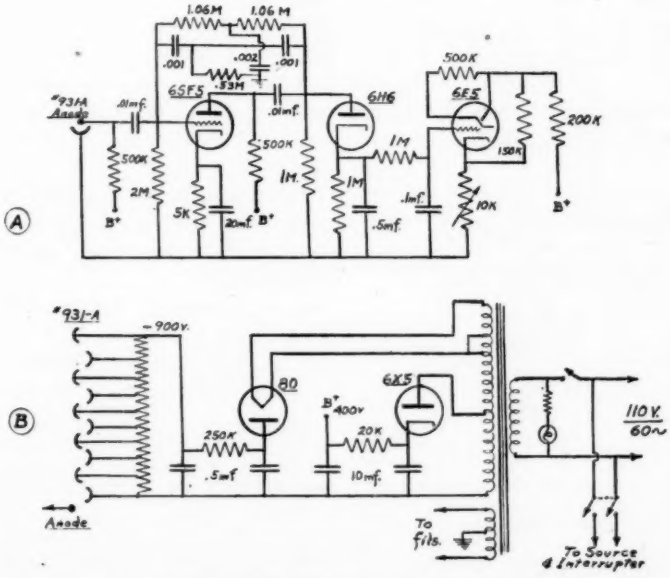

FIG. 4. Complete electronic schematic of the Model 2.

the "magic eye" to an optimum reading position for any light level.

The light receiver is the RCA 931-A.[6] The dark current is of the order of 2×10^{-8} ampere, the noise fluctuations in dark current of the order of 5×10^{-10} ampere. The average sensitivity is given by RCA as 2.0 amperes/lumen for a standard lamp, or 1800 amperes/watt at 3750A. It is to be noted that at present the available tubes show very wide variations in characteristics. The ultimate limit in light measurement is set by the dark current fluctuations.

The amplifier stage is a triode tuned by the twin-*T* resistance capacitance filter operated as a plate to grid feedback network.[7] The band width for half-maximum-response is 45 cycles, adequately narrow for this application. The peak frequency is adjusted to the frequency of alternation of light beams, approximately 150 c.p.s. Rectifier, indicator, and power supply circuits are given in the schematic and are typical.

The use of the electron multiplier tube eliminates one practical difficulty in the measurement of very low light intensities by photo-tubes. With an ordinary high vacuum photo-tube, where the minimum detectable light intensity produces a current of the order of 5×10^{-15} ampere, the fluctuating (noisy) components of the terminal leakage currents must be kept below this order of magnitude. With the electron multiplier this low level photoelectric current flows only between the first two electrodes within the evacuated envelope, and by careful manufacture the leakage currents in the tube can be reduced to a minimum before evacuation. The output current is brought out at a level which may be made as high as 300,000 times above the current in the photo-cathode. At this level leakage currents are negligible. In addition the electron multiplier is probably the simplest and most economical method of obtaining a pre-amplifier.

The advantages of the light chopping method are several. The use of a single receiver eliminates dark current corrections and drifts due to changes in dark current or photo-tube sensitivity. Especially to be noted is the elimination of the effect of fatigue (loss in sensitivity as a function of the total energy which has recently fallen on the cathode), which is found in all photo-tubes.

In the specific application to the Baird Associates densitometer, the improvements over the Model 1 design were: (1) 60-sec. warm-up time; (2) elimination of dark balance; (3) light balance not subject to draft; (4) reproducibility over long time periods is within .02 density over the entire range of the instrument (density 0–3); (5) response time of 0.5 second is uniform over the entire range; (6) effect of leakage currents reduced; and (7) selection of tubes less critical.

Possible modifications will suggest themselves for other applications: (1) elimination of the comparison beam, chopping the measured beam at a suitable frequency, and measuring the light level with a suitable vacuum tube voltmeter; (2) use of the photo-multiplier without chopping, with a galvanometer or d.c. amplifier to measure the light level, correcting for dark current at low intensities.

Acknowledgment is made to the entire development staff of Baird Associates for ideas, suggestions, and valued assistance on this development.

[6] For properties of these tubes see manufacturer's data and G. H. Dieke, "The use of multiplier phototubes in spectrographic analysis," OPRD-WPB, Report No. W-193, May 1, 1945.

[7] H. H. Scott, "A new type of selective circuit and some applications," Proc. I.R.E. **26**, 226 (Feb., 1938).